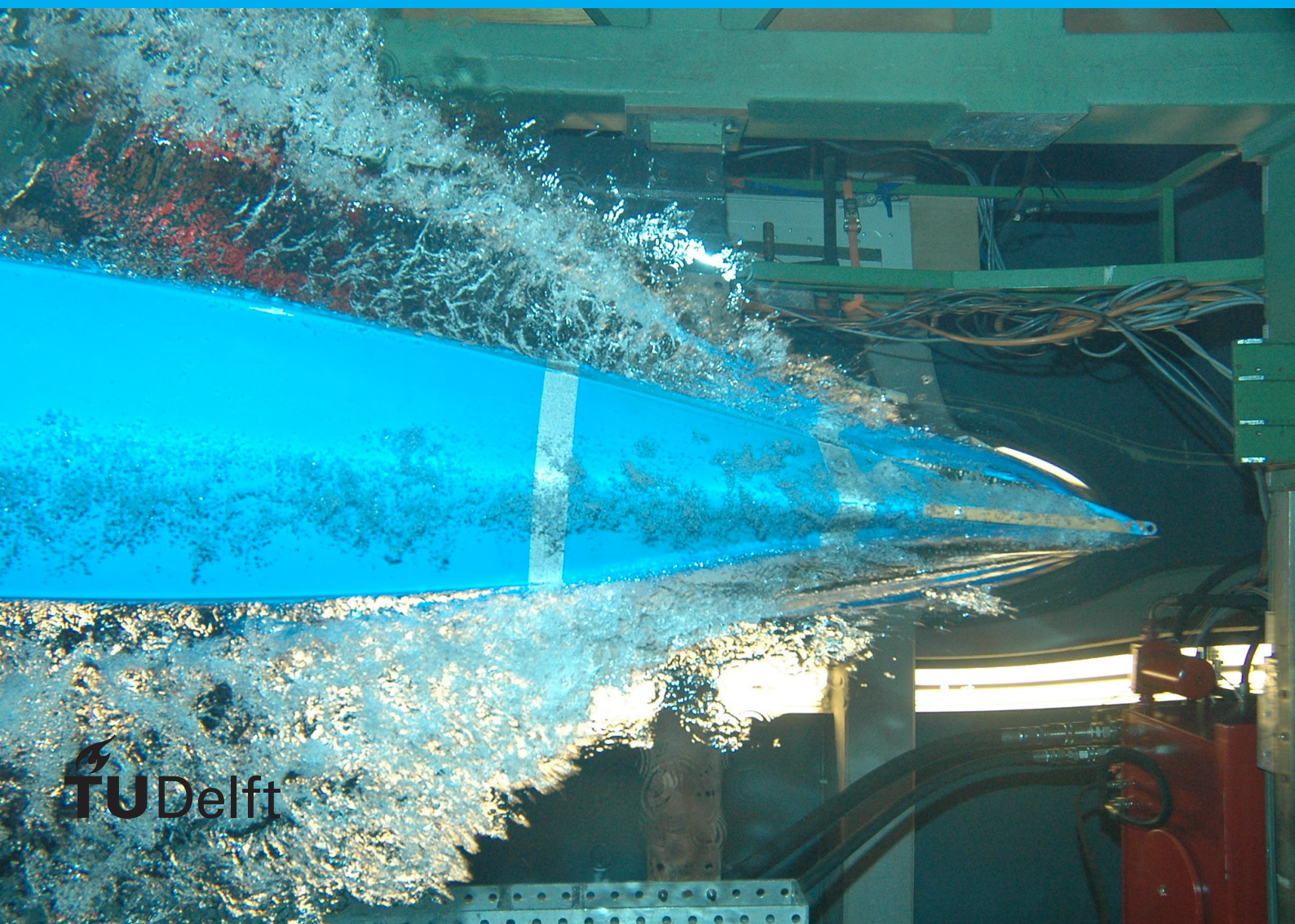


# An alternative Ocean Cleanup system

Conceptual design of a mobile Great Pacific Garbage Patch plastic catching system

B. Delfos

ISBN 978-94-6186-742-1





# An alternative Ocean Cleanup system

## Conceptual design of a mobile Great Pacific Garbage Patch plastic catching system

by

B. Delfos

to obtain the degree of Master of Science,  
from the faculty of offshore & dredging engineering,  
at the Delft University of Technology,  
with a specialization in bottom founded and floating structures,  
to be defended on October 20, 2016 at 13:00 AM.

Student number: 4019210  
Project duration: January 1, 2016 – October 20, 2016  
Thesis committee: Prof. dr. ir. A. Metrikine, TU Delft, supervisor  
Ir. A. Jarquin Laguana, TU Delft  
Ir. A. Tjallema, The Ocean Cleanup

*This thesis is confidential and cannot be made public until December 31, 2016.*

An electronic version of this thesis is available at <http://repository.tudelft.nl/>.





# Abstract

Eight million tons of plastic enters the ocean every year, causing damage to the environment, to human health, and to the economy. Due to rotating currents, called 'Gyres', large quantities of that debris accumulate in five areas around the world. In an attempt to clean up the most polluted area, being the Great Pacific Garbage Patch, Boyan Slat (founder of the Ocean Cleanup) proposed to install a fixed moored, 100km long, v-shaped barrier, to passively catch, concentrate and extract the plastic (Figure 1). However, due to the recent discovery of the presence of a highly variable current direction, in combination with the huge costs projections for the fix moored barrier, the Ocean Cleanup came to the conclusion that it would be appropriate to initiate a research into alternative cleaning systems. The first phase that followed is this thesis, with the objective of developing a conceptual design of a alternative cleaning system.

The thesis accomplishes this objective by first analyzing all possible cleaning strategies and strategy specific concepts in a high level and structured process. Using methods such as brainstorming, multi-criteria analysis (MCA), and morphological overviews, strategies and concepts were developed and evaluated. Four strategies are proposed, of which a passive concept with sea-anchors, driven by ocean currents, is selected as the most promising concept for further feasibility analysis. A high level concept that is completely flexible and uses hydrodynamic lift to force the barrier open perpendicular to the flow, is subsequently selected for feasibility analysis using a numerical model. Besides that, a experimental test program is proposed to evaluate a concept which uses a large surface covering membrane.

The feasibility analysis of the concept, is subsequently divided into two steps. The first step focuses on the design of a suitable sea-anchor to generate stable lift. For which a three-dimensional model was constructed using a lumped mass approach, in which the system is build-up out of massless springs and all forces are superimposed on the nodes, being; mass, buoyancy, tension, drag, and added-mass. The model is subsequently used to simulate the behavior of a 'Window-shade drogue' (sea-anchor for meteorological research) to partially validate the model. After which the sea-anchor design is adapted to show that stable lift can be generated. Besides this, a one-degree of freedom model gives insight into the parameters required to ensure anchor stability.

The second step focuses on the construction and evaluation of a three-dimensional model of the complete concept, and multiple variations. It is shown that the high level selected concept is not feasible, and that the efficiency both in terms of current following capability as in shape retainment, is low. The concept is not able to adequately follow a median changing current direction of 16 degrees/hr at 0.17 m/s, leading to entanglement of lines and a collapse of the system. Following from these results, a new concept is proposed which requires torsional and bending stiffness in the anchor and barrier configuration, to prevent entanglement, and uses a two sided catching mechanism to catch plastic from all directions. Furthermore, additional research is suggested for individual components as well as for the newly proposed concept.



# Preface

This thesis was the first step of the Ocean Cleanup in the search for alternative plastic catching systems. The research objective of developing a conceptual design of a mobile Great Pacific Garbage Patch plastic catching system, was therefore extremely broad. As a result the first two months were highly conceptual. To enable a structured process I organized and lead several brainstorm sessions, during which possible cleaning strategies were developed. Furthermore, in the early stages of concept formulation, the opportunity arose to participate in a HYDRALAB+ program (subject of part 3). The HYDRALAB+ program opened up the possibility to test one of the concepts in a offshore wave basin in Denmark, and was therefor thought to be a valuable opportunity for this thesis. As a consequence I started working together with Reijnder de Feijter, to develop a scientific test program proposal. Reijnder de Feijters focus was thereby on large scale system movements, whereas my focus was on actual concept behavior. Unfortunately the proposal was not approved, but the feedback (Appendix A) can be used to submit a new proposal before the 1st of December. After the submission of the test program the thesis period mainly focused on the development of a three dimensional model of a high level selected concept. However, during this period I attended several brainstorm sessions at the Ocean Cleanup, in which I contributed to the in-house development of conceptual design, which started four months after the beginning of this thesis. This final thesis document is therefor not the only contribution to the Ocean Cleanup, but can be considered as the result of a conceptual design process.

I would hereby foremost like to thank Reijnder de Feijter for his contribution to the experimental test program in part 3. Secondly I would like to thank Prof. dr. ir. A. Metrikine for his support as my supervisor. And thirdly I would like to thank Ir. A. Jarquin Laguana, Ir. A. Tjallema, and Ir. L. Boot, for their support as daily supervisors.

Lastly I would like to thank the Ocean Cleanup for giving me the opportunity to help develop a system to clean the worlds oceans.

*B. Delfos  
Delft, January 2016*



# Contents

<b>List of Figures</b>	<b>xi</b>
<b>List of Tables</b>	<b>xiii</b>
<b>1 Introduction</b>	<b>1</b>
1.1 The Ocean Cleanup problem statement. . . . .	1
1.2 Thesis objectives . . . . .	3
1.3 Research approach . . . . .	4
1.4 Work structure . . . . .	5
1.5 Contribution to the body of knowledge . . . . .	6
<b>I Concept generation</b>	<b>7</b>
<b>2 Operating conditions</b>	<b>9</b>
2.1 Environmental forcing . . . . .	9
2.1.1 Current . . . . .	9
2.1.2 Tidal. . . . .	9
2.1.3 Wind. . . . .	10
2.1.4 Waves. . . . .	10
2.1.5 Extreme statistics. . . . .	10
2.2 Plastic. . . . .	12
2.2.1 Release . . . . .	12
2.2.2 Concentration. . . . .	12
2.2.3 Size and mass distribution . . . . .	13
2.2.4 Vertical distribution . . . . .	13
2.2.5 Buoyancy . . . . .	13
<b>3 Strategy formulation</b>	<b>15</b>
3.1 Idea generation. . . . .	15
3.2 Proposed strategies . . . . .	16
3.2.1 Drones targeting hotspots . . . . .	17
3.2.2 Actively towing or pushing a barrier . . . . .	17
3.2.3 Encircle plastic and contract . . . . .	18
3.2.4 Passive system with sea-anchor. . . . .	18
3.3 Strategy selection . . . . .	19
<b>4 Concept formulation</b>	<b>21</b>
4.1 Base case. . . . .	22
4.1.1 Relative current. . . . .	22
4.1.2 Size . . . . .	22
4.1.3 Risks . . . . .	23
4.2 Working principles . . . . .	23
4.2.1 Retaining shape . . . . .	23
4.2.2 Catch plastic . . . . .	25
4.2.3 Maintain heading . . . . .	25
4.2.4 Plastic retention. . . . .	26
4.2.5 Sea anchor . . . . .	26
4.3 Proposed concepts . . . . .	27
4.3.1 The Hydroforce . . . . .	28
4.3.2 The Parachute . . . . .	28
4.3.3 Gate wheel . . . . .	28
4.3.4 The liquid Island . . . . .	29



4.4	Concept selection . . . . .	29
<b>II</b>	<b>Experimental test program</b>	<b>31</b>
<b>5</b>	<b>HYDRALAB+</b>	<b>33</b>
5.1	Environmental contribution. . . . .	33
5.2	Scientific objectives . . . . .	34
5.3	Methodology . . . . .	35
5.4	Test program . . . . .	36
5.5	Test set-up . . . . .	38
<b>III</b>	<b>Sea-anchor feasibility</b>	<b>41</b>
<b>6</b>	<b>Defining solution space</b>	<b>43</b>
6.1	Previous research . . . . .	43
6.2	Practically feasible TOC sea-anchors . . . . .	45
6.3	Risks . . . . .	46
<b>7</b>	<b>Three-dimensional sea-anchor model</b>	<b>49</b>
7.1	Test-cases and evaluation procedure . . . . .	50
7.2	Assumptions . . . . .	51
7.2.1	The Algorithm. . . . .	51
7.2.2	Anchor representation . . . . .	51
7.2.3	Damping and stiffness . . . . .	51
7.2.4	Environmental loading . . . . .	53
7.2.5	Added-mass and drag coefficients. . . . .	53
7.2.6	Hydrodynamics . . . . .	55
7.3	Algorithm . . . . .	58
7.3.1	2-D local matrix transformation . . . . .	59
7.3.2	3-D local matrix transformation . . . . .	61
7.3.3	3D matrix assembly . . . . .	65
<b>8</b>	<b>Model evaluation</b>	<b>67</b>
8.1	Test 1 . . . . .	68
8.2	Test 2 . . . . .	72
<b>9</b>	<b>Sea-anchor evaluation</b>	<b>75</b>
9.1	One degree of freedom stability analysis . . . . .	75
9.2	Sea-anchor design . . . . .	79
<b>IV</b>	<b>Concept feasibility</b>	<b>85</b>
<b>10</b>	<b>Three-dimensional concept model</b>	<b>87</b>
10.1	Test-cases and evaluation procedure . . . . .	88
10.1.1	Functionality . . . . .	89
10.1.2	Efficiency . . . . .	90
10.1.3	Anchor evaluation . . . . .	91
10.2	Assumptions . . . . .	91
10.3	System set-up . . . . .	92
10.4	Convergence test. . . . .	93
<b>11</b>	<b>Concept evaluation</b>	<b>95</b>
11.1	Hydro-force boom . . . . .	95
11.2	Hydroforce-boom with anchor connector . . . . .	98
11.3	Hydroforce-boom with surface rudders . . . . .	99
11.4	Concept variation evaluation. . . . .	101
11.5	Proposal of a new concept. . . . .	103

<b>V Research evaluation</b>	<b>107</b>
<b>12 Discussion</b>	<b>109</b>
12.1 Part: Concept generation process . . . . .	109
12.2 Part: Experimental test program . . . . .	110
12.3 Part: Sea-anchor feasibility . . . . .	110
12.3.1 The approach . . . . .	110
12.3.2 The results . . . . .	111
12.4 Part: Concept feasibility . . . . .	112
<b>13 Conclusion &amp; Recommendations</b>	<b>113</b>
13.1 Part: Concept feasibility . . . . .	113
13.1.1 The conclusions . . . . .	113
13.1.2 The recommendations . . . . .	113
13.2 Part: Sea-anchor feasibility . . . . .	114
13.2.1 The conclusions . . . . .	114
13.2.2 The recommendations . . . . .	115
13.3 Additional recommendations . . . . .	115
<b>Bibliography</b>	<b>117</b>
<b>A HYDRALAB+</b>	<b>121</b>
A.1 Application form . . . . .	123
A.2 Feedback . . . . .	126



# List of Figures

1.1	The Gyres . . . . .	1
1.2	The Ocean Cleanup barrier . . . . .	2
1.3	Fixed barrier in different current directions . . . . .	2
1.4	The Ocean Cleanup Value Drivers . . . . .	3
2.1	Annual non-tidal surface current and tidal surface current, by Metocean Solutions	10
2.2	Annual wave and wave conditions, by Metocean Solutions . . . . .	11
2.3	Annual densityplots, by Metocean Solutions . . . . .	11
2.4	Concentration of plastic in the GPGP, by the Ocean Cleanup . . . . .	12
3.1	Brainstorm program . . . . .	16
3.2	Strategy overview . . . . .	16
3.3	Strategy MCA scoring . . . . .	19
4.1	Morphological overview . . . . .	21
4.2	Current velocity profile and difference in current direction over the year 2012 .	22
4.3	Proposed retention methods . . . . .	26
4.4	Morphological overview with working structures . . . . .	27
4.5	Concept overview . . . . .	28
4.6	Concept MCA results . . . . .	29
5.1	Passive parachute barrier . . . . .	34
5.2	Passive flexible floater . . . . .	35
5.3	Experiment set-up . . . . .	39
6.1	Schematic of a 'Window-shade drogue', and anchor orientation to the current direction, as depicted by William A. Vachon [43] . . . . .	45
6.2	Tristar and SVP drifter [29] . . . . .	48
7.1	Window-shade drogue as simulated in this thesis . . . . .	49
7.2	The three sea-anchor test to be performed . . . . .	50
7.3	Model schematic and arbitrary tether stiffness curve . . . . .	52
7.4	Drag and added-mass coefficients for a plate by Keulegan, Garbis H and Car- penter, Lloyd H . . . . .	53
7.5	Drag and added-mass coefficients for a cylinder by Sarpkaya, T . . . . .	54
7.6	Drag and added-mass coefficients for a sphere by Sarpkaya, T . . . . .	54
7.7	Added-mass for sea-anchor and 'window-shade drogue' [27] . . . . .	55
7.8	Drag and lift coefficients depending on the angle of attack for an airfoil and flat plate . . . . .	56
7.9	Hydrodynamic center as function of the angle of attack . . . . .	57
7.10	Moment coefficient depending on the angle of attack . . . . .	58
7.11	Visual representation of calculation of lift and drag . . . . .	61
7.12	Representation of a 3-D transformation of a global to local coordinate system .	63
7.13	Visual representation of individual element matrices combined into one system matrix . . . . .	65
8.1	Visual explanation of the representation and the calculation of the angle of attack	68
8.2	Results of the first test of the window drogue in surface current only . . . . .	69
8.3	Time traces of the tension in long anchor lines . . . . .	69
8.4	Effect of line length . . . . .	70

8.5 Results of the first test of the window drogue in surface current only . . . . .	70
8.6 Time traces of the tension of pretensioned anchor lines . . . . .	71
8.7 Schematic of anchor orientation with and without pretension . . . . .	72
8.8 Time traces of the anchor with pretensioned lines . . . . .	72
8.9 Time traces of the anchor without pretensioned lines . . . . .	73
8.10 Schematics of median anchor orientation simulated and measured . . . . .	73
9.1 One degree of freedom anchor schematic . . . . .	75
9.2 Adopted anchor configurations . . . . .	80
9.3 Angle calculation and relative velocity direction representation . . . . .	80
9.4 results of straight tow of the triangular adopted anchor . . . . .	81
9.5 Boxplots of angle of attack versus forced anchor angle . . . . .	81
9.6 Result of anchor with hydrodynamic center dependency under a forced angle .	82
9.7 Visual explanation of anchor behavior . . . . .	82
9.8 Boxplots with the angle of attack versus mass variations . . . . .	83
9.9 Result of an anchor with high bi-normal added-mass . . . . .	83
9.10 Result of an anchor with rigid bars to force the angle . . . . .	84
10.1 Three basic system designs derived from the high level concept selected in chapter 3 . . . . .	87
10.2 Probability of median rate of change of the surface current direction . . . . .	88
10.3 The three different test executed for the concept feasibility analysis . . . . .	89
10.4 Visualization of functional limits and projected span width . . . . .	90
10.5 Matrix assembly of the first model . . . . .	93
10.6 Convergence test for system 1 . . . . .	93
11.1 Selected concept schematic and three-dimensional model . . . . .	95
11.2 Time trace of the left anchor with rigid angle forcing . . . . .	96
11.3 The first two variations of the selected concept . . . . .	97
11.4 Time trace of the Direction and Opening efficiency of the first three variations, with indication of first moment of failure . . . . .	97
11.5 The first two variations of the system with anchor connector . . . . .	98
11.6 The concept variations with anchor connector with drag-line and pilot anchor .	98
11.7 Time trace of the Direction and Opening efficiency of the anchor connector variations, with indication of first moment of failure in red . . . . .	99
11.8 The first two variations of the selected concept . . . . .	100
11.9 The first two variations of the selected concept . . . . .	100
11.10 Time trace of the Direction and Opening efficiency of the surface rudder variations, with indication of first moment of failure in red . . . . .	101
11.11 Boxplots of the total, directional, and opening efficiency of all system variations	102
11.12 Boxplots of the total, directional, and opening efficiency of all system variations for the longer barrier . . . . .	102
11.13 New concept schematics . . . . .	104
11.14 Visualization of new efficiency determination . . . . .	105
11.15 Proposed barrier for the new concept . . . . .	105



# List of Tables

2.1	100-year extreme values, by Metocean Solutions . . . . .	12
5.1	Scaling concept 2 with a 100 meter span width . . . . .	36
5.2	Summary of the test-program . . . . .	38
9.1	Parameters for one degree of freedom stability analysis . . . . .	78
10.1	System parameters . . . . .	92



# Introduction

## 1.1. The Ocean Cleanup problem statement

Eight million tons of plastic enters the ocean every year, causing environmental damage, human health damage, and economic damage. The Ocean Cleanup's goal is to extract, prevent, and intercept that plastic, by initiating the largest clean-up in history. It aims to achieve this by creating awareness, but primarily by installing a large moored floating barrier, which can passively concentrate plastic debris, by using the ocean currents. The idea of a moored barrier originated from the fact that a large part of all ocean debris is over time concentrated in five areas around world, where the current follows a circular pattern, called Gyres (Figure 1.1).

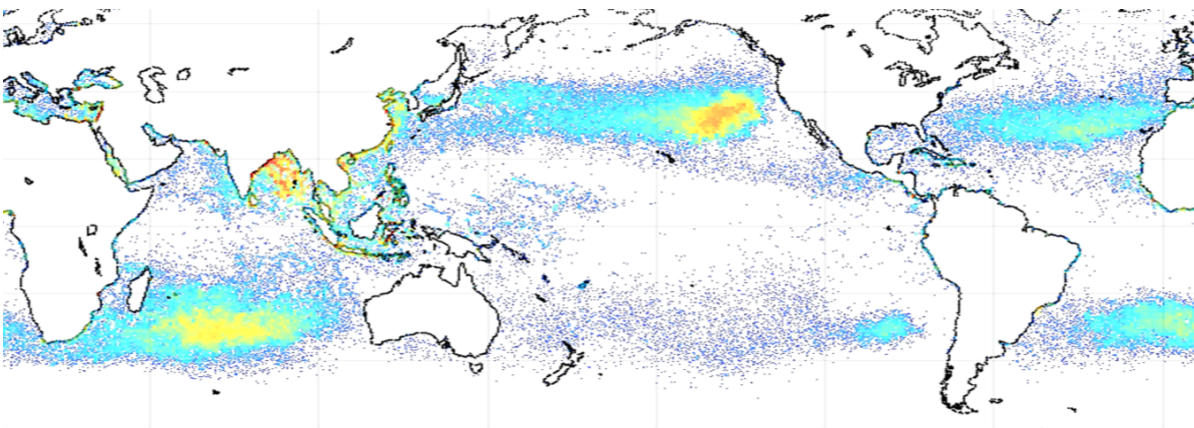


Figure 1.1: The Gyres

This circular pattern sparked Boyan Slat's (founder of the Ocean Cleanup) vision to position a V-shaped barrier in the outer edge of the flow pattern, thereby passively collecting all plastic present in that flow. The area with the highest concentration and total mass of plastic, being the North Pacific Gyres, was subsequently selected to be the first intended location for an Ocean Cleanup plastic catching system (30 N, 138 W). The intended barrier, which can be seen in Figure 1.2, has a length of more than 100 kilometers, and has a screen of 2 meters below the waterline. Which is, according to several physical experiments performed by the Ocean Cleanup, deep enough to ensure that every plastic particle is caught. The barrier would have to be moored in a specific high plastic concentration area within the patch, and directed with the 'open' side towards the mean current direction. The plastic would then be concentrated in a single area, extracted, stored, and eventually transported back to shore for recycling.

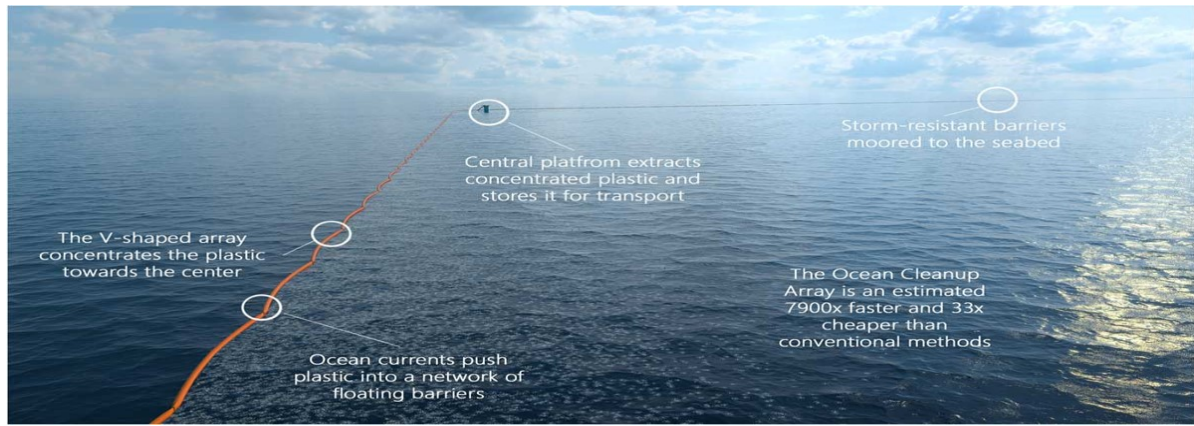


Figure 1.2: The Ocean Cleanup barrier

However, more recent studies performed by the Ocean Cleanup show that the current does not flow in a circular pattern on the scale of the barrier. Although the barrier would be the longest floating structure ever build, it is still 'small' in comparison to the size of the North Pacific Gyre. What on a large scale appeared to be a slow rotating current, proved to be a flow pattern with many vortices on a smaller scale. Simulations have shown that due to these vortices the efficiency of the fixed barrier is drastically lower than expected. Figure 1.3 shows a simulation of the fixed barrier at the intended deployment locations. Whereas at one moment in time the barrier concentrates the plastic (Figure 1.3a), at another moment the plastic flows out of the concentration area (Figure 1.3b), and all plastic is lost. In situation in Figure 1.3a) the current is coming from the left as intended and the plastic is concentrated. However in Figure 1.3b) the current is coming from the right, being the 'closed' side, and cannot be concentrated.

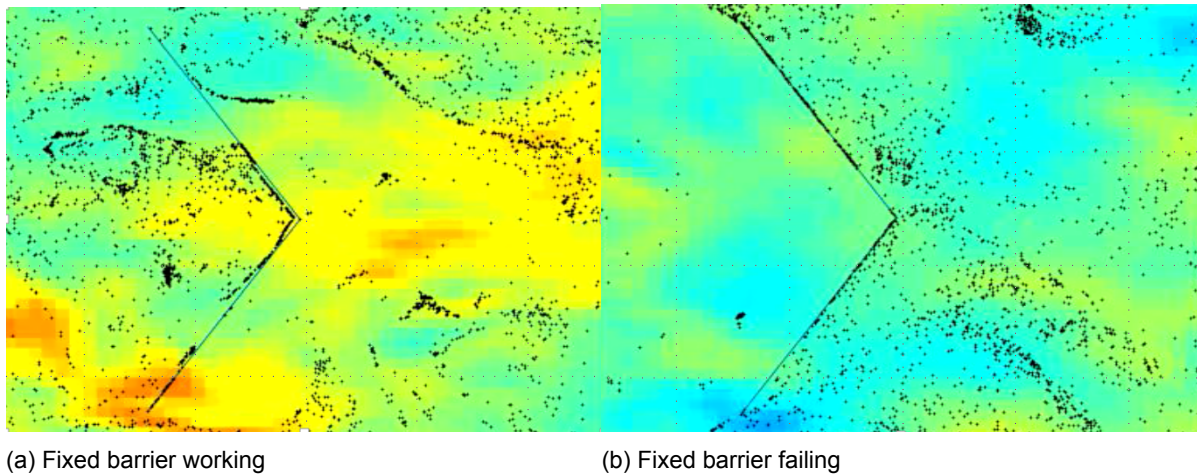


Figure 1.3: Fixed barrier in different current directions

These findings, in combination with the projections of the huge mooring costs involved in installing the barrier in water depths of around 4500 km, led to the decision that it would be appropriate to start a research into alternative cleaning systems.

## 1.2. Thesis objectives

The masters thesis presented herein, is the very first step by Ocean Cleanup towards designing a alternative ocean cleanup system. Since an alternative system could either be moored or mobile, the decision was made by the Ocean Cleanup to have this thesis focus on a mobile system, and that the organization would internally develop moored alternatives. Furthermore, the objective was narrowed by focusing on North Pacific Ocean, and on catching the actual plastic. The main objective of this thesis therefor became:

**To develop a conceptual design of a mobile Great Pacific Garbage Patch plastic catching system.**

The objective on itself was still extremely broad since there were no boundaries to the design at the start of the research. Meaning that, according to the book Engineering Design [32], the task at hand needed to be clarified first. However to be able to do so, significant research resources had to be contributed to defining a list of requirements, or in this thesis called: the system value drivers. Through a process of several brainstorm sessions and discussions with the Ocean Cleanup, the Value Drivers were defined as in Figure 1.4.

Inspirational	Low environmental impact	Efficiency	Scalability	Low CAPEX & OPEX	Short timeline to 'First plastic'
<ul style="list-style-type: none"> <li>• For funding</li> <li>• For attention</li> <li>• For motivation</li> </ul>	<ul style="list-style-type: none"> <li>• During production</li> <li>• During installation</li> <li>• During operation</li> <li>• During decommission</li> </ul>	<ul style="list-style-type: none"> <li>• In plastic/week</li> <li>• In retention</li> <li>• In use of material</li> <li>• In use of personnel</li> </ul>	<ul style="list-style-type: none"> <li>• In numbers</li> <li>• In size</li> <li>• In locations</li> </ul>	<ul style="list-style-type: none"> <li>• Of the shelfe</li> <li>• Minimal maintenance</li> <li>• High survivability</li> <li>• Easy logistics</li> </ul>	<ul style="list-style-type: none"> <li>• Technology readiness</li> <li>• Fast construction</li> <li>• Fast installation</li> <li>• 'Obeyes' maritime law</li> </ul>

Figure 1.4: The Ocean Cleanup Value Drivers

The value drivers are depicted in order of importance from left to right. With the first value driver being 'Inspirational'. The Ocean Cleanup is completely dependent on funding and publicity, therefor it was deemed of the utmost importance that a system would be developed that could enable support by the general public. Secondly the system would need to be completely environmentally friendly since the goal of the Ocean Cleanup is to improve the environment. Thirdly the system would have to be efficient in all of its aspects. Fourth, the system would have to be scalable to other locations around the world, but mostly in numbers or size. This would ensure that a small system could be tested and if proven to work, could be expended. The fifth value driver is low CAPEX&OPEX since funding is limited. And the sixth and last value driver being 'short timeline to first plastic'. Which is needed to prove, as fast as possible, that the system works, without loosing media attention and investors. Besides these value drivers one major requirements was introduced, for the overall and final concept comparison. Being that: the complete system implementation, meaning one or more systems, should lead to a 50% reduction of plastic volume in the Great-Pacific-Garbage-Patch, within 10 years. Based on this final criteria, concepts that would be low costs, low efficiency, but of which many could be implemented, could be compared to highly efficient, high cost systems.



### 1.3. Research approach

To fulfill the stated objectives a thorough research approach was set-up. The approach needed to enable creativity and efficiency at the same time, due to the highly innovative and ambitious objective of conceptual designing a mobile plastic catching system. As a baseline for the approach, research by Gerhard Pahl and Wolfgang Beitz, presented in the book Engineering design, was used [32]. The process of performing a conceptual design, described in this book, was considered to be appropriate, however some adaptations needed to be made.

According to the author the first step of a conceptual design is to ask the following questions:

- Has the task been clarified sufficiently to allow the development of a solution in the form of a design?
- Is a conceptual elaboration really needed, or do known solutions permit direct progress to the embodiment and detail design phases?
- If the conceptual stage is indispensable, how and to what extent should it be developed systematically?

If the answer to all questions could be answered in favor of a conceptual design, the research could continue to the next step. The formulation of the system Value Drivers, presented in section 1.2, followed from the first question. Whereas the second and the third question were respectively answered with, yes it is needed since no comparable systems exist, and the design needs to be developed creatively since out of the box solutions are required. Subsequently, the list of requirements, or in this thesis called the Value Drivers, was used as input for the following steps. Whereby step 7 and 8 were not performed since only one conceptual design could be made and evaluated in this thesis.

#### 1. Abstract to identify the essential problems

- Define the actual problem to be solved, independent of possible solutions

#### 2. Establish functions structures, Overall functions-sub functions

- The neutral and abstract overall system function needs to be defined
- Sub-functions which are necessary to fulfill the overall function need to be defined

#### 3. Search for working principles that fulfill the sub functions

- Determine the physical methods that can be used to fulfill the sub-functions

#### 4. Combine working principles into working structures

- Select appropriate combinations of physical methods to fulfill the sub-functions

#### 5. Select suitable combinations

- Select the most suitable combinations defined in the previous step

#### 6. Firm up into principle solution variants

- Get a thorough understanding of the actual behavior and feasibility of combinations

#### 7. Evaluate variants against technical and economic criteria

- Define which concepts are best performing

#### 8. Principle solution

- Concept is chosen

## 1.4. Work structure

### Step 1

Following this process the first step was to further abstract the problem. Besides the Value Drivers, it was unclear at the time, with what kind of conditions the concept would have the coop. These conditions were therefore analyzed and are discussed in part 1, chapter 2. Where the current, wind and wave conditions are analyzed in section 1 and the actual plastic distribution and concentrations are discussed in section 2.

### Step 2-5

The solution space of a possible system was subsequently investigated according to steps 2-5, in which the working principles were not considered to be physical effects but considered to be strategies (Part 1, chapter 3). At step 5 a strategy was chosen based on the value drivers (section 3.3), after which the process continued to step 2 for the development of strategy specific concepts (chapter 4). The steps 2-5 were subsequently performed and a high level most promising concept was selected in step 5 (part 1, chapter 4).

### Step 6

Step 6 has been approached in three different ways, of which 1 is an experimental approach and the latter two are successive phases of concept analyzes with a three-dimensional numerical tool. In an early phase of the research the opportunity arose to participate in a HYDRALAB+ experimental test program. In order to participate in this program a proposal was written based on two concepts that were at the time deemed most promising. One of the concepts was intended to be tested qualitatively whereas the other was deemed to be tested for the determination of hydrodynamic coefficients. The program can be read in part 2, chapter 5. As for the numerical analyzes the research was divided into two parts of which the first focused on the design and analysis of a critical component of the most proposing concept, being a sea-anchor/rudder (part 3, chapter 6, 7, and 8). Chapter 6 gives a literature overview of research into current following drogues that are used for meteorological research. After which the construction of the three-dimensional numerical model is explained in chapter 7. Subsequently, the model is partially validated in chapter 8.1 by comparing the results to experimental test results[43], and a suitable sea-anchor is designed in chapter 8.2. In part 4, chapter 9 the test cases for assessing concept feasibility are defined and the three-dimensional model of the complete system is discussed. In chapter 10, the thesis describes the design and evaluation of all concept variations of the concept selected in chapter 4. Whereby the chapter finishes with the proposal of two new concepts, based on the lessons learned.

The thesis is finalized in part 5 with a discussion and conclusion in respectively chapter 11 and 12. The discussion is gives a critical overview of the approach, assumptions and justifications. Whereas the conclusion elaborates on the accomplishment of the research objective and the recommendation of additional research.

## 1.5. Contribution to the body of knowledge

The research presented in this thesis provides a very structured overview of the combination of innovative and a scientifically substantiated conceptual design process. This innovative process leads to the design, and construction of a three-dimensional model of a system that has not been discussed in any other research up to the moment of writing. Thereby the thesis is the first research to shed light on the design of a floating structure that is passively controlled by sea-anchors. It shows that in the North Pacific Ocean such a system can only function when designed such that it can always recover from any failures in its function. Besides that it indicates that any passive cleanup system should have a rigid structure. Furthermore, the thesis provides a partially validated numerical tool of a meteorological drogue that has not been investigated for the past 20 years. Whereby an analysis with the tool shows interesting dependency of the drogues performance on line tension. Next to this, a one-degree of freedom system of a vertically hinged flat plate in a uniform flow, indicates that the Window-Shade Drogue can maintain static stability during any straight tow, without the introduction of torsional stiffness, but that a specific amount of structural damping is needed to prevent dynamic instability. With respect to the design of a sea-anchor for passive control the research shows that a flexibly constraint anchor for lift generation can always fail due to its tendency to stream parallel to the apparent current direction, which is an unstable position. All in all, this thesis contributes to the body of knowledge on three levels: it provides insight into an innovative conceptual design process, it provides a numerical tool for analyzing meteorological drogues and sea-anchors, and it shows that a passive and flexible plastic catching system is unable to follow a rotating current.

# **Part I**

## **Concept generation**





# 2

## Operating conditions

The intended location for a fixed moored barrier was based on the combination of the mean plastic catching concentration and water depth. However, the optimal location for a mobile system is uninfluenced by the water depth and can be varied to constantly maintain a position in a high plastic concentration area. Nevertheless, for the investigation of environmental loads, and plastic concentration, the originally intended installation location is used. Which is at 30 N, 138 W at about 1000 nautical miles west of Los Angeles, with a water depth of approximately 4000 meters. The following chapter is intended to give a thorough overview of the weather conditions and the implications that these conditions might have on a permanently moored Ocean Cleanup barrier system versus a mobile system. All figures and tables in section 2.1 are provided by Metocean Solutions.

### 2.1. Environmental forcing

#### 2.1.1. Current

The current profile was originally thought to flow in circular pattern. However, according to a desktop study by Metocean Solutions the current direction at the intended location is very diverse. The plastic was thought to be rotating within the Gyres but instead it converges in the 'eye of the gyres' where the current has a mean velocity of 0,09 m/s. The annual surface non-tidal current rose plot in Figure 2.1a shows currents in the 'going to' directional reference, according to oceanographic directional conventions. From this plot it is clear that any cleanup system should be able to catch plastic from any direction. There is a dominant flow to the North-West but if the system would be fixed to catch plastic flowing in that direction, the overall efficiency would be very low. Furthermore, the maximum monthly current velocity is between 0.3 and 0.6 m/s according to Metocean Solutions, but has a median of 0.17 m/s. Which indicates that any system would have to coop with a reasonably low current velocity.

#### 2.1.2. Tidal

The tidal rose plot in Figure 2.1b ('going to' direction) shows a maximum tidal current of 0.03 m/s. Indicating that the tidal current will be of practically no influence on a mobile system. However, since the 10th percentile surface current velocity is around 0.06 m/s, the tidal currents will be of importance 10% of the time.

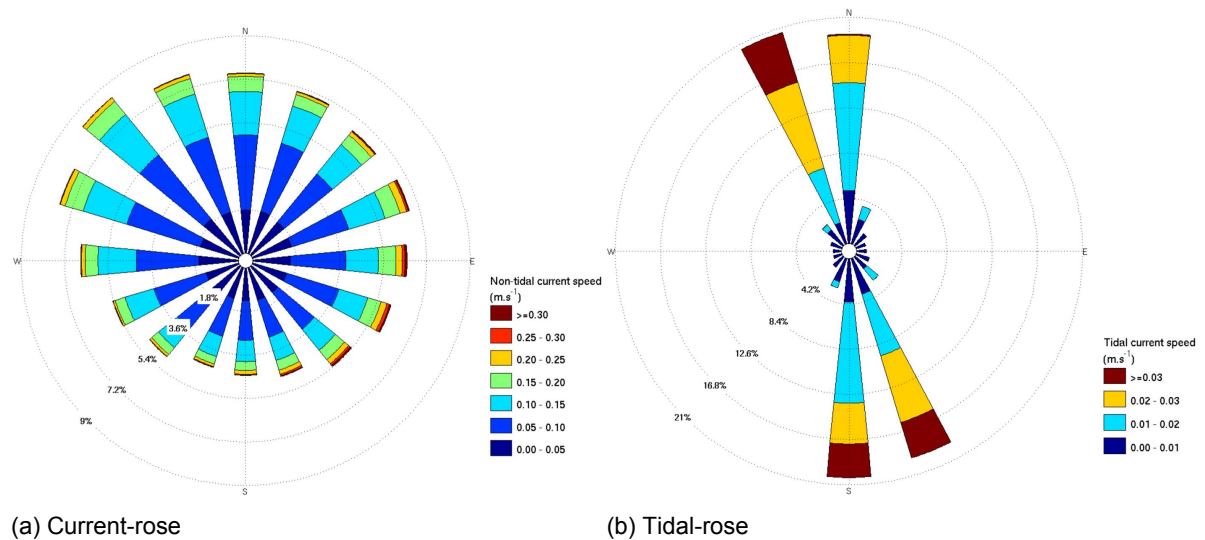


Figure 2.1: Annual non-tidal surface current and tidal surface current, by Metocean Solutions

### 2.1.3. Wind

The wind is predominately coming from the North-East, with a low but present directional variability in all directions. However, during winter the directional variability increases, leading to frequent strong winds coming from the South-(West) (**Appendix**). The annual and seasonal wind roses (Figure 2.2a) show winds in the ‘coming from’ directional reference, according to directional conventions. According to Metocean Solutions the annual mean wind speed is 6.4 m/s, while Wind speeds exceeding 12 m/s can occur throughout the year. Besides that, wind direction can change very suddenly which implies that a mobile system needs to be able to resist sudden changes in wind direction and speed, as to retain optimal plastic catching efficiency and prevent damage. Furthermore, the high wind speeds from predominantly the North-East could theoretically be used to propel a wind driven cleaning system, or could be used to generate energy for propulsion.

### 2.1.4. Waves

The wave rose plot in Figure 2.2b and the density plot in Figure 2.3b show that waves are predominately coming from the North-West, with a period of 12-14 seconds. Furthermore, Figure 2.3a indicates that these waves mostly have a significant wave height of around 2 meters, but can also have significant wave heights of around 7 meters. These long waves of reasonable height indicate that any mobile plastic catching system will have to operate in benign day to day conditions, and that wave propulsion could be used.

### 2.1.5. Extreme statistics

With respect to the extreme conditions that a mobile system will have to cope with, Metocean Solutions provided tables regarding the 1,10,100 and 1000 year return periods. According to Ship and Offshore structures XIX [39], a return period of around 20/25 years is taken into account during the design process of ships. However, it is also indicated that for offshore structure usually a return period of 100 and sometimes even a 10000 years is taken into account. Since the objective of this thesis is to make a conceptual design of a mobile system, one could regard it as a ship. However, depending on the type of mobile system to be designed, and the expected lifetime and deployment time, the system could also be regarded as an offshore structure. For that reason Figure 2.1 shows the 100 year return period. Whereby one has to consider that the total cleanup operation is expected to take 10 years. The probability of encountering the 100 year return period conditions are therefore:

$$p = (1 - \exp(\frac{-L}{T})) = (1 - \exp(\frac{-10}{100})) = 0.0952 \quad (2.1)$$

Where,  $p$  is the probability of encounter,  $L$  is the lifetime and  $T$  is the return period.

The provided data indicates that there is a 10% change that the mobile system will encounter winds of ....., waves off ....., and currents of, ....., Meaning that the current maximum is apparently not above the monthly maximum, but that maximum significant wave height and wind speed are around twice as high as the yearly maximum.

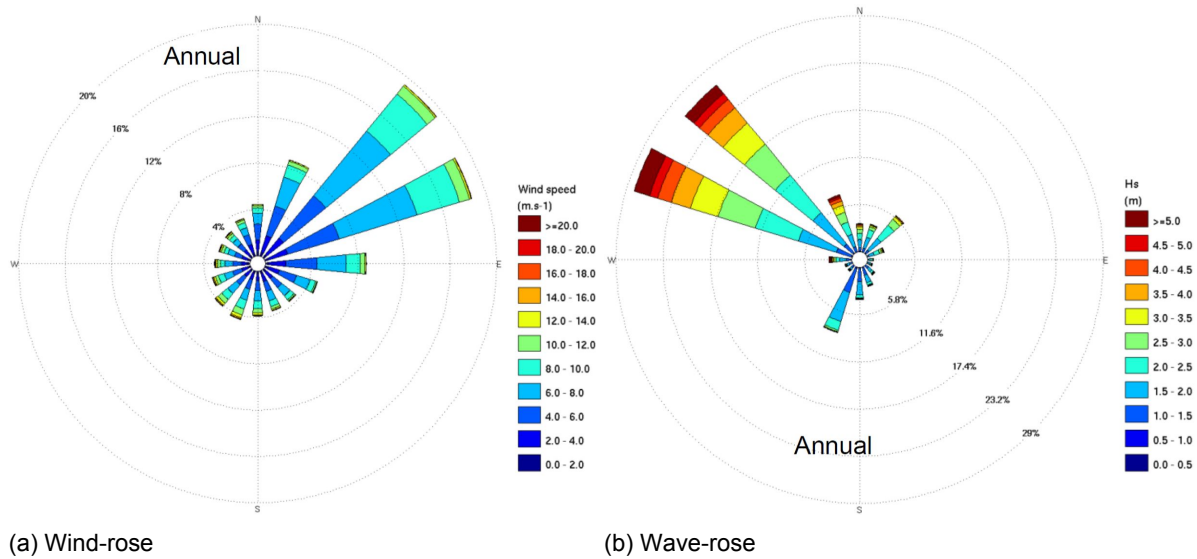


Figure 2.2: Annual wave and wave conditions, by Metocean Solutions

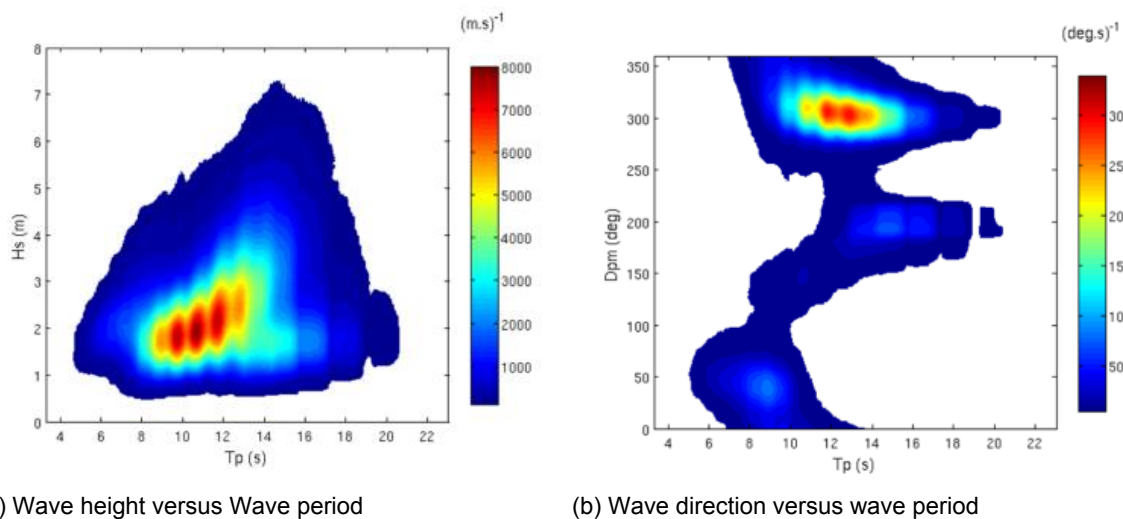


Figure 2.3: Annual densityplots, by Metocean Solutions

Table 2.1: 100-year extreme values, by Metocean Solutions

100-year return period	Symbol	Units	Direction from (degT)								Omni
			337.5-22.5	22.5-67.5	67.5-112.5	112.5-157.5	157.5-202.5	202.5-247.5	247.5-292.5	292.5-337.5	
10-min averaged wind speed	$U_{10min}$	m.s <sup>-1</sup>	16.56	16.13	16.92	17.62	21.78	21.76	20.57	17.95	25.25
Significant wave height	$H_s$	m	7.58	5.22	-	5.18	5.51	-	14.87	12.41	13.84
Spectral peak wave period	$T_p$	s	15.82	10.46	-	9.90	14.02	-	20.76	21.16	21.74
Maximum wave height	$H_{max}$	m	15.41	11.74	-	11.05	10.73	-	27.02	23.09	26.96
Maximum wave crest	$C_{max}$	m	8.21	6.14	-	5.78	5.61	-	15.36	12.67	15.18
Non-tidal surface current speed	$U_{so}$	m.s <sup>-1</sup>	0.30	0.37	0.44	-	-	-	0.28	0.32	0.58

## 2.2. Plastic

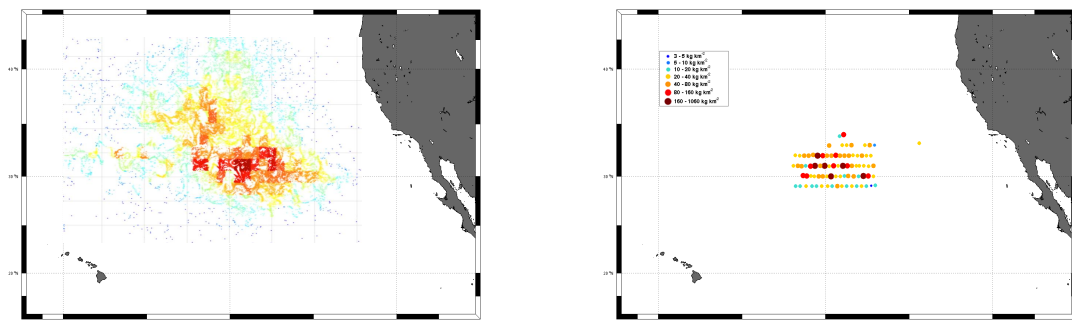
The overall goal of The Ocean Cleanup is to remove plastic debris from the ocean. In order to come up with a good strategy, a basic understanding of the plastic behavior is needed. This section discusses the concentration, mass distribution, vertical distribution, and buoyancy of the plastic, since all these aspect influence the possible catching strategies.

### 2.2.1. Release

The release of plastic determines the type of plastic present in the great pacific garbage patch, and could thereby influence the the type of screen and barrier needed to catch the plastic. Plastic is released from either land based or marine sources. It is estimated that over 80% of the plastic debris within the oceans originates from land based sources. The remaining 20% is marine based debris containing large fishing nets or otherwise called 'ghost nets', buoys, etc [22]. Thereby, the influence of environmental disasters such as tsunami's and hurricanes is considered to be small. The type of plastic released can therefor be very different and a system should be able to catch all types of plastic.

### 2.2.2. Concentration

Within the Great Pacific Garbage Patch (GPGP), which is an area of around 1000 x 1000 km, there is a large difference in the absolute concentration. It can be stated that when looking on a global level the GPGP is an area of high plastic concentration. However, in this area there are higher concentrations as well. Even on the scale of a 100 km barrier the plastic is widely dispersed. Figure 2.4 shows this wide dispersion, where Figure 2.4a is based on a numerical model produced by the Ocean Cleanup, and Figure 2.4b is based on data gathered during the Ocean Cleanup Mega expedition. The average concentration was found to be 60 kg/km<sup>2</sup>, however the concentration depending on the location might be a factor X higher.



(a) Plastic concentration model by the Ocean Cleanup (b) Plastic collected during Mega Expedition

Figure 2.4: Concentration of plastic in the GPGP, by the Ocean Cleanup

### 2.2.3. Size and mass distribution

The major part of the plastic garbage consists out of particles larger than 10 cm [34]. Within this distribution, ghost's nets are included, which make up almost all of the debris size larger than 50 cm and which make up 80% of the total plastic mass. However since the concentration of ghost's nets is low, they will most likely need to be removed by a different dedicated system. Therefore it is assumed that most of the plastic mass caught by the mobile barrier will be in the 10-50 cm size range. When looking at the number of particles the concentration is dominated by the smaller pieces, so called micro plastics. To be able to catch these micro plastics the screen is required to be completely sealed.

### 2.2.4. Vertical distribution

The plastic pieces floating in the ocean are vertically distributed across the first meters of the water column. The mass of plastic decays faster with depth than the number of pieces. This is explained by the increased buoyancy of larger pieces, which dominate the mass of plastic, and therefore have higher rising velocity. These pieces will subsequently be at the surface of the ocean. Turbulence in the top layer of the ocean mixes buoyant particles. Wind and waves influence this turbulence, therefore the amount of mixing that takes place is dependent on the sea state and wind conditions[21].

### 2.2.5. Buoyancy

The average density of surface plastic debris is found to be  $965 \text{ kg/m}^3$  [21]. The low density particles have an effective area above the water surface, making them vulnerable to wind. In general, during beach clean-ups the major part of the collected debris consist out of lightweight plastic compounds. Furthermore, large quantities of lightweight plastic are found on the shoreline of Alaska, and during the Ocean Cleanup Mega expedition the collected debris primarily consisted out of low buoyant material. Consequently, it is assumed that, lightweight wind-driven plastic will not be collect in the GPGP, and the Ocean cleanup barrier should be designed for current driven plastic.

Another aspect of plastic buoyancy that needs to be taken into consideration for design purposes, is the rising velocity. Recent tests pointed out that the rising velocity fluctuates significantly between plastic debris type, but indicate that a screen of approximately 2 meters under the waterline, should be enough to prevent the plastic from being transported under the barrier[16]. However, trial tests with the prototype in the North Sea indicate the plastic passes under a barrier with a screen of only 2 meters deep at a current velocity of 0.5 m/s. Additional test with respect to plastic buoyancy therefore have to be executed. For this thesis a screen of 2 meter below the waterline is assumed.



# 3

## Strategy formulation

The second step after understanding the operating conditions was to define cleaning strategies that could be used to clean the North Pacific Garbage Patch. These strategies are high level approaches which differ significantly in their method of 'catching' the plastic. Within the conceptual design process discussed in Engineering Design [32], the strategies defined here would be considered as complete working structures, and the specific elements within these strategies as working principles.

In this section the strategy formulation process will first be discussed, after which the strategies are evaluated on a high level, taking the working principles into consideration. This approach, in which the strategies are defined before their working principles are analyzed, is in this case applicable since strategies can be defined without specific knowledge on the underlying working principles. However, the feasibility of the strategies does depend on their working principles.

### 3.1. Idea generation

Innovative idea generation can be done in numerous ways, where there has been made a distinction between intuitive and logical methods. With intuitive methods being the stimulation of the unconscious thought process to come up with unstructured but innovative solutions, and logical methods being a structured process such as problem decomposition [38].

The Authors of 'Evaluation of Idea Generation Methods for Conceptual Design', Jami J. Shah, Santosh V. Kulkarni and Noe Vargas-Hernandez, subsequently make a distinction between Germinal, Transformational, Progressive, Organizational, and Hybrid conceptual designs, where Germinal design focuses on the development of a completely new product.

Within Germinal design there are methods such as Morphological Analysis [47], Brainstorming [19], and the K-J Method [17], that can be used for idea generation. For this thesis it was appropriate to make use of brainstorming as the main idea generation method. If brainstorming is properly executed the knowledge of experts from different areas can be combined, and an innovative environment can be established. Both of which were thought to be necessary for the complicated objective of designing a mobile Ocean Cleanup system. However it needs to be emphasized that the final formalized strategies do not form a collectively exhaustive overview of all the possibilities. Which is inherent to a innovative conceptual design process.

As part of this thesis a Brainstorm session was organized at Bluewater b.v. During this Brainstorm session 9 professionals with various backgrounds attended. The Brainstorm session was organized as to stimulate creativity using the step-wise program see in Figure 3.1.

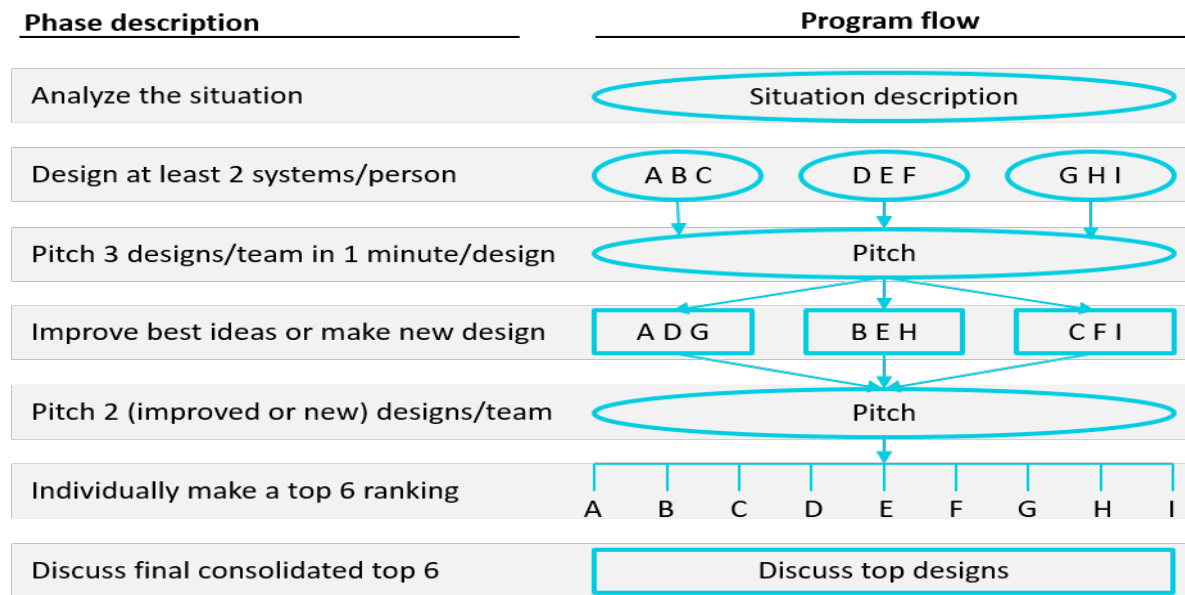


Figure 3.1: Brainstorm program

## 3.2. Proposed strategies

During the Brainstorm a wide variety of cleaning strategies came forward, which could be combined into the cleaning strategies depicted in Figure 3.2.

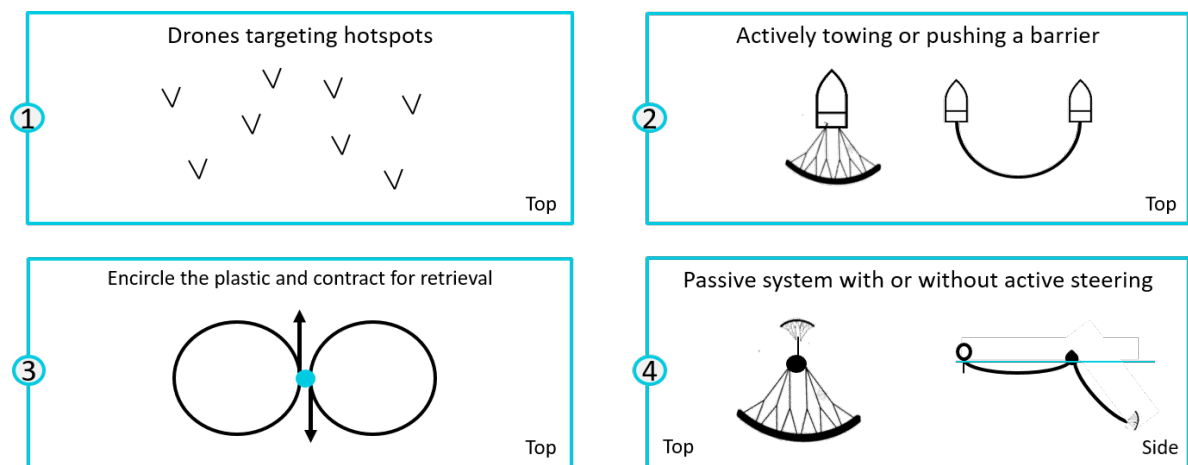


Figure 3.2: Strategy overview

The strategies defined during the brainstorm have been analyzed on a high level and the major pros and cons have been determined based on the value drivers. Thereby acknowledging the fact that all strategies would need to clean 50% of the North-Pacific-Garbage-Patch in 10 years. Which means that all strategies are considered to have a similar cleaning rate, and that the number of systems needed for a specific strategy has to be chosen such that this cleaning rate can be met. Furthermore, since the inspirational and environmental value driver are of up-most importance, it was decided in collaboration with the Ocean Cleanup, that any system would have to be driven by renewable energy/propulsion sources.



### 3.2.1. Drones targeting hotspots

The first strategy to be proposed was the use of drones, deployed from consecutively larger ships (ship in ship in ship), to clean the high density areas. After the drone storage area would be filled it would return to the 'motherships' for plastic extraction.

Main advantages:

1. Drones can be considered to be very inspirational in the year of writing
2. Drones would be very material efficient, meaning that a small number of systems could be used
3. No offshore personnel would be required which would reduce costs and improve safety

Main disadvantages:

1. Drones would have a low technology readiness
2. Drones would be expensive to produce

### 3.2.2. Actively towing or pushing a barrier

The second strategy is to simply use a conventional sailing ship or any other ship with renewable propulsion/energy sources, to tow or push a large barrier through the water and thereby collect all the plastic along the way.

Main advantages:

1. The technology would be ready tomorrow when existing sailing boats or boats with kites are used to tow the barrier
2. The system behavior is known and proven to work since oil spill barriers are deployed behind ships

Main disadvantages:

1. Offshore personnel is needed (otherwise considered to be a drone), which would result in high OPEX
2. The system can be considered not-inspirational according to the Ocean Cleanup
3. Acquiring sufficient ships is presumed to result in high CAPEX
4. If specially designed ships are necessary, the time to first plastic will rise and CAPEX will rise considerably

### 3.2.3. Encircle plastic and contract

The third strategy is to use mechanical contraction to collect the plastic. With this strategy low amounts of energy would be necessary since there would be no efficiency losses due to the propeller/water interaction. A very large flexible barrier would have to be positioned in a circle around the plastic, after which the deployment ship leaves and the system will slowly contract the plastic into a small area, from which it can subsequently be extracted.

Main advantages:

1. This strategy was considered to be inspirational by the Ocean Cleanup
2. Low energy consumption and therefore great for the environment and CAPEX
3. No offshore personnel required for long periods

Main disadvantages:

1. Unproven technology with respect to development, production, and working principle. Resulting in high CAPEX, and long time-line to first plastic
2. Needs to be redeployed every time the system has contracted the plastic, which would result in high OPEX

### 3.2.4. Passive system with sea-anchor

The fourth and final strategy to be considered plausible, was the use of a sea-anchor to benefit from the difference in ocean currents at different depths. Deploying an anchor from a passive barrier system could reasonably slow down the system to a required catching speed. Plastic could be concentrated automatically and would need to be extracted in intervals, depending on the plastic retention method.

Main advantages:

1. The strategy is considered to be very inspirational by the Ocean Cleanup since it fulfills the company vision: let the oceans clean themselves
2. The strategy could result in a relatively low CAPEX and OPEX solution, respectively depending on the system design and extraction interval
3. If one system can be proven to work, the technology can be easily scaled in numbers or in size

Main disadvantages:

1. The strategy has a low technology readiness what could result in high CAPEX and long time line to first plastic
2. Plastic extraction could result in high OPEX depending on the plastic retention system
3. System could drift into shipping lanes, causing high additional OPEX

### 3.3. Strategy selection

For the evaluation of the defined strategies the value drivers were analyzed and compared to the value delivered by the strategies. Structured this resulted in a multi-criteria analysis (MCA). The value drivers and their ranking, are respectively converted into evaluation criteria and weighting. In turn the strategies were judged qualitatively with a ++ to – score. The scoring itself was based on engineering experience in collaboration with various experts, and on a qualitative research into feasibility of the proposed strategies. Which are included into the pros and cons of the previous section. The results from the multi-criteria analyses can be seen in Figure 3.3.

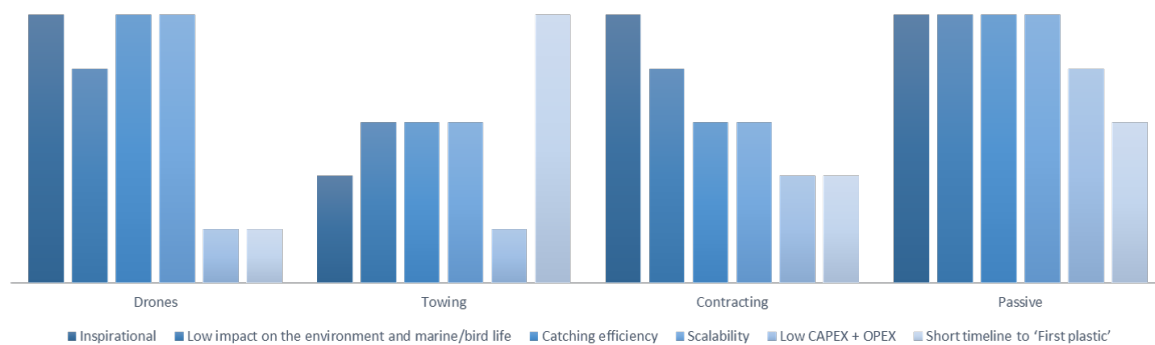


Figure 3.3: Strategy MCA scoring

The MCA output clearly shows that the passive strategy scores highest on all the ocean cleanup value drivers. First, the strategy is considered to be extremely inspirational as it follows the vision of the ocean cleanup, being: "let the oceans clean themselves". Second, it has low impact on the environment, because theoretically no active propulsion is needed, limiting the need for fuel or batteries. Thirdly, from the first plastic drifting simulations performed by the Ocean Cleanup, the passive strategy seems to be even more efficient than a fixed barrier. Fourth, the strategy is highly scalable in numbers, due to its presumed relatively low costs. Fifth, the sum of capital and operational costs is presumed to be lower than all other strategies, since no fuel is needed, maintenance necessity is lower since there are no active components, material costs are relatively low, and there is no need for offshore personnel other than the personnel needed during the extraction intervals. And last but not least, the requirement of a short timeline to first plastic is considered to be feasible.

All in all the main reason for the selection of the passive strategy was the vision of the ocean cleanup. The Ocean Cleanup is fully depended on funding from investors and individuals, and an inspirational system is therefore extremely important. There are already a multitude of existing plans by other organizations to use special ships or drones to collect the plastic, and it is presumed that the current success of the Ocean Cleanup is related to its passive cleanup strategy.



## Concept formulation

The strategy specific concepts, related to the chosen strategy, could be designed in many ways. To make a thorough analysis of the possible concepts, a morphological matrix was used, as described in Engineering Design [32] (See Figure 4.1).

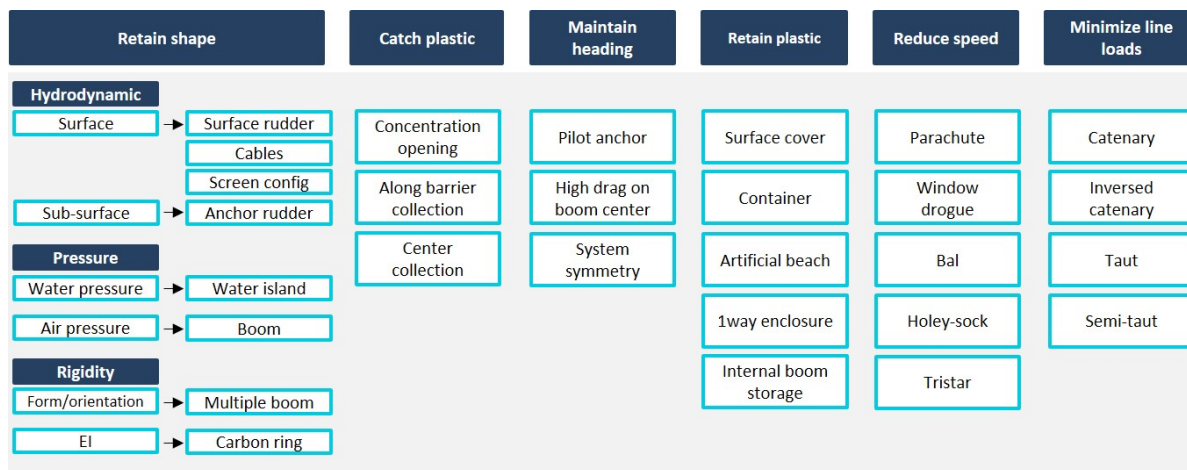


Figure 4.1: Morphological overview

The morphological matrix used here is specially designed and shows the sub-functions of the passive strategy on the horizontal axis, and possible solution principles to those sub-functions in the rows below. The solution principles of those sub-functions are derived from the related risks. However, in order to assess those risks, additional research into current profile over the water depth was needed, and a base case needed to be proposed. It has to be noted that the plastic extraction method is not specifically taken into consideration for the system design. Extraction can be executed in numerous ways, and can be adopted to the system design. On the other hand, the retention of plastic is taken into consideration, since this can influence the system design.

## 4.1. Base case

### 4.1.1. Relative current

The current profile in the North-Pacific-Garbage-Patch is of vital importance to the passive cleaning strategy. It determines the ability to slow down the system, and it is the primary driver behind the system trajectory. The strength of the surface current was already investigated in chapter 2, however up to this point in the research, the exact velocity profile over the depth was unknown. The information required to determine these variables, was found in the HYbrid Coordinate Ocean Model (HYCOM). Analyzing the data from several coordinates around the intended deployment location led to current profile seen in Figure 4.2. The figure indicates that the current velocity drops with almost 50% over the first 100 meters. Which shows that the use of a sea-anchor would be definitely plausible, depending on the required speed reduction. However, the direction of the current was also found to vary over the depth. Figure 4.2b one can see the difference in direction between the surface current and the current at -150 meters, over the year 2012. The high variability indicates that any system would have to coop with a difference in direction as well as speed, over the depth.

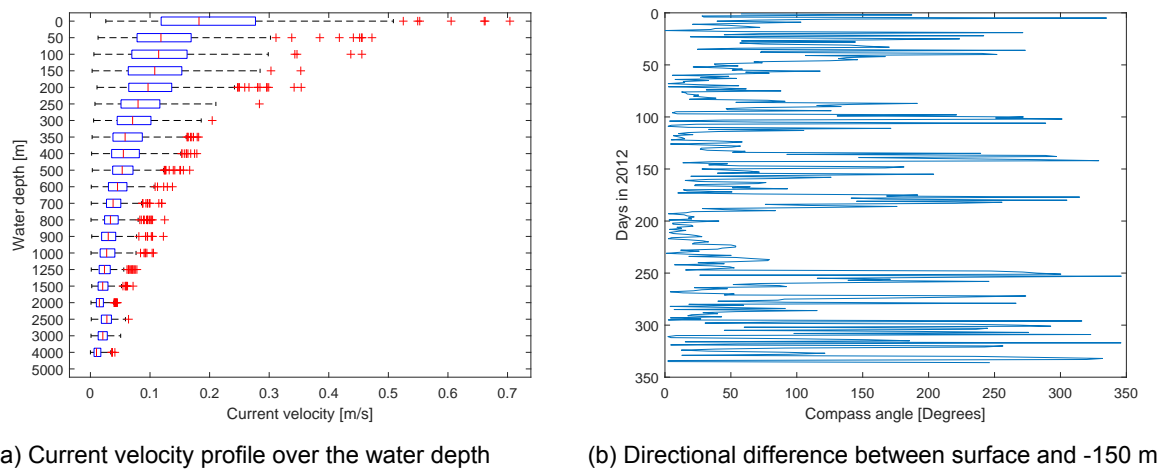


Figure 4.2: Current velocity profile and difference in current direction over the year 2012

### 4.1.2. Size

The required speed reduction primarily determined the estimated force needed in the opposite direction of the system movement and the required force needed to open the barrier. Since the barrier would collapse if no 'opening force' is applied, due to the current flowing against and under the barrier, and not around it. The required reduction was determined to be 10%, which was in sharp contrast to the educated guess made earlier in the process, being that the highest reduction would result in the highest efficiency. However, according to several simulations done by the Ocean Cleanup, a 10% reduction would ensure that the system flows with the plastic and automatically flows into 'hotspot areas' (high concentration areas). Furthermore the required force is also influenced by the drag area of the barrier. It was therefor decided to take a base case barrier for comparison purposes. Where the original barrier was planned to be 100 km long, the smaller passive base case was set on 1km span width. Besides that the screen was taken to be 2 meters deep, since this was determined to be a sufficient height for the prevention of 'underspill' (loss of plastic due to plastic flowing under the barrier). Besides these major influences on the required force, the length of the barrier in relation to the constant span width of 1km, also influences the force since the drag force decreases with a decreasing angle of attack.

### 4.1.3. Risks

Subsequently the risks related to the passive cleaning strategy had to listed, in order to define the correct strategy sub-functions are related working principles.

#### Surface system:

- cannot maintain the intended shape in current, wind, and waves, which could cause:
  - loss of plastic
  - reduced span width of the catching opening
  - damaged due to scrambling
- is unable to follow a changing current direction while keeping the 'open' side perpendicular to the current
- has a barrier that does not precisely follow the waves, leading to high forces and possible plastic loss

#### Sea anchor system:

- would require a very large sea-anchor or a very deep anchor position, due to a depth current profile with low steepness
- causes the system to change it's heading due to a depth current in a different direction from the surface current
- cannot deliver a constant drag load

#### Mooring system:

- could experience shock-loading due to wave loads on the system in combination with high drag of the sea-anchor
- could get entangled in the highly dynamic environment

Furthermore, besides these risks, risks such as collisions, or entering a shipping lane are not taken into account for this thesis. These risks will be evaluated in a separate research. With as input the final proposed conceptual design form this thesis.

## 4.2. Working principles

### 4.2.1. Retaining shape

The shape stability of the system is the first and possibly the most difficult design aspect. Designing for shape stability has an effect on all value drivers, and the technology required is never been used on the scale of a mobile Ocean Cleanup barrier (1km span width). Furthermore, as discussed in the risk overview, the inability to retain shape can have serious consequences on the system performance. If the shape is lost plastic might be pushed out of the system by the barrier itself. The catching opening could be reduced to zero, which would practically render the system to be useless. Lastly, the loss of shape could damage the system and the system might not be able to return to it's intended shape.

Shape retainment can be created in several way's, but the principle of guaranteeing shape is to ensure a form of rigidity or constant tension exist in the system. However, enabling rigidity or more precisely, bending-stiffness, on this scale is extremely difficult, since length scales to the power of five in the formula for rigidity per unit mass. Considering a deflection  $\delta = \frac{\omega \cdot L^4}{8 \cdot E \cdot I}$  of a rod of length  $L$ , under a load per unit length  $\omega$ . Having a Young's modulus  $E$ , density  $\rho$ , and circular section of radius  $r$ , the formula for rigidity per unit mass is:

$$\Gamma = \frac{\omega \cdot \delta}{m} = \frac{8 \cdot E \cdot I}{L^4 \cdot m} = \frac{2 \cdot E \cdot r^2}{L^5 \cdot \rho} \quad (4.1)$$

Where,  $I = \frac{\pi \cdot r^4}{4}$  and  $m = \rho \cdot \pi \cdot r^2 \cdot L$ .

This strong dependency of rigidity on the length of the system causes significant difficulties. However, several methods of ensuring stability are proposed in the swimming-lane. Where there has been made a explicit difference between the use of the hydrodynamic force generated by a relative current velocity, the use of a rigid structure, and the use of pressure. Whereby the use of hydrodynamic force ensures there is tension in the system, leading to the retention of shape. The proposed methods of ensuring shape are:

## **Tension**

### **Surface rudder**

The barrier could be equipped with very large rudders to generate lift to open the system perpendicular to the current. However the amount of rudder area would have to be extremely large, since the relative velocity, which is preferred to be 10% of the surface current velocity, has a median around 0.017 m/s.

### **Cables**

The use of an almost infinite amount of cables could redirect the force on the barrier directly to the anchor. Which in turn would cause the system to open by water pressure alone. However, the large amount of lines could block the plastic inflow, reduce extraction options, and could be harmful for marine and bird life.

### **Screen configuration**

The use of screen that could act as a 'one-way-gate' could ensure that the system shape would be unaffected by a rotating current. Meaning that when the current turns around the system, it can pass through the barrier, inducing a very low drag force. However, in this configuration the plastic would have to be directly retained to ensure it doesn't flow out of the system.

### **Anchor rudder**

Rudder anchor is a theoretical sea-anchor, that can be oriented with an 'angle of attack' to the relative current direction. Orienting the anchors under the correct angle could deliver enough drag to slow down the system, and generate enough lift to open the barrier perpendicular to the current. Using Rudder anchors would be preferable to normal rudders since the relative velocity at anchor depth is significantly higher (depending on the anchor depth), which reduces the rudder anchor area needed for generating the required lift force. Thereby, since the rudders would function as both anchor and 'rudder', no other drag devices are needed. Besides this, the rudders could be completely decoupled from waves or other surface effects, thereby making them less sensitive to damage.

## **Pressure**

### **Water island**

Creating bending stiffness could also be enabled by exerting pressure in the opposing direction as the applied force. One way of introducing this pressure into a mobile cleanup system, is with a combination of water and air pressurized in a flat floating fabric. Figure 5.2 shows a schematic of this configuration, where water acts both as a method of increasing the weight of the system (to make it less sensitive to wind), and as a medium that pushes outward in the horizontal plane. Besides that, the air layer also acts as a medium for exerting outward force. When a load is introduced in the horizontal plane the air layer is either pushed up or down, which due to the buoyancy of the air layer results respectively in an upward reaction force when pushed down, and due to the weight of the water layer, results in a downward reaction force, when pushed upwards. The combination of the water and air, results in a



'water island' that could hold itself open perpendicular to the current. The question is how much force could be handled by such a water barrier. Furthermore, the dynamics of such a barrier would be very interesting. It should be noted that the 'water-island' has an infinite amount of lines since its fabric completely covers the area between anchor and barrier. For all solutions holds that when lines are introduced along the barrier system, forces could be directed to the anchor. Thereby reducing the amount of tension, pressure or rigidity needed to open the barrier.

### **High pressure barrier**

A high pressurized barrier could enable the system to stay open under a low relative current. However, the pressure would need to be very high. This type of rigidity would prevent the barrier from following the waves, leading to plastic loss and high forces in the barrier.

## **Rigidity**

### **Multiple barriers in the horizontal plane**

By binding multiple barriers behind each other, rigidity could be enabled in the horizontal plane, while the 'barrier' remains flexible in the vertical direction. The description of multiple barriers is one of the many configurations that are possible when enabling stiffness in the horizontal plane, but retain flexibility in the vertical plane.

### **Rigid pipe**

Another solution for introducing rigidity is by simply using a rigid material. The pipe could be submerged at 30 or 40 meters under the waterline, supported by buoys. A completely flexible barrier could then be connected between those buoys. Which would enable the barrier to precisely follow the waves.

## **4.2.2. Catch plastic**

The strategy function of catching plastic is of course the primary function but is closely related to the retention of shape. Any system covering a wide area could in theory be used to catch plastic. For this thesis there are however 3 specific methods presented, in which this theoretic structure or barrier could be used to catch plastic. The first method is by creating a concentration shape, such as the V shape proposed by Boyan Slat. If the 'open' side of this structure is directed perpendicular to an incoming plastic flow, the plastic is concentrated and can subsequently be extracted. The second method is to form a circle and allow plastic to enter this circle from any side of the structure, but prevent the plastic from leaving the circle. The third method is to collect the plastic at every point along the barrier by implementing a direct retention method.

## **4.2.3. Maintain heading**

The heading of the opening of the system is of high influence on the systems efficiency if a catching method of type one or three is used. As will be discussed in part 4, the efficiency decreases when the projected span width, perpendicular to the flow, decreases. If the systems cannot not follow a rotating current or the angle of the system with the current decreases, due to any type of irregularity, an efficiency drop could occur. The first proposed option to prevent the loss of a correct heading is a pilot anchor, which is a surface system with a high drag coefficient and a large submerged area, connected to the front of the mobile cleanup system. This arbitrary drag device could pull the system with the current direction. The second proposed option is to simply increase the drag area of the barrier screen in the 'tip' of the mobile cleaning system. The third option is to design the system in such a way that every side of the mobile cleaning system can act as the 'tip' and thereby enabling any side to act as a 'catching opening', e.g. a circular system such as presented as catching method two.

### 4.2.4. Plastic retention

A efficient retention method would limited the number of extractions per year, thereby reducing the cost for offshore extraction. Retention methods can vary from low-tech surface covers to prevent over-topping of the barrier in wave conditions, to fully enclosed containers in which the plastic can be automatically stored for a long period of time. Furthermore, innovative solutions such as a artificial beach (proposed by the Ocean Cleanup), internal barrier storage, and a '1-way-gate' principal are proposed, through which plastic is collected and retained. Figure 4.3.1 shows the working-principle of a surface cover, Figure 4.3.2 that of an artificial beach, Figure 4.3.3 shows the internal barrier storage, and Figure 4.3.4 the 1-way gate used in a circular catching system.

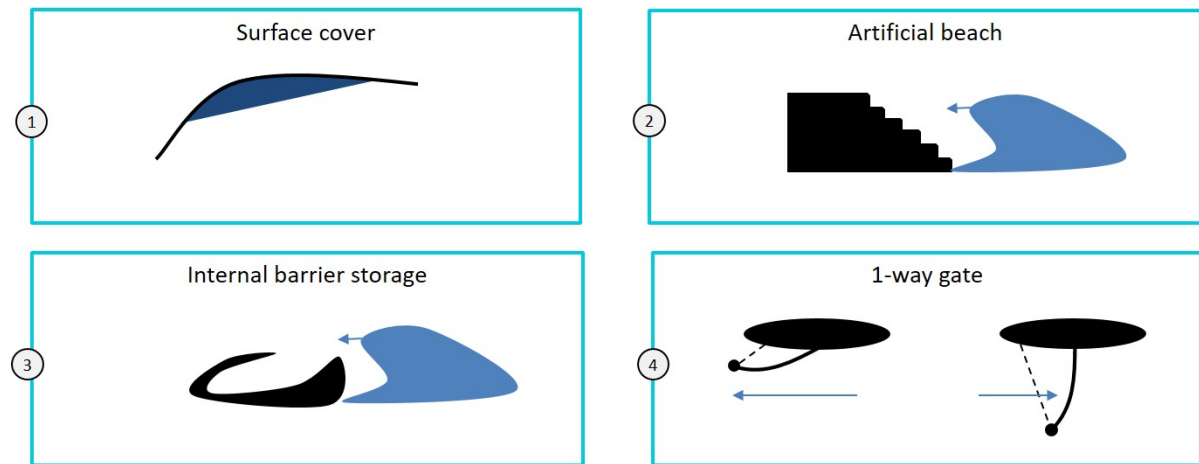


Figure 4.3: Proposed retention methods

### 4.2.5. Sea anchor

The sea anchor is one of the most critical components in all the possible concepts. For some concepts, drag in the opposite direction of the surface system movement will be sufficient, for others however, a specific lift force might be necessary to open the barrier. The design of a suitable sea anchor will be discussed in detail in chapter 6, 7, and 8. But several existing options are discussed in this section.

#### Parachute

The first type of sea-anchor is frequently used in the naval industry. When a boat is adrift in storm conditions, one can deploy these anchors from the bow, which will then pull the front of the ship into the dominant weather direction, thereby lowering the forces on the boat and preventing the ship from drifting-off. However, although these types of sea-anchor might be suitable under storm conditions, they are not suitable for low current speeds. According to William A. Vachon, a parachute anchor needs a initial velocity before it completely unfolds and before it is able to deliver a high stable drag load [42].

#### Window-shade drogue

Between the 1970's and 1980's over 300 window-shade drogues were deployed as part of meteorological research into ocean currents. These 'Window-shade drogue' being exactly what the name indicates, namely a screen between two rigid bars, similar to a window-shade. When a line is attached precisely above the center-line of the screen, the screen will turn normal to the the relative current direction, due to a pressure difference between the leading and trailing edge. The flat configuration perpendicular to the flow, ensures it has a high normal drag coefficient of 2.6 [43].

### Bal anchor

A 'Bal anchor' is one of the most simplistic drag devices available [43]. A large spherical screen can be filled with ambient water and subsequently be pressurized. The drag coefficient of a sphere is relatively low in comparison with the 'window-shade drogue' (0.5), but due to its configuration it has no reasonable theoretical limit in size, and can be easily installed. However, increasing the size of the anchor can cause the system to be present in multiple different current layers with different speeds and direction, which could harm its effectiveness. Furthermore, the added mass of such an anchor would be enormous, leading to high inertial forces when the system frequently changes direction or speed.

### Holey sock

The Holey-sock or 'SVP drifter' is currently in wide spread use all over the world, and has replaced the 'Window-shade drogue' as measuring equipment of ocean currents [12]. It is a tested system and it has proven to be effective in delivering drag. Its configuration is a vertical cylinder with rigid rings to maintain its shape. Depending on the required size the installation would be more difficult than that of a ball anchor. Besides that it would have the same problem of enduring different current speeds and directions, as a large ball anchor.

### Tristar

The Tristar drogue was another proposed alternative to the 'Window-shade drogue'. Although it proved better at following a specific current than the SVP drifter, it was deemed less suitable due to higher manufacturing costs and difficult deployment [29]. The Tristar configuration has 6 rigid spokes sticking out from a center at 90 degree angles with respect to each other. In between the tips of the spoke is a fabric, leading to a high drag coefficient in all directions.

Of all these anchor types, only the window shade drogue could be directly adopted to deliver a specific lift force. By positioning it under an angle, lift and drag force could be generated in a required direction to open the barrier perpendicular to the current.

## 4.3. Proposed concepts

The start of concept formulation was executed in the form of a new brainstorm, again with industry experts and layman. All the here proposed concepts are primarily different in their way of retaining shape, with some concepts being different in the application of a certain design element, or in the use of a completely different design element. The final morphological overview with defined working structures can be seen in Figure 4.4. Where every number symbolizes a working structure. These working structures or otherwise called high level concepts are considered to be good combinations based on engineering feeling.

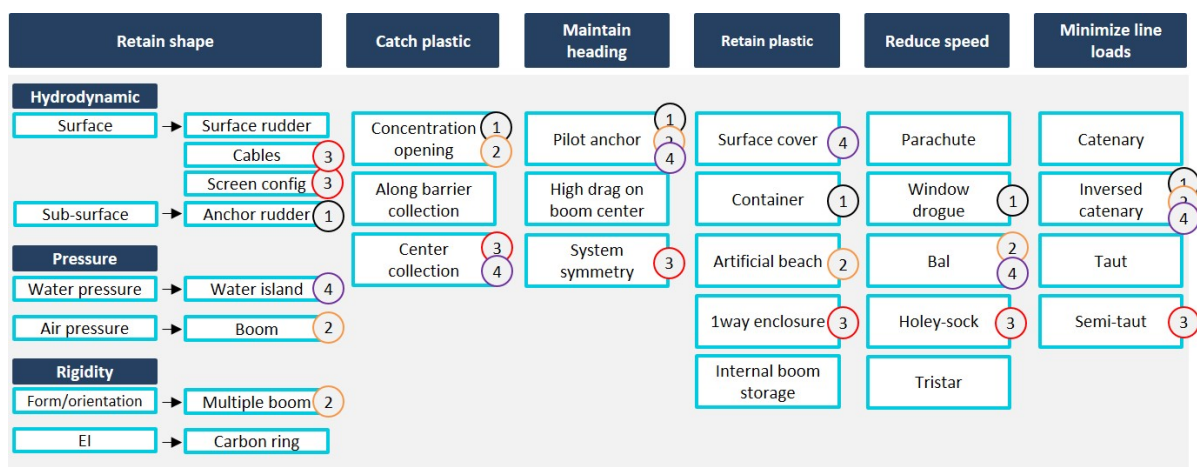


Figure 4.4: Morphological overview with working structures

The schematics of the concepts that follow from these combinations of design elements can be seen in Figure 4.5. These four concepts are considered to be fundamentally different. Which ensures that any research into one specific concept, through which several configurations will come to exist, will have no overlap with the other concepts. This way the concepts can be properly analyzed in separate work-flows.

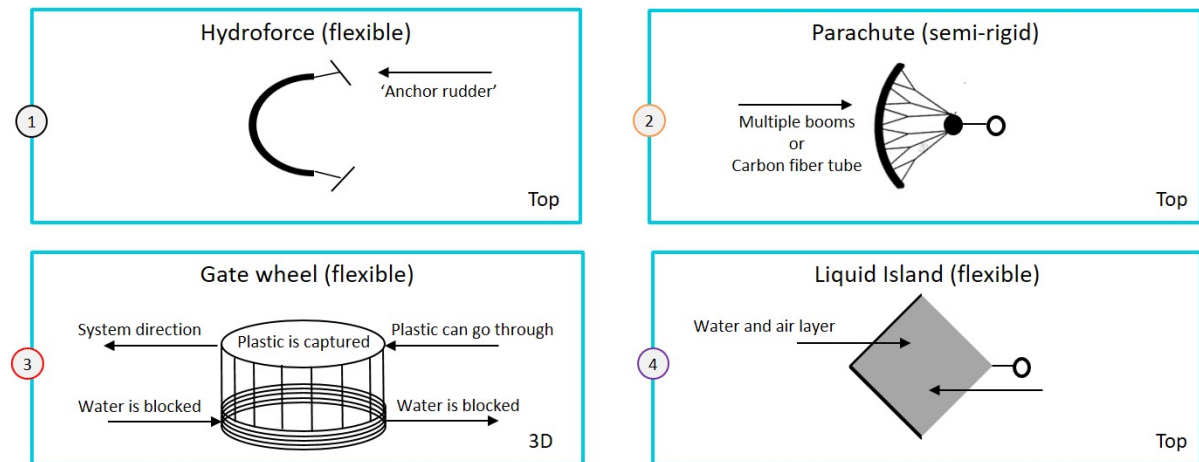


Figure 4.5: Concept overview

The concepts proposed here are high level configurations and need to be analyzed thoroughly before their feasibility can be assessed. However as a first proposal these four high level concepts were considered plausible and a good guideline in narrowing the research.

### 4.3.1. The Hydroforce

The Hydroforce, of which the schematic can be seen in number 1 of Figure 4.5, makes use of the relative velocity of the current to induce tension in the barrier. The relative velocity is generated with the use of two submerged rudder anchors, which also open the barrier by generating an outward lift force. The barrier is chosen to be completely flexible since this would enhance the wave following capabilities, and reduces chances of plastic over-topping. The use of two submerged rudder anchors also reduced the 'closing force' of the barrier in comparison with an anchor at a central point. On the other hand there were several complications identified. Two anchors might reduce the ability of the system to follow a fast turning current, and a completely flexible barrier could be difficult to maintain in the desired shape. However at this point in the research process all the data pointed towards a slow moving current with a slowly varying direction on system scale.

### 4.3.2. The Parachute

The parachute system was the first concept that followed from the passive strategy. It uses air pressure, but primarily multiple barriers behind each other to form a rigid system in the horizontal plane, but retain flexibility in the vertical plane. Furthermore, it uses a number of lines to redirect the force from the barrier to the anchor, to reduce the amount of bending stiffness needed to maintain open perpendicular to the current direction. As an anchor system it could make use of any of the simple drag devices, of which a Holey-sock or Tristar, would be the most suitable since it is proven technology and no lift force generation is required.

### 4.3.3. Gate wheel

The Gate Wheel uses a barrier with a 1-way-gate screen, through which plastic can enter from all sides, but is stopped on the inside from floating outwards. Directly below the barrier there is a continuous sea-anchor (resembling a large 'Window-shade drogue') that is thought

to be enable an automatic shape stability. Flow from any direction exerts a load on the barrier which is directly redirected to the anchor below. Due to the large anchor area, the anchor could be located at around 20 meters of water depth, to slow down the system by 10%.

#### 4.3.4. The liquid Island

The liquid Island is named after its shape stability method. The use of a large water-filled layer could potentially be very effective, but the technology is unproven. Forces induced by waves could be damaging and the influence of wind friction might be large depending on the volume above the waterline. Although the system is not regarded as the most plausible concept is was deemed worth investigating. In chapter 5 a test program for the liquid Island is proposed.

### 4.4. Concept selection

Based on the proposed concepts a high level evaluation was made to determine the most plausible concept for feasibility analysis. This evaluation was done in collaboration with the Ocean Cleanup and based on the mobile system value drivers, which can be found at the first page of the chapter (see Figure 1.4. The concepts were again evaluated with a multi-criteria analyses against the mobile system value drivers, following a -, -, +/-, +, ++, system. The results are depicted in Figure 4.6.

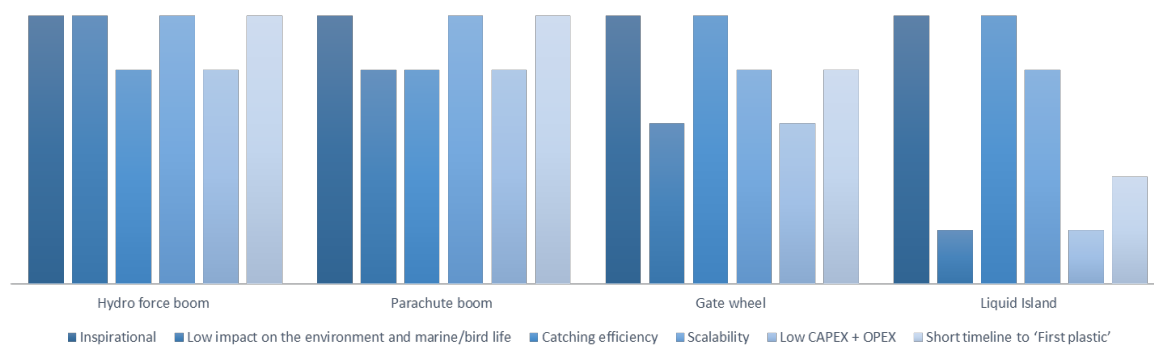


Figure 4.6: Concept MCA results

It can be seen that both the Hydroforce and the Parachute score very high on the mobile system value drivers, although all systems are considered to be inspirational. According to experts on marine biology, the Hydroforce would have the lowest impact on the environment, since it makes use of a minimal amount of material, whereas the Liquid Island is at the other end of the spectrum by very large surface area, under which various fish pieces could manifest itself in a unnatural ecosystem. Assessing the catching efficiency, all systems score high, but the Gate-wheel and Liquid-Island are presumed to be more effective. The Gate-wheel is able to catch plastic in any current condition, and the liquid island could be equipped with a similar 1-way-gate system, giving it a superb retention system. As to scalability, the Hydroforce and Parachute are easily scalable in numbers due to a reasonably low amount of material needed, whereas the Gate-wheel and Liquid Island are potentially easily scalable in size since their behavior is independent of current direction. Furthermore, the Gate-Wheel en Liquid-Island are, due to the amount of material needed and the technology readiness, considered to require a high CAPEX, and have a longer period to first plastic. On the other hand OPEX would be quite low for the 'Liquid-Island, due to its large retention area. The Hydroforce and Parachute are expected to have, the same OPEX, CAPEX, and time to first plastic, due to respectively the same logistical process, a special type of anchor versus a rigid barrier, and a similar expected design, production, and installation process.

It is at this point in the research process that was decided to continue with a feasibility analysis of the Hydroforce. As mentioned before the Hydroforce was considered to be preferred above all systems due to the simplicity and thereby high score on all Value Drivers. However, a new type of sea-anchor had to be designed first; a rudder anchor. The design of this anchor is the subject of part 3. Whereas the feasibility of the concept is determined in part 4.

However, the next part elaborates on the a experimental test-program focused on the behavior of the parachute system and the 'liquid-Island'. The reasoning behind this choice is that gaining understanding of behavior of the parachute system would be a first step in understanding the fully flexible Hydroforce, and that the 'Liquid-Island' was at the time of the call for proposal deemed to be worth investigating.

## **Part II**

# **Experimental test program**





After the strategy formulation phase the opportunity arose to participate in the HYDRALAB+ project, through which free access to an experimental offshore basin could be gained. Since, performing an experimental research into the concept feasibility was considered to be extremely valuable, a proposal was written. The most plausible concept at that time was thought to be the Liquid Island, which was therefor the main topic of this proposal. To obtain access to the program, a scientific test-program needed to be written according to the following steps:

1. Description of the environmental contribution
2. Test methodology
3. Test program
  - Scientific need to use the chosen offshore wave basin
  - Proposed analysis of results
  - Data storage and documentation
  - Publication plan & dissemination
4. Test set-up

The proposed test-program was unfortunately not directly approved but deemed to require improvement on several areas. The program is discussed in the following paragraphs, whereas the feedback and application form can be found in the appendix.

## 5.1. Environmental contribution

Every year eight million tons of plastic enters the worlds oceans. This plastic pollution has a negative effect on aquatic life, economy and human health. In addition, recent research by M. Cole [7]. has shown an effect of micro-plastics on the amount of carbon being transported to the deep ocean. This may in turn affect the carbon controlling capabilities of the ocean. In this way, plastic pollution might even contribute to global warming.

The Ocean Cleanup's goal is to extract, prevent, and intercept this plastic pollution by initiating the largest clean-up in history. It aims to achieve this by installing a large moored floating barrier, which can passively concentrate plastic debris by using the ocean currents. The 100 kilometer long moored barrier has been tested extensively but has some major drawbacks. Especially the inconsistent current direction and the average water depth of 4500 meter, impose big challenges and high costs.

For this reason, the Ocean Cleanup is currently researching mobile alternatives in close collaboration with the Delft University of Technology. Out of several cleaning strategies, one strategy has been selected for further development. It relies on a passive but mobile cleaning system, which uses large sea anchors at around 100 meters water depth to create a relative velocity with the surface current. The concept is designed in such a way that it maintains a zero degrees azimuth heading into the current (the plastic flow). The result is a passive system (1 kilometer span width) that continuously captures plastic while drifting within the garbage patch. Following the strategy, two concepts have been developed (Figure 5.1 and 5.2).

A first conceptual study has shown the high potential of the mobile systems. Key advantages are the low CAPEX and the significant improvement of catching efficiency with respect to a moored system. The first simplified ‘mega-scale’ numerical models used for evaluating the feasibility of the cleaning strategy show a 10 times higher plastic production per meter of barrier length than the current seabed-moored system.

## 5.2. Scientific objectives

The core objective of the current phase of the research into a mobile plastic catching system is to investigate the feasibility of both the designed concepts and the cleaning strategy. However, since modeling the non-linear behavior of the concepts requires complex models with high computational costs, and the accuracy of current numerical models is limited, a test program with the following goals is proposed:

1. Verify the feasibility of two different concepts and ensure that all important physical phenomena are adequately understood and accounted for, see Figure 5.1 and 5.2.
2. Input generation for, and validation of, numerical tools used for simulating mega-scale hydrodynamic behavior, and system behavior.

The novelty of the research is that it focuses on analyzing the behavior of an extremely flexible mobile VLFS (Very Large Floating Structure) in deep water. Until now, experiments on VLFS have taken place in coastal simulated environments, with a fixed moored position and a relatively high rigidity compared to the Passive Mobile Ocean Cleanup system. The proposed test program therefore enables a whole new field of research into deep water offshore VLFS, such as floating farms, and offers additional data to benchmark new and existing models. Besides that, research into the dynamic behavior of the passive parachute generates additional knowledge on the behavior of floating barriers used for large oil spill clean-up operations.

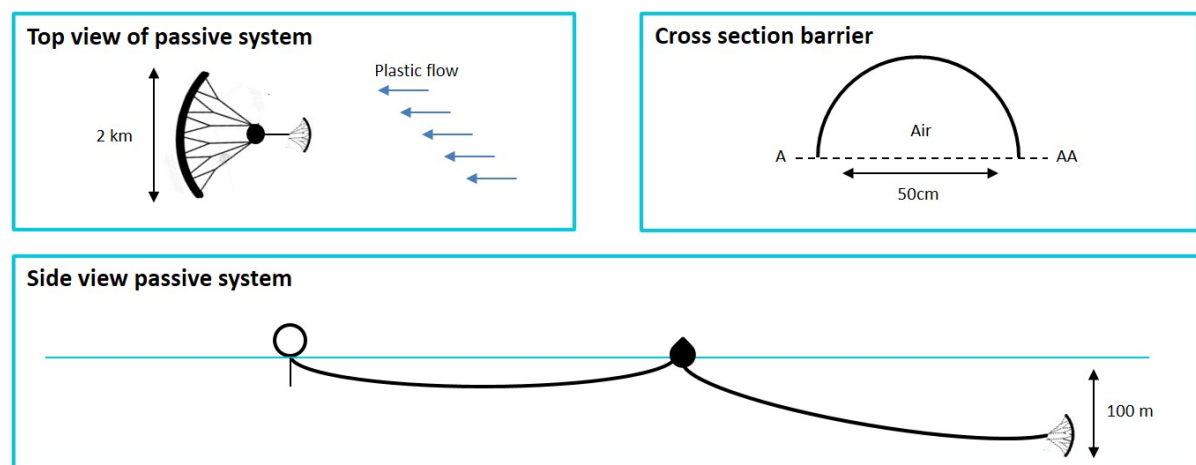


Figure 5.1: Passive parachute barrier

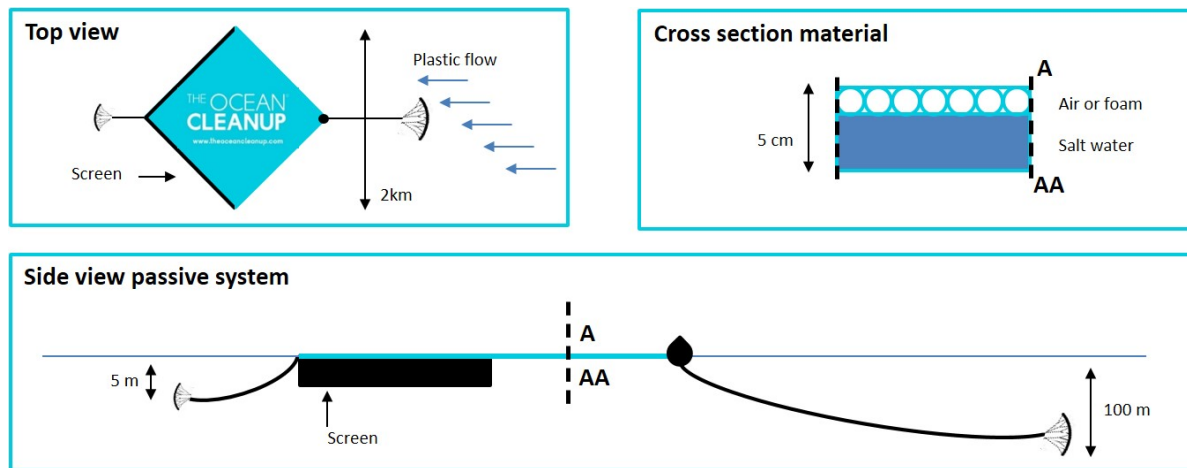


Figure 5.2: Passive flexible floater

## 5.3. Methodology

To increase the efficient use of the testing facility, the physical model of the concepts is divided into two parts. By splitting the model into the sea anchor and the surface system, their behavior can be tested independently at different locations. Several sea anchor designs will be tested at a one directional towing tank located at the Technical University of Delft.

The research goals will be reached in two testing phases using two different types of physical models. The first phase focuses on verifying the feasibility of the different concepts and ensuring that all physical phenomena are understood and accounted for; this will be done using flexible models. The following versions will be tested and the effect on the dynamic behavior will be evaluated:

1. Two different line configurations of the line set-up of concept 1, see Figure 5.1.
2. Two different designs of the floating elements in concept 2, see Figure 5.2.

The second phase uses an experimental set-up with a rigid barrier to determine the hydrodynamic coefficients used in the mega-scale numerical model. Subsequently, this numerical model will be validated by means of numerical reconstruction of data obtained from the model test.

A rigid barrier is needed for a captive test in which the hydrodynamic coefficients will be determined. In addition, using a rigid model ensures the outcome of usable data which will provide insight into the maximum potential of the cleaning strategy, independent of the feasibility of the different concepts. In this way, it is ensured that the second goal of the test program can be reached, independently of the outcome of the first phase.

However, the physical modeling of the surface system, which can be seen as a 'Very Large Floating Structure' (VLFS), introduces some challenges. The first challenge is related to the physical size of the concepts, which is very large in the horizontal plane, but very small in the vertical plane. Scaling the entire 1 kilometer span width system would create significant scaling and model effects causing unusable results. Therefore, since the test is intended to give insight into physical aspects and investigate the general behavior of floating flexible systems, a 100 meter span width system will be modeled. The feasibility of the cleaning strategy for the 1 km system will be evaluated by extrapolating the numerical model validated by the rigid model tests.

A factor of 1/18 will be used to scale down the concepts, which is approximately the scaling factor used by The Ocean Cleanup in recent 2D and 3D model tests at Marin and Deltares. These provided usable and scalable results. The knowledge gained during these previous test will be used in the construction of the model and is used to set up the experiment (see appendix).

Secondly, the elastic properties of the model need to be correctly scaled. According to Watanabe Wang [45] shearing rigidity, inertia of rotation of the cross section and structural damping can be neglected for a VLFS. Subsequently, the law of the similarity for making a model VLFS becomes as in table 1 (column 2), which results in the model units in column 4. Model tests with similar dimensions have been performed for floating airfields by Takagi and Nagayasu [40].

Table 5.1: Scaling concept 2 with a 100 meter span width

$\alpha = \frac{1}{18}$	Scaling formula	Prototype scale	Model scale
Geometrical condition	$L_m = \alpha \cdot L_p$	100m	5.56m
Mass	$M_m = \alpha^3 \cdot M_p$	50000 kg dry-weight	8.57kg
Time condition	$T_m = \sqrt{\alpha} \cdot T_p$	10 (average wave period)	2.36s
Bending stiffness	$EI_m = \alpha \cdot E \cdot \alpha^4 \cdot I_p$	Negligible	ALARP

Polyethylene has been chosen for the flexible model. This material was previously used by Watanabe Wang [45] to simulate zero rigidity when testing VLFS. Buoyancy will be scaled by adding polyethylene foam with a lower density. This will cause an incorrect scaling of the axial stiffness, however, since the expected strain is small and the focus is on the overall behavior of the system the effect on the outcome will be acceptable.

## 5.4. Test program

### Phase 1: Verify the feasibility of the two different concepts and variations thereof

By isolating current, wind and wave loads, the influence of the individual parameters on the dynamic behavior of the system can be evaluated. In addition, specific related forces will be measured and evaluated, which in turn is invaluable input for the design optimization. The following steps will be executed in sequence per concept (version), with the exception of the second test in phase C. An overview of the test program can be found in section 5.5.

#### A. Current only

##### Verify feasibility in different current speeds from head-on

This test will be used to investigate whether characteristic or specific responses, such as fishtailing, will occur in the current speed domain. The models will each undergo a test with a very slow increase of current speed. During the test the forces in the mooring line will be measured and the movements will be captured by the motion capturing system (MCS). The increase will be sufficiently slow in order to avoid dynamic behavior induced by changing current speeds.

**Verify feasibility under a change in current direction** This test will be used to investigate the qualitative behavior of the system when the direction of the current changes. The concepts will be placed at an angle towards the current rack (10 degrees azimuth) after which the lowest possible current will be induced. The MCS will be used to qualitatively compare the dynamic behavior of the concepts.

#### B. Wind and current test

##### Verify feasibility in a variety of wind conditions

To validate whether wind can be neglected as a driving force, and to investigate if there is a risk of wind lifting the system, a wind test is needed. The test will be executed under an angle of 135 degrees, this is the angle for which both concepts are expected to have the highest

responses. Thereby, the wind speed will be slowly increased and a low head-on current will enable the measurement of the force fluctuations in the mooring line. With the help of MCS the effect on the different concepts can be compared.

### **C. Waves and current test**

#### **Verify feasibility of the system in different wave conditions**

To verify the feasibility in operational conditions but to limit the time needed, only two wave tests will be executed for each concept. The first being an irregular wave field from head-on, the second being from beam on. Thereby, a low head-on current will enable the measurement of the force fluctuations in the mooring line. Again motion capturing will be used to evaluate the effect on the different concepts. At the end the best performing concept will undergo one additional test where a one year storm condition will be simulated.

#### **Phase 2: Input generation for, and validation of, numerical tools**

The objective of phase two is to provide the hydrodynamic coefficients for the equation of motions which will be used in the mega-scale numerical model. Subsequently, it will be evaluated if the movements recorded during the test can be replicated by the numerical model. During this phase a rigid barrier will be used. The hydrodynamic coefficients will be obtained from a captive test where the model will be fixed in its horizontal position at the center location of the barrier. However, the model will not be limited in its heave, pitch, and roll motion. It will be ensured that lines present in the system will be slack during this test to avoid unwanted reaction forces. The tension force in the mooring line and the reaction forces in the surge, sway, and yaw direction will be measured. The rigid barrier will be tested under different current speeds to investigate the dependency of dynamic forces on the current speed. The same forces as stated above will be measured in a steady current conditions for multiple angles relative to the current. The data which will be used in the validation of the numerical model will be obtained by testing the rigid barrier in a free test. The testing conditions in this procedure will be similar to the test performed in 1A. The anchor force and horizontal movements of the system will be recorded such that it can be evaluated if the numerical model shows similar movements and anchor forces.

#### **Scientific need to use DHI offshore wave basin**

The DHI Offshore Wave Basin is primarily required for the available equipment. This enables an efficient, realistic and complete test program. The 3D wave generator is capable of simulating the desired one year extreme values and different combinations of current and wave headings can be simulated by replacing the current rack within the tank. The available wind generators eliminate the need for additional wind tests in other facilities. Secondly, the depth of the basin is required, since the sea anchor has to be modeled at a depth of approximately 5.5 meters (scaling factor of 1/18).

#### **Proposed analysis of the results**

The majority of the test output will be in the form of qualitatively recorded dynamic behavior of the two mobile cleaning systems. This data is invaluable for the feasibility study, design optimization and for future research into Very Large Floating Structures. Secondly, the quantitative data on the forces and the dynamic response in the mooring line, of the flexible system in current and wave conditions, will be used to assess any unknown specific responses and could therefore result in new knowledge on the behavior of flexible floaters. Additionally, the data is of key importance for design optimization and validation of the numerical model on vertical system movements. Thirdly, the quantitative results on the rigid model tests will be used to simulate the mega-scale system movements in the ocean. This will in turn lead to knowledge on the plastic catching efficiency of the system and insight in the operational risks that might occur from these unmanned drifters.

To conclude; when the passive mobile cleaning system seems feasible, the next team will continue the detailed development of the concept and execute any additional test programs.

## Data storage and documentation

Data obtained from the model tests will be stored at The Ocean Cleanup and on the servers of the TU Delft. By storing the test data at the TU Delft it is ensured that it will be accessible for other researchers and institutions. In addition the papers and theses will be uploaded into the open access institutional repository of the TU Delft.

## Publication plan & dissemination

The obtained results are intended to be published in conference and journal papers. The following journals are considered for a publication:

1. Marine Pollution Bulletin
2. Ocean Engineering
3. IEEE Journal of Oceanic Engineering
4. Environmental Science and Technology

The detailed results will also contribute to two MSc theses that focus on the development of the new system, and will contribute to a wider scientific knowledge on flexible floaters. Furthermore the research contributes to the knowledge about the behavior of flexible floaters in waves and is therefore valuable for future studies. Knowledge gained during these model tests can be applied to other research areas, such as sea farming and floating oil barriers. Lastly, the reputation of The Ocean Cleanup will contribute to the fast dissemination of the results, therefore leading to a high promotional value for the HYDRALAB+. Vertical movements of the lines within the system will be recorded with an underwater video camera.

## 5.5. Test set-up

Experts from DHI will be involved throughout the entire process. A close collaboration is very important since the primary researchers of the team are first time users. The team is supported by an extensive group of experienced professionals. However, regarding the practical implications of the test program and the facility, the local teams input will be invaluable. The test program as presented section 5.5 is summarized in Table 5.2. Each test performed with a flexible model will be executed for the different concepts. Experiences from previous model tests within The Ocean Cleanup will be used during the construction of the physical models.

Table 5.2: Summary of the test-program

Test	Objective	Concepts to be tested	#	time / test	time / test	Total
1.A.1	Feasibility in stable current	2 flexible versions of both concepts	4	2 hours	2 hours	8
1.A.2	Feasibility in altering current direction	2 flexible versions of both concepts	4	1 hours	1 hours	4
1.B.1	Feasibility in wind	2 flexible versions of both concepts	4	2 hours	2 hours	8
1.C.1	Feasibility in waves	2 flexible versions of both concepts	8	3 hours	3 hours	24
2.A	Generating data for validation of numerical model in stable current	Rigid version of best performing concept	1	2 hours	2 hours	2
2.B	Generating data for validation of numerical model in changing current direction	Rigid version of best performing concept	1	3 hours	3 hours	3
2.C	Determining hydrodynamic coefficients	Rigid version of best performing concept	1	2 hours	2 hours	2
2.D	Determining hydrodynamic coefficients	Rigid version of best performing concept	1	2 hours	2 hours	2
Total test time						53
Installation time						10
Basin adjustments						6
Calibration time						24
Days (6 hours)						15

The sea anchor will be represented by a roller support with three degrees of freedom, namely: heave, pitch, and yaw. In this way, the degrees of freedom of the sea anchor, relevant for this test, are represented. During the tests at the towing tank of the TU Delft the other relevant degrees of freedom of the sea anchor are tested. The tension force in the anchor line is measured at the single point mooring by a force transducer. With this can be computed. A potential meter will measure the height of the sea anchor during every test. Horizontal movements of the system will be recorded by the motion capturing system. During every

test the entire force and the weight of the single point mooring system the horizontal force acting on the surface elements model will be recorded from above with a normal camera and from the side by an underwater camera. An impression of the experimental set-up is given in Figure 5.3, which will be used during all the tests. The arrangement will have to be replaced once in order to test beam wave conditions. During these tests the current rack will be located at the dotted green line in combination with the relocated roller support at the north side of the pit.

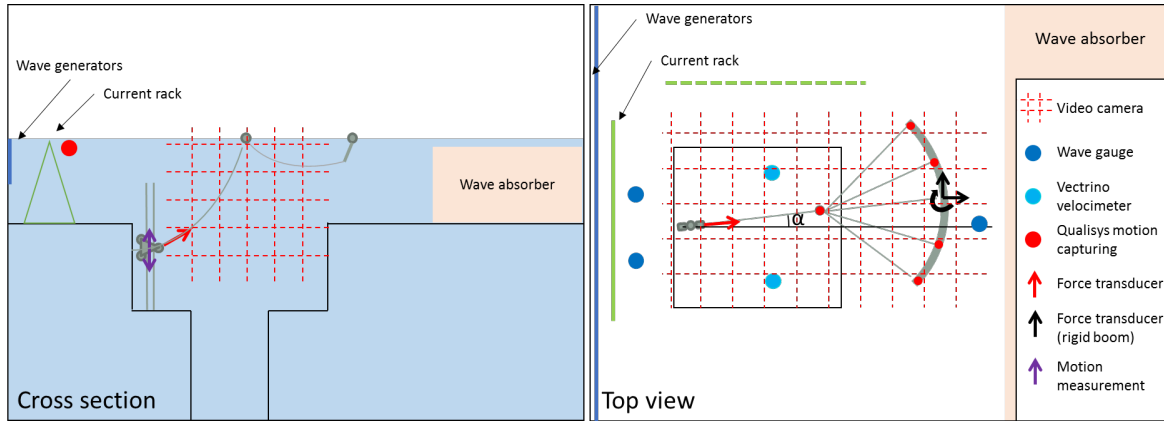


Figure 5.3: Experiment set-up





## **Part III**

# **Sea-anchor feasibility**



## Defining solution space

Designing a system requires a thorough understanding of the behavior of its components. Taking the previously proposed concepts into account, it is clear that there is one primary aspect, common to all concepts, that can greatly influence the feasibility of those concepts: the sea-anchor. Furthermore, the concept that was selected for further investigation, the 'Hydroforce-barrier', makes use of anchor rudders to generate lift, to open the barrier perpendicular to the current. The first step in concept feasibility analysis was therefore focused on the design and simulation of the sea-anchor component. However, the use of sea-anchors for passively controlled lift generation was non-existent up to this thesis. Past applications for sea-anchors or otherwise called 'drogues', have been limited to the improvement of storm survivability of ships, and to the use of measurement of deep ocean currents. Although in both applications the generation of a lift force is tried to be minimized, there are still similarities to the sea-anchor required for a passive mobile Ocean Cleanup system. Respectively being, delivering a very high drag load, and locking on to a specific depth in the water column. On the other hand sea-anchors for survivability are only used in storm conditions, and 'drogues' are used to precisely follow a current at a specific depth and not to slow down a surface system. To identify the best of both worlds and to design a suitable sea-anchor, both applications were taken into consideration and will be discussed in this chapter. Starting with a literature overview, after which practically feasible anchors are selected and risks are identified.

### 6.1. Previous research

Research on the subject of 'drifters', 'drogues', or in this thesis called sea-anchors, intensified around the 1970's, when satellite tracking became in use [12]. The research originated from the interest in investigating the ocean currents at specific depths. Which could provide information on climate patterns. Up to that point in time most research had focused on surface currents and no scientific research existed to support the effectiveness of proposed sea-anchor designs [25]. In 1973 William A. Vachon published a report on the experimental test results of forty different sea-anchor designs [42]. These designs were based on previously used configurations for meteorological research [25] and expected performance. Furthermore the parachute sea-anchor used for ships in storm conditions had also been used for meteorological research due to its simplicity of deployment, and was therefore also analyzed in this thesis.

The forty configurations consisted out of nine completely different shapes and variations thereof:

Previously existing:

1. Parachute

2. Bucket
3. Conical
4. Two axis crossed vanes
5. Fishing net

New configurations:

1. Three axis crossed vanes
2. Vertical cylinder
3. Sphere
4. Plastic sheet in the form of a window-shade

Thereby the anchors were judged on the following criteria:

1. Ease of installation (simplicity)
2. Drag coefficients as function of relative velocity
3. Influence of buoy-induced dynamic heave motion on 'drogue' performance

Based on these tests the 'window-shade drogue' (number 4 of new configurations) was considered to be the most suitable sea-anchor for meteorological research into ocean currents (see Figure 6.1). The 'window-shade drogue' consisted out of a rigid top and bottom bar with a screen in between (resembling a window-shade), with the bottom bar having a weight of at least one and a half times the expected drag force on the screen. Attaching the mooring-line precisely above the center-line of the anchor, ensures the system turns normal to the current, thereby delivering the highest drag load. The ability of the anchor to turn normal to the current direction is caused by a changing hydrodynamic center depending on the angle of attack. If the anchor turns away from the normal the hydrodynamic center moves from the center of the screen to the leading edge, thereby creating a returning moment around the center-line.

The anchor design is easy to install, has a mean drag coefficient of 2.6, and when decoupled from the wave motions the performance would be solely dependent on current. Other shapes and/or configurations had either lower drag coefficients, were more difficult to install, or needed a deployment velocity to achieve the full drag coefficient. The latter was specifically a problem for the parachute anchor. Which, according to the tests, needs a full scale deployment velocity of 0.05 to 0.15 knots, depending on the configuration. Furthermore, configurations such as the parachute and bucket are shown to oscillate, depending on the current velocity, and tend to stream at large angles to the current.

In 1975 William A. Vachon published a report specifically focused on full scale ocean tests of a 'window-shade drogue' [43], [41]. In this report detailed results, such as the measured horizontal drag coefficient of 2.6 and vertical coefficient of 0.03 are presented. Besides that, the tests were focused on finding the correlation between the slippage velocity (the expected velocity based on estimated forces – the actual velocity) and associated drogue forces, to the environmental forcing such as wind and waves. Through which, in contrary to earlier tests, it was concluded that a window-shade drogue does not turn completely normal to the relative current at anchor depth. Of which the unexpected alignment is shown at the right side in Figure 6.1.

At the time the lack of understanding was deemed related to the use of inadequate measuring equipment. Equipment used during the test to measure the actual current and anchor depth, was another but larger 'window-shade drogue', which at the time was thought to give accurate results. Decreasing the surface float area and increasing the drogue area was thought to

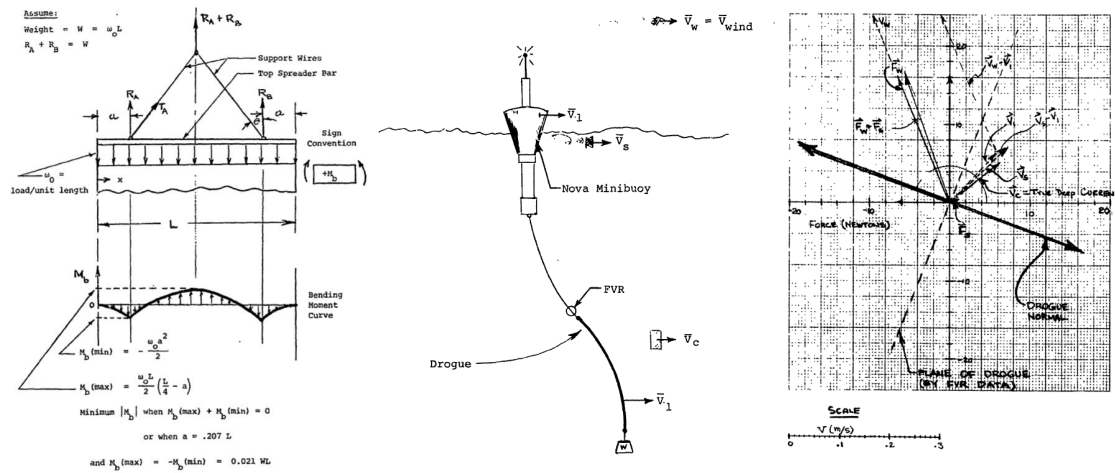


Figure 6.1: Schematic of a 'Window-shade drogue', and anchor orientation to the current direction, as depicted by William A. Vachon [43]

increase the measurement accuracy. However, not only the the use of inaccurate equipment, but also the physical properties of the window-shade drogue itself contributed to a lack of understanding. As will be discussed in chapter 7 and 8.

Although over 300 window-shade drogues were deployed after the research performed by William A Vachon, there had still been a lot of discussion in the scientific community with respect to it's effectiveness. In 1982 the World Climate Research Program (WCRP) recognized that a global array of drifting buoys ("drifters") would be invaluable for oceanographic and climate research [12]. But to ensure such a array would come to existence a 'drifter' or sea-anchor had to be designed that could be easily deployed from aircraft's and from any boat available, whereby the costs had to remain low. As a result new researches where initiated, that eventually led to the development of the Tristar, and SVP drifter (see Figure 6.2). The Tristar drifter was shown to have better current following characteristic but since the SVP drifter was easier to produce and deploy, the decision was made to standardize the Surface Velocity Program (SVP) drifters [12], [29]. These drifters consist out of a long cylindrical fabric with opposing holes to reduce vortex induced vibrations, and rigid rings to maintain it's shape. The SVP drifters are still in use today.

## 6.2. Practically feasible TOC sea-anchors

Whereas the purpose of an 'drifter drogue' is to follow a current direction at a certain specific depth, it is the purpose of an Ocean cleanup sea-anchor to ensure that the surface system can follow the surface currents as precisely as possible at a specific relative velocity. This requirement followed from research performed by the Ocean Cleanup [34], which has shown that the plastic in the Great Pacific Garbage Patch is mostly submerged, therefore the plastic movement is only current driven. Furthermore, simulations performed by the Ocean Cleanup have shown that a speed decrease of 10% relative to the surface current, is the optimal system speed. At this speed the system automatically moves with the plastic to so called 'hot-spot areas'. Which are areas where plastic accumulates due to rotating currents.

The total list of operational sea-anchor requirements for the selected concept or further investigation, is the following:

1. Open the barrier to the current
2. Slow down the system to 90% of the surface current velocity
3. Enable the system to follow the surface current

Taking into account the requirements for an 'Mobile Ocean Cleanup' sea-anchor, the window drogue system was deemed most feasible type of anchor, for the following reasons:

1. It could act as a plate/wing and could thereby be used to generate a controlled lift force
2. It is reasonably easy to deploy in comparison to several other designs
3. The high drag coefficient results in a reasonably sized anchor

However, the weathering ability of the 'window-shade drogue' has been discussed thoroughly in research [13], [18], [28], [30], and was deemed not stable. The window drogue is therefore adopted in chapter 8, to design a suitable anchor with a stable angle towards the relative current. Besides the window-shade drogue, the ball anchor was deemed most suitable for drag elements that didn't require steering capabilities. Primarily it's simplicity in installation and operation, and the fact that there is almost no limit as to its size, make it an interesting system.

### 6.3. Risks

The sea-anchor to be designed in chapter 8, will need to uphold to the previously described Value Drivers (Figure: 1.4). Testing this ability asks for a specific test program. In the next paragraph the test program and evaluation parameters will be discussed. Additional to the Value Drivers, the 'window-shade drogue' specific risks that could 'hurt' those value drivers had to be defined. Following from the literature, two main risks remained for the 'window-shade drogue'.

As mentioned earlier, from the tests results of Willam A. Vachon, it could be concluded that the understanding of the behavior of a 'window-shade drogue' was inadequate [43]. More precisely, it was unclear why the anchor didn't turn normal to the relative current velocity vector. A significant risk following from this behavior could be that the anchor would turn parallel to the current when force under an angle for lift generation.

Furthermore, according to J.E.W. Wichers 1976. [46] A system such as a tanker, attached to a single point mooring will experience slow oscillating movements when the 'equilibrium position' of the tanker is unstable. This instability can be caused by wind and current only, and increases when the angle between the current and wind decreases. Besides that when the 'equilibrium position' is stable in current and wind, but a oscillating force, such as irregular waves, work on the ship, the instability can occur as well. When comparing the described situation and analyses with a system pulling a sea anchor, one can notice several similarities. These similarities could indicated that 'fishtailing' of the sea anchor could occur. Together with wave forces, a combinations of forces could come to exist that could lead to high shock loading in the mooring lines [46]. Thereby possibly damaging the system.

The similarities are found in the environmental conditions that could cause an unstable 'equilibrium position'. These conditions are:

- The surface current direction and the current direction at anchor depth can differ, causing the the anchor to be pulled into a different direction then the current direction.

- When the anchor is used as a wing to open the barrier into the current, the anchor will be pulled to the middle of the system due to the closing force, even while the surface current, and current at anchor depth are aligned.
- Since a certain 'slippage' might occur between the expected normal position of the anchor towards the current vector, 'fishtailing' effects could increase.

The most interesting part about the possibility of the occurrence of 'fishtailing', is that it could occur on both 'ends' of the system. Namely, besides the similarities described, between a sea-anchor attached to a moving surface system, and a tanker attached to a buoy. The surface system could experience fishtailing, since it is moored to the sea anchor, and experiences current, wind and wave forces. The fishtailing effects on both ends could thereby influence each other, making it a difficult behavior to analyze.

Another risk that was identified, is the risk on torsional and rotational galloping as described in Flow Induced Vibration by Robert D.Blevins [5]. According to Blevins all non circular cross sections are susceptible to galloping and flutter. Where galloping is the term used in civil engineering and is used to describe the hydrodynamic instability of a structure, that arises when self induced oscillating fluid flows increase the vibration of the structure. With the self induced oscillation originating from the fact that the hydrodynamic coefficients are dependent on the orientation of the structure to the flow. Which in turn means that the 'Window-shade drogue' or any to be designed sea-anchor could start vibrating with a large amplitude.

Furthermore, vortex induced galloping or flutter, vortex induced vibrations and autorotation, are risks that have to be acknowledged in the detailed design of a sea-anchor, but are not discussed in this thesis, several methods exists to limited the driving vortices.

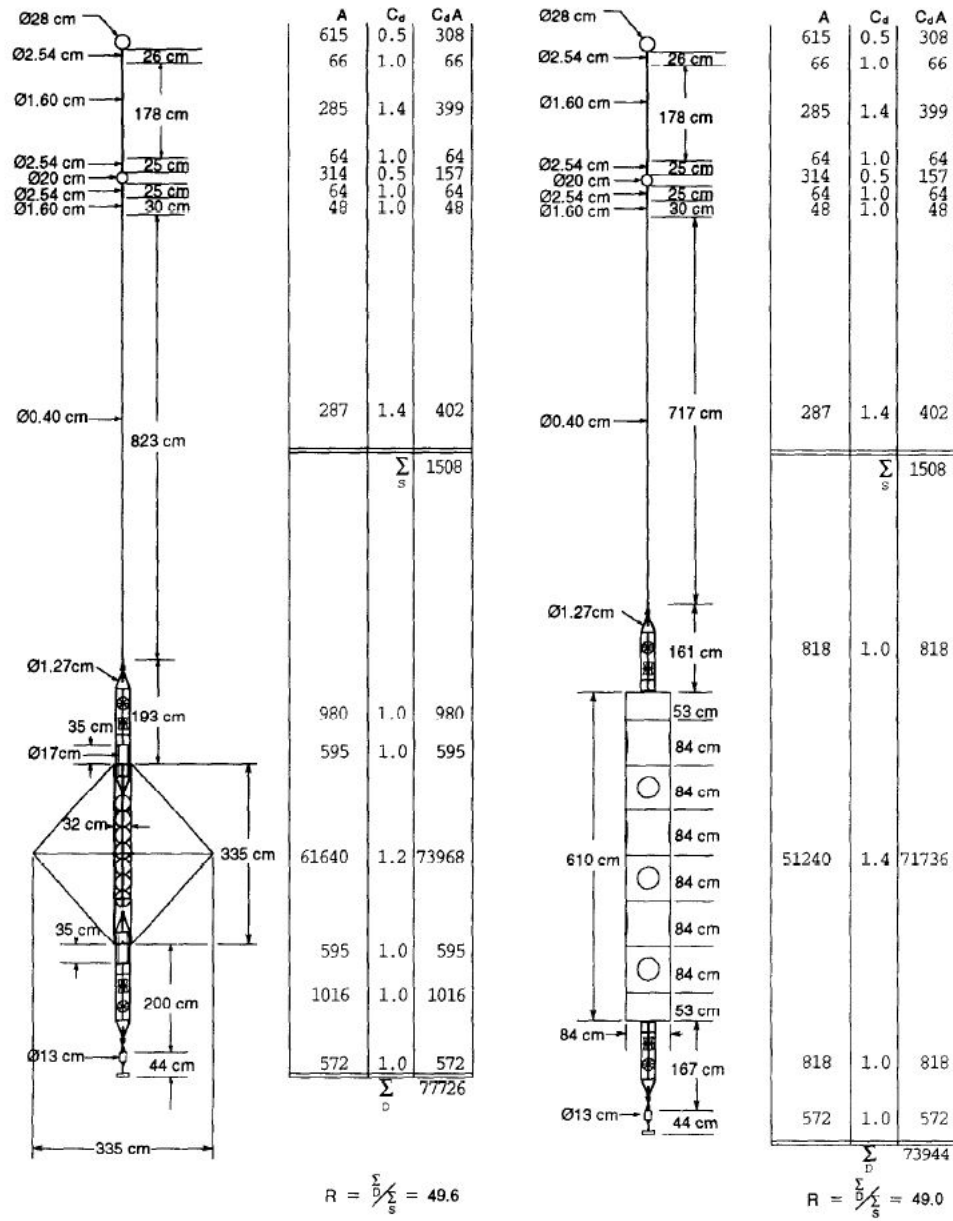


Figure 6.2: Tristar and SVP drifter [29]



## Three-dimensional sea-anchor model

To enable the analysis of the solution space and design a new suitable sea-anchor, a three-dimensional model needed to be constructed. Since, the anchor had to be able to move up and down in the water column, was expected to show interesting behavior in the horizontal plane, and would have to be integrated in complete concept simulation. The first step in the set-up of the three-dimensional model was to define a test program. Besides this a validation method was defined. This program and validation method are the bases for the required model input and assumptions. The model is subsequently constructed around the set-up of a 'Window-shade drogue', which led to the simulation seen in Figure 7.1. After which the model is evaluated and new sea-anchor system are tested in chapter 8 .

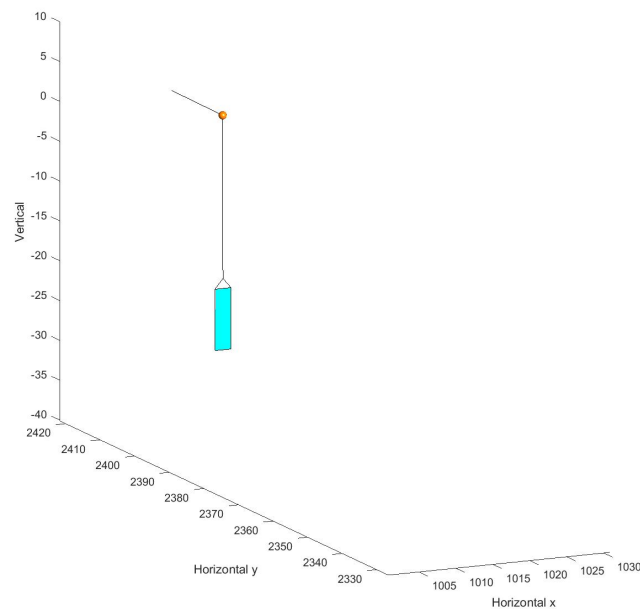


Figure 7.1: Window-shade drogue as simulated in this thesis

## 7.1. Test-cases and evaluation procedure

To make a detailed design of an anchor which is not subjected to any of the previously described risks, requires an specially dedicated research. However, this thesis is focused on making a conceptual design of the complete system. Therefor it was decided to firstly construct a 3-D sea-anchor model, and to simulate one of the tests done by William A. Vachon. Thereby comparing the results for a partial model validation. After which no further validation or verification was planned, but a focus was set on optimizing the sea-anchor design to fulfill it's function in the model. That being, to generate a stable lift force. As part of this objective the 'Window-shade drogue' was modeled as a one-degree of freedom system. Where specific attention was given to the determination of required structural damping and torsional stiffness, to stabilize the anchor in a uniform flow.

Waves were not taking into account for the modeling and testing of the sea-anchor as a separate system. Primarily because the effect of waves on the surface system would be of great influence on the sea-anchor behavior, and the forces experienced by the sea-anchor could therefor be completely different. Besides that, the literature on 'Window-shade drogues' primarily describes tests in benign environments, and states that the behavior of the drogue can be greatly influenced by waves, and therefor the drogue needs to be completely decoupled [43]. Taking this advice the anchors in the eventual system will have to be decoupled, therefor making influence of waves on the anchor of secondary interest.

The steps in testing and evaluating the sea-anchor as a separate system were the following:

1. Model 3-D window drogue
2. Compare behavior to behavior as described by Willam A. Vachon and J.E.W. Wichers
  - (a) Test if the system turn normal to the relative current vector with inline depth current profile
  - (b) Test the system with different current direction at the surface and at anchor depth to evaluate if 'slippage' occurs
3. Adapt the anchor through an iterative process and analyze behavior
4. Analyze anchor behavior when the anchor is placed under an angle to the current
5. Finalize the testing procedure with the recommendation of an anchor configuration for 3-D system modeling.
6. Model the 'Window-shade drogue' with one-degree of freedom and analyze stability

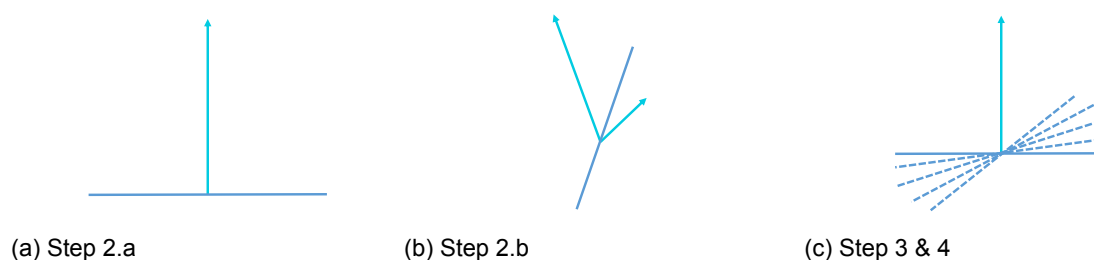


Figure 7.2: The three sea-anchor test to be performed

For step 2, the exact same sea-anchor parameters have been used as by William A. Vachon in 1975 for a 'ocean test'[43]. Using these parameters it is intended to perform a partial model validation in chapter 8.

For step 3 and 4 the same environmental conditions were used as in step 2.a. Furthermore, the anchor area was kept the same and the anchor depth was also kept at 24 meters. However, the shape and suspension of the anchors were changed. In step 4 the angle of attack of the anchors is forced varied from 0 degrees up to 20 degrees, with steps of 5 degrees. Subsequently the anchors have been evaluated on:

- stability
- lift generated
- failure angle

Besides these basic test-cases, which focus on the sea-anchor as a separate system, the sea anchor is evaluated again as part of the complete system evaluation.

## 7.2. Assumptions

### 7.2.1. The Algorithm

The first step in setting-up the model was to choose a representative modeling method, which would capture all the relevant physical phenomena. For this purpose a lumped mass approach was chosen. An approach described extensively by Van den Boom, with respect to mooring-line analysis. [44]. The Lumped Mass approach is shown to be of great relevance in analyzing dynamic mooring-line tension, which will be present in the sea-anchor as a separate system and the complete concept. According to Van den Boom, a dynamic tension amplification effect of a mooring-line, is strongly effected by elasticity, drag and catenary effects. All of which can be modeled with the lumped mass approach. Since the dynamic problem of a sea-anchor in a unstable equilibrium will be effected by dynamic forces in the mooring-line, the Lumped Mass Model was thought to be at least sufficient on this level. Furthermore, Van den Boom shows that the Lumped Mass model is an effective tool in analyzing the dynamic behavior of multi-component mooring configurations. And that the algorithm is suitable to study the influence on mooring tension on the low frequency movements of the complete system.

### 7.2.2. Anchor representation

The anchor modeled in this chapter will be simply represented by four nodes, each representing a corner of the anchor screen (see Figure 7.3a) The corners are horizontally connected by a bar and vertically connected by tethers. The calculation of in plane tension is therefor not possible, and the line between the bottom and top bar of the anchor will always be straight. However, the bottom bar can rotate with respect to the top bar. This representation can be justified since the weight of the bottom bar will at minimum be 1.5 times higher then the maximum expected drag load. The anchor is there assumed to be tensioned through the tethers and a force in the middle of the screen is not expected the alter the shape of the anchor.

### 7.2.3. Damping and stiffness

The Lumped Mass model is usually set-up without material damping, bending and torsional moments according to Van den Boom. Which is a simplification that is also quite suitable for the modeling of the sea-anchor system. The length and rigidity of the mooring line and anchor fabric, result in a bending stiffness that can be neglected. Besides that torsional effects can be of interest on anchor behavior but is neglected here since research by William A Vachon states that the behavior is primarily dependent on hydrodynamics [41]. Furthermore, material damping can also be neglected in comparison to the viscous damping [8]. Other types of damping can also be neglected according to Keulegan and Carpenter, since the damping force acting on a submerged member are usually relatively small [20]. However,

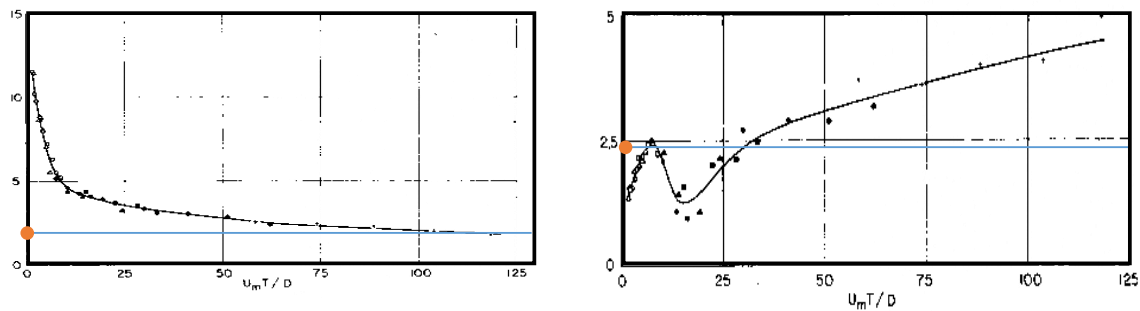


### 7.2.4. Environmental loading

With respect to the external forces acting on the sea-anchor system, waves and wind are left out of the calculations. Both can definitely have a strong effect on the sea-anchor behavior as state by William A Vachon [43]. But by decoupling waves from the sea-anchor in the final system, wave effects on the anchor will be minimized. Although When a surface rudder is used, the analyses of wave effects will be of great importance. Wind is simply considered to be another constant force effecting the surface system, which in this model is incorporated into a surface current force. The sea-anchor system modeled as is, is therefor only subjected to the relative current, thereby it is subjected to fluid loading due to drag (relative velocity squared) and added mass (virtual mass/inertia), caused by relative velocity and acceleration of the anchor through the water. Other loads that are induced are mass, buoyancy.

### 7.2.5. Added-mass and drag coefficients

The added mass and drag coefficients are determined based on the full scale test results by William A. Vachon [43], and based on research done by Keulegan, Garbis H and Carpenter [20], and research by Sarpkaya [37]. William A. Vachon determined that the normal drag coefficient of a 'window-shade drogue' was 2.6, which is a high coefficient compared to what can be find in other literature. Assuming the 'Window-shade drogue' acts like a flat plat, the coefficient of 2.6 could explained by analyzing Figure 7.4a form Keulegan, Garbis H and Carpenter research [20].



(a) Frequency dependent  $C_d$  for a plate

(b) Frequency dependent  $C_m$  for a plate

Figure 7.4: Drag and added-mass coefficients for a plate by Keulegan, Garbis H and Carpenter, Lloyd H

The value of 2.6 is above the low frequency measurements (around 2), which is the frequency level that is expected to have occurred during William a. Vachons tests. However, the high frequency measurements indicate that the value of 2.6 is possible if the frequency of the plate increases. Thereby either there were significant vibrations present during William A. Vachons test, or the 'window-shade drogue' used during the test, did not have sufficient tension to be represented by a flat plate. However, based on these two data points it was assumed that the normal drag coefficient of the sea-anchor has a value of 2.5. Furthermore, William A. Vachon concluded that the vertical drag coefficient was 0.03, which is assumed to be true for the Ocean Cleanup sea-anchor as well. Besides this, the bi-normal drag coefficient is assumed to be 0.03 as well.

The drag coefficients for the mooring-lines are based on Sarpkaya's research into forces on cylinders and spheres in a sinusoidal oscillating fluid, which can be see in Figure 7.5a [37]. In which he determined a value of 1.5 for low frequency movements for a cylinder in normal direction, which will represent the value for a mooring-line elements in this theses. And that of the cylindrical buoy supporting the sea-anchor.

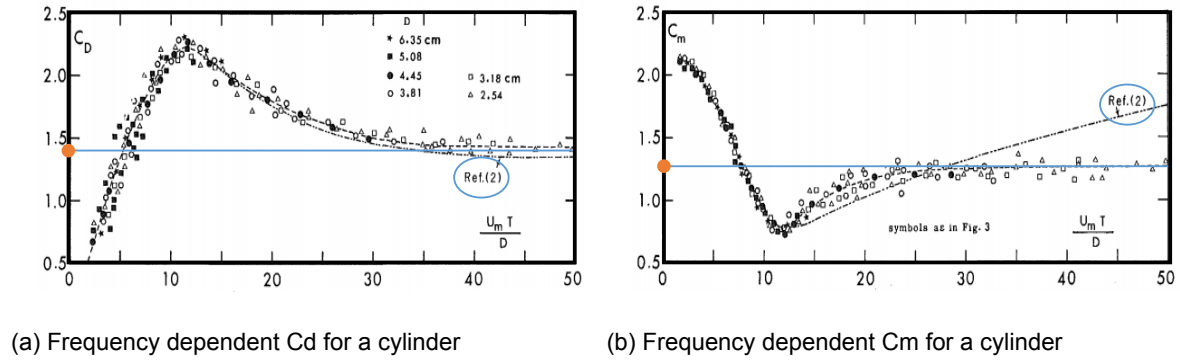


Figure 7.5: Drag and added-mass coefficients for a cylinder by Sarpkaya, T

As for the added mass coefficients Sarpkaya determined a value of 1.25 for a cylinder at low frequency in normal direction, which contradicts the value of 1.75 determined by Keulegan, Garbis H and Carpenter ('ref 2' in Figure 7.5b). Sarpkaya proved the value of 1.25 to be true and concluded that the values of the drag coefficients determined by Keulegan, Garbis H and Carpenter, were correct. The frequency dependent added mass for a plate at low frequency, determined by Keulegan, Garbis H and Carpenter, could therefore not be trusted, resulting into a coefficient value of 2.5 to be chosen for this thesis. Which is in line with the value at the frequency, as of which Sarpkaya determined a constant added mass value for a cylinder. This value of 2.5 holds for the normal direction. For the tangential direction a added mass value of 0.01 was chosen for both the mooring-line and the sea-anchor fabric, since the displaced water in these directions can almost be neglected. The same holds for the drag coefficient off the mooring-line in tangential direction. The value for added mass off the anchor could be higher depending on the density of the rigid bar used on the top and bottom of the anchor. If the density is low but the required tension, and thereby weight is high, a significant volume might have to be installed. Indicating that in that case a coefficient of 1.25 should be used for both bottom and top bar in normal and bi-normal direction.

Furthermore, the buoy to which the anchor is connected has a spherical shape. The drag and added-mass coefficient used for these elements can be seen in Figure 7.6

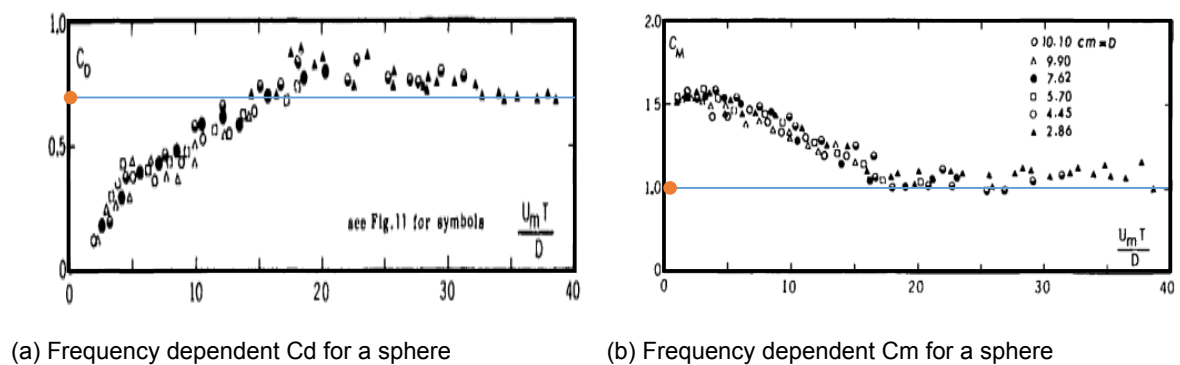
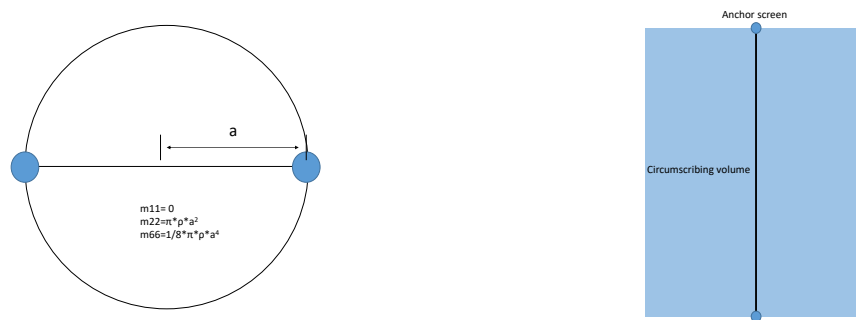


Figure 7.6: Drag and added-mass coefficients for a sphere by Sarpkaya, T

### 7.2.6. Hydrodynamics

The hydrodynamics of the 'window-shade drogue', and adopted sea-anchor are very complex. A lot of assumptions have already been made with respect to added-mass and drag coefficients, but the actual added-mass and drag force calculation is determined by additional factors. First a circumscribing fluid volume around the anchor screen has to be determined, which defines the added-mass. Secondly, the hydrodynamic coefficients depending on the angle of attack have to be assumed. Third and last, the hydrodynamic center, which is the location on the anchor screen where the forces are calculated, has to be assumed.

Since the anchor screen is represented to be a flat plate, literature indicates that the fluid circumscribing the screen can be represented by a cylinder with a diameter of the screen width in normal direction [27]. However, in tangential and bi-normal direction the circumscribing fluid can be assumed to be zero (see Figure 7.7a). As for a spherical shape the added-mass volume is assumed to be half the volume of the sphere, and for a cylinder, the volumes can be assumed to be the exact volume occupied by the cylinder itself, in normal direction, and zero in tangential direction (for a cable).



(a) Top view circumscribing fluid cylinder

(b) Side view circumscribing fluid cylinder

Figure 7.7: Added-mass for sea-anchor and 'window-shade drogue' [27]

Since the 'window-shade drogue' is presumed to resemble as a flat plate, flat plate aerodynamics are assumed for the computation of lift and drag forces. Where Figure 7.8a show the lift and drag coefficient of an airfoil under all angles of attack, Figure 7.8b shows the theoretical lift and drag coefficient for a flat plate, and thus for the anchor presented in this thesis. The coefficients assumed earlier are therefore the values used at a 90 degrees angle of attack. The drag and added-mass calculation is subsequently only dependent on the decomposition of the relative velocity and acceleration vector. To obtain the real drag and lift coefficients for the 'Window-shade drogue' experimental test need to be performed.

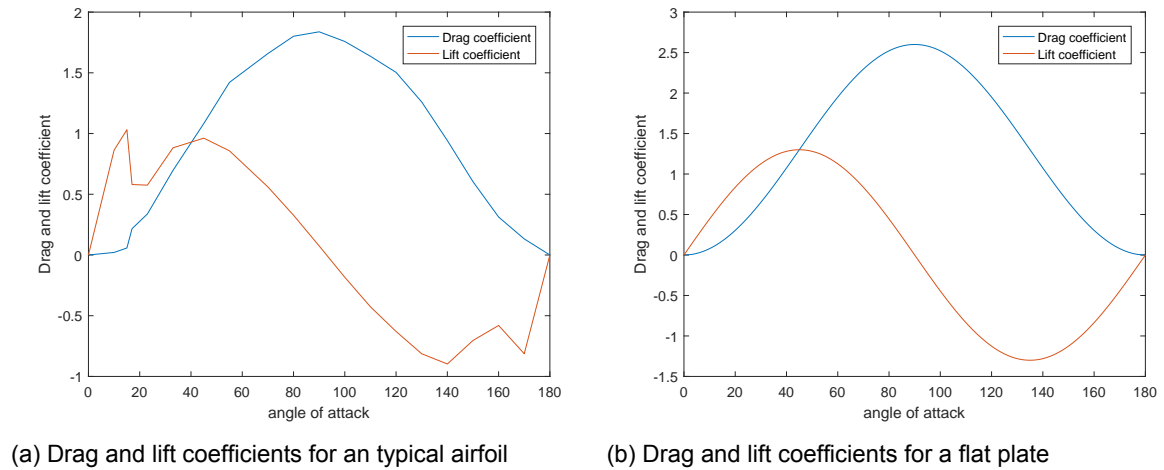


Figure 7.8: Drag and lift coefficients depending on the angle of attack for an airfoil and flat plate

Lastly, the 'hydrodynamic center' or 'center of pressure' of the anchor needs to be assumed, which is the point where the sum of the total pressure field acts on the body. This point is therefor used to superimpose all pressure forces, and the location is often not similar to the location of the center of mass, causing a moment around the center of the anchor. William A. Vachon states that the working principle of the 'Window-shade drogue' is completely dependent on an increasing drag force on the leading edge of the anchor [43]. Meaning that when the anchor turns into the current with a decreasing angle of attack, the force on the leading edge increases and a moment around the center-line forces the anchor back to a position normal to the current. The increase of drag on the leading edge is due to the relocation of the center of pressure or aerodynamic/hydrodynamic center, which changes with the angle of attack. Furthermore the location is also very much dependent on the shape and aspect ratio of the plate as described in a recent research by Xavier Ortiz, David Rival and David Wood [31], [14]. Meaning that a rectangular anchor and a square anchor would have very different dynamic behavior. Furthermore, other research into falling plates of different shapes and sizes, indicates that for example a triangular shape glides down in a helical path, whereas a rectangular shape tumbles or flutters down in a single plane [2],[1],[33]. Which in turn shows the complexity of the behavior of possible different anchor shapes.

For the assumption of the hydrodynamic center, the graph in Figure 7.9a, in combination with the graph in Figure 7.9b is used. Where in Figure 7.9a, -1 is the leading edge, 0 the center of the plate, and 1 the trailing edge. With AR being the aspect ratio of a tested plate, and is defined as height/width in the case of sea-anchor. Whereby the high aspect ratio tests are the most relevant for the design of a sea-anchor, since this configuration would be the easiest the construct and deploy. It can be seen that there is a large different is the location of the center of pressure for the various aspect ratios. The effect of the location of the hydrodynamic center on the design should be investigated thoroughly, but for since this thesis focuses on the conceptual design of the complete system, one specific angle dependency is assumed. Taking Figure 7.9b into consideration, presented in the Journal of Hydrodynamics [24], one sees that the obtained experimental data shows similar results as the formula of the center of pressure as formulated by Kirchhoff. Where  $\theta$  is  $90 - \text{the angle of attack}$ , and  $c * b^{-1}$  indicates the center of pressure towards the leading edge.



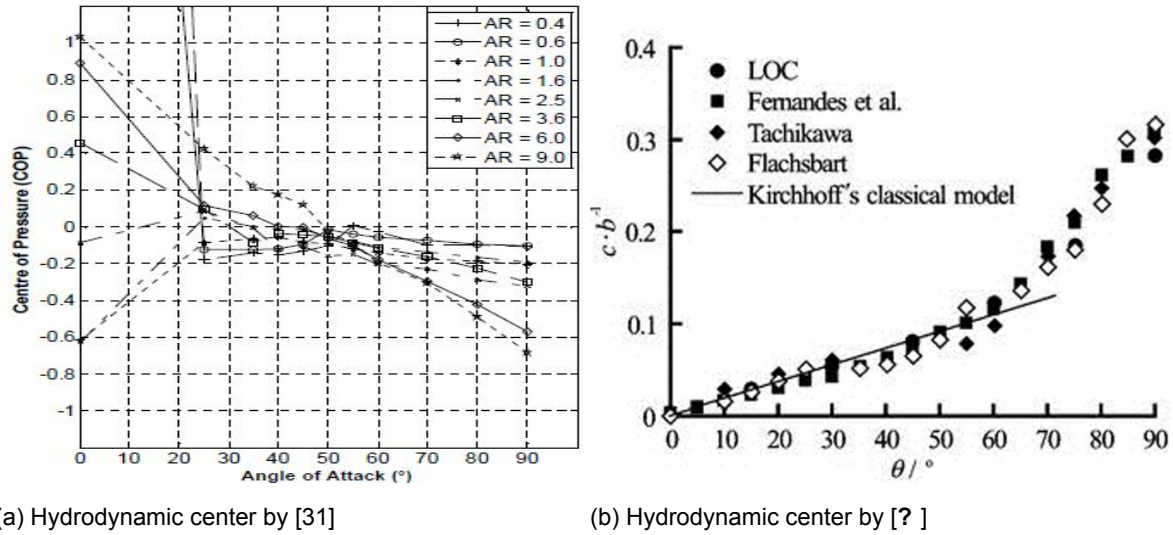


Figure 7.9: Hydrodynamic center as function of the angle of attack

Fernandes expands this formulation of the center of pressure based on additional experimental data seen in Figure 7.9b, [11]. They propose two linear formula's to describe the dependency of the center of pressure on the angle of attack. Being:

Kirchhoff:

$$(c/b) = 0.0933 \cdot \theta + 0.003 \quad (7.1)$$

For an angle of  $0^\circ \leq \theta \leq 55^\circ$ , where  $\theta = 90^\circ - \text{angle of attack}$

Additional:

$$(c/b) = 0.381 \cdot \theta - 0.2745 \quad (7.2)$$

For an angle of  $55^\circ < \theta \leq 90^\circ$ , where  $\theta = 90^\circ - \text{angle of attack}$

When comparing both results one sees the data is similar for higher aspect ratios although the data in Figure 7.9b is obtained from a plate with an aspect ratio of 1. Furthermore, according to the authors of Figure 7.9a, the data presented is not to be trusted in the higher angle of attack range. Therefore, since the data in the lower angle of attack range shows similar dependency as in Figure 7.9b, and the test results in Figure 7.9a are obtained in a windtunnel, whereas the test results in Figure 7.9b are obtained in a uniform fluid flow, equations 7.1 and 7.2 are used throughout this thesis.

Subsequently Mirzaeifath, Sina and Fernandes, Antonio Carlos, give the following two formula's to describe the moment coefficient as a function of the angle of attack [24]:

Streamline theory:

$$C_m = \frac{-3}{2} \cdot \frac{\pi \cdot \sin(2 \cdot \theta)}{(4 + \pi \cdot \sin(2 \cdot \theta))^2} \quad (7.3)$$

For an angle of  $0^\circ \leq \theta \leq 75^\circ$ , where  $\theta = 90^\circ - \text{angle of attack}$

Munk moment:

$$C_m = \frac{-\pi}{4} \cdot \sin(2 \cdot \theta) \quad (7.4)$$

For an angle of  $75^\circ < \theta \leq 90^\circ$ , where  $\theta = 90^\circ - \text{angle of attack}$

Resulting in the moment coefficient curve seen in Figure 7.10. Which is used to calculate the dynamic behavior of the sea-anchor in the one-degree of freedom model.

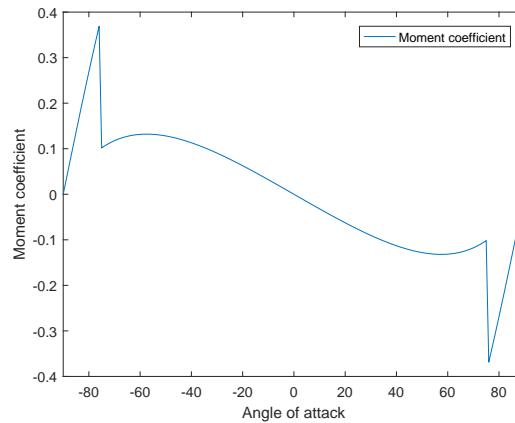


Figure 7.10: Moment coefficient depending on the angle of attack

### 7.3. Algorithm

The lumped mass method is a numeric approach to solve non-linear equations related to mooring systems, by representing the system as a multitude of masses connected by mass-less springs. The springs between the masses, represent the elements that would be present between those masses (see Figure 7.3a). The forces acting on these elements, of which the orientation is described by the springs, are then simulated to act on the connected masses. Increasing the amount of masses would thereby result in a better representation of reality but can significantly increase computation time. Through the lumped mass algorithm the equations of motions for each element can be connected by simply connecting their respective, mass, stiffness, damping, and added-mass matrices at the position of interaction. Following from this technique is a discrete set of equations of motion.

To able to properly calculate all the mooring-line forces the calculations have to be executed in a local coordinate system. Where drag loads act normal, bi-normal and tangential to the elements. With the same being true for added mass, since it is dependent on the direction of acceleration due to the unsymmetrical shape of the system elements (symmetrical normal and bi-normal but not in tangential). In addition, the tension forces are also calculated in local coordinates.

In order to enable this calculation in local coordinates, a method of coordinate transformation has to be incorporated in the following sequence:

1. The system is subjected to external loads in a global-coordinate system
2. The coordinated system is transformed into a local system
3. Forces are calculated on a local level
4. The coordinated system with local forces is transformed back into a global system
5. System response is calculated
6. Sequence repeats from 1

To enable this, the systems equations of motion have to be defined, following from the mass, buoyancy, stiffness, drag, added mass matrices. These matrices have to be transformed in two steps to enable direct global-coordinate input and global-coordinate output, while computing the forces in a local system. Subsequently they have to be combined into one large system matrix. In 2-D the sea-anchor system has the set up seen in Figure 7.3a. The

resulting equations of motion in global coordinate, of the complete system are depicted in equation 7.5.

$$(M + Ma(t)) \cdot \ddot{x}(t) = F(t) \quad (7.5)$$

Where:

$$F(t) = -K(t) \cdot x(t) - C(t) \cdot \dot{x}(t) + Fb + Fg \quad (7.6)$$

Where:

**x(t)** = displacement vector

**M** = mass matrix

**Ma(t)** = time dependent added mass matrix

**K(t)** = time dependent stiffness matrix

**C(t)** = time dependent drag matrix

**Fb** = buoyancy force vector

**Fg** = gravity force vector

### 7.3.1. 2-D local matrix transformation

For the 2-D example in Figure 7.3a, the global added mass and drag matrix can be derived from the local matrices, which depend on the normal and tangential fluid forces. The global stiffness matrix can be derived from the local stiffness matrices, which depend on the tangential position of two subsequent (spring connected) masses. Whereby, all three matrices are time dependent, since the added mass and drag are dependent on the orientation of the element, which changes every time step. And since the stiffness of 'string' elements is dependent on the tangential distance between two masses.

Since the matrices depend on length and orientation of a complete element, every element has to be treated separately. In 2-D the the local matrices for a single element can be seen below. Where  $x(t)$  is the local displacement vector. The matrix of any 2-D element consists out of left upper-part, which is representative of the contribution to the mass on one side of the element. And it consists out of a right lower-part, which is representative for the contribution to the other side of the element. Together being the combined equations of motions of two masses representing the element.

$$[m] = \begin{bmatrix} mt & 0 & 0 & 0 \\ 0 & mn & 0 & 0 \\ 0 & 0 & mt & 0 \\ 0 & 0 & 0 & mn \end{bmatrix} \quad (7.7)$$

Where:

$$mn = \frac{1}{2} \cdot elementmass \quad (7.8)$$

$$mt = \frac{1}{2} \cdot elementmass \quad (7.9)$$

Here,  $mn$  and  $mt$  are the normal and tangential mass which are off course the same.

$$[ma] = \begin{bmatrix} at & 0 & 0 & 0 \\ 0 & an & 0 & 0 \\ 0 & 0 & at & 0 \\ 0 & 0 & 0 & an \end{bmatrix} \quad (7.10)$$

Where:

$$an = \frac{1}{2} \cdot \rho \cdot c_{an} \cdot \frac{\pi}{4} \cdot D^2 \cdot l(t) \quad (7.11)$$

$$at = \frac{1}{2} \cdot \rho \cdot c_{at} \cdot \frac{\pi}{4} \cdot D^2 \cdot l(t) \quad (7.12)$$

Here,  $an$  and  $at$  are the respective normal and tangential added mass. With  $c_{an}$  and  $c_{at}$  being the respective coefficients.  $D$  being the diameter of the element, and  $l(t)$  being the length of the element depending on time.

$$[c] = \begin{bmatrix} ct & 0 & 0 & 0 \\ 0 & cn & 0 & 0 \\ 0 & 0 & ct & 0 \\ 0 & 0 & 0 & cn \end{bmatrix} \quad (7.13)$$

Where:

$$cn = \frac{1}{2} \cdot \rho \cdot c_{cn} \cdot D \cdot l(t) \quad (7.14)$$

$$ct = \frac{1}{2} \cdot \rho \cdot c_{ct} \cdot 2 \cdot \pi \cdot r \cdot l(t) \quad (7.15)$$

Here,  $cn$  and  $ct$  are the respective normal and tangential *drag – relativevelocity*. With  $c_{cn}$  and  $c_{ct}$  being the respective coefficients.  $r$  being the radius of the element, and  $l(t)$  being the length of the element depending on time.

$$[k] = \begin{bmatrix} kt & 0 & -kt & 0 \\ 0 & 0 & 0 & 0 \\ -kt & 0 & kt & 0 \\ 0 & 0 & 0 & 0 \end{bmatrix} \quad (7.16)$$

Where:

$$kt_{constant} = ks \quad (7.17)$$

$$kt_{variable} = \frac{ks}{2} + \frac{ks}{2} \cdot \tanh(1 \cdot (l(t) - l_0 - 0.1)) \quad (7.18)$$

Here,  $kt(constant)$  and  $kt(variable)$  the respective constant and variable stiffness of an element with maximum stiffness  $ks$ , time actual time dependent length  $l(t)$  and intended length  $l$ .

And  $x(t) = [T, N, T, N]$ , being the local displacement vector.

Next, these matrices have to be transformed, following the steps as described at the beginning of the paragraph. To enable this transformation, directional matrices have to be used.

The effect of these directional matrices is best explained according to a visual example, in which drag forces are calculated in local coordinate system, by transforming the global relative current vector, and after which the normal drag is calculated and is decomposed in a lift and drag force, seen in Figure 7.11. Where a 2D top-view of a 'window-shade drogue' under an angle is depicted.

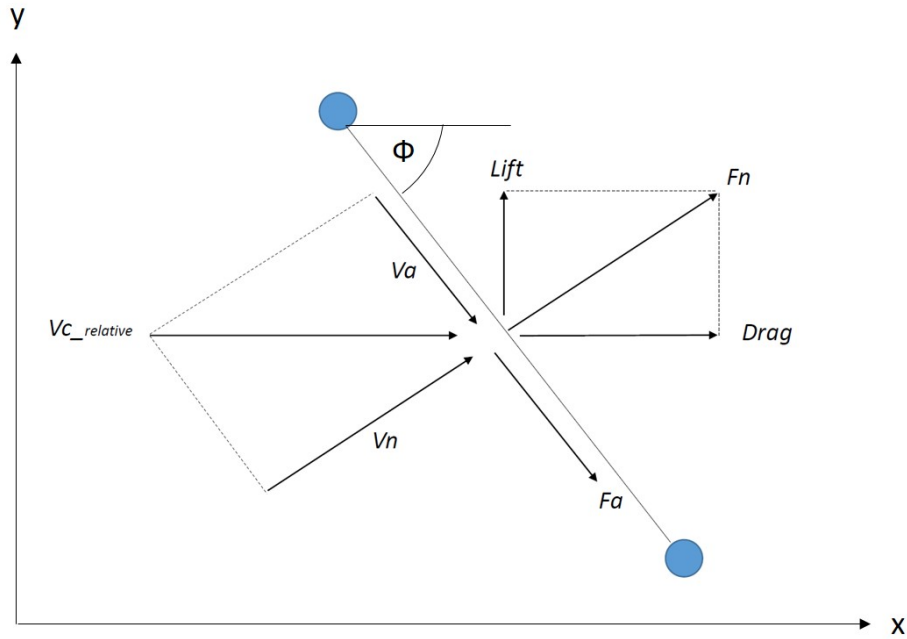


Figure 7.11: Visual representation of calculation of lift and drag

The directional matrix for the transformation of a 2-D global coordinate system into a local coordinate system is as follows:

$$[T] = \begin{bmatrix} \cos(\phi) & \sin(\phi) & 0 & 0 \\ -\sin(\phi) & \cos(\phi) & 0 & 0 \\ 0 & 0 & \cos(\phi) & \sin(\phi) \\ 0 & 0 & -\sin(\phi) & \cos(\phi) \end{bmatrix} \quad (7.19)$$

Writing this in a form without the use of cosine and sine decreases the chances on computational errors. Otherwise called a vector notation.

$$[T] = \begin{bmatrix} dX/l(t) & dY/l(t) & 0 & 0 \\ -dY/l(t) & dX/l(t) & 0 & 0 \\ 0 & 0 & dX/l(t) & dY/l(t) \\ 0 & 0 & -dY/l(t) & dX/l(t) \end{bmatrix} \quad (7.20)$$

Where,  $dX$  is the x distance between the two ends of the element,  $dY$  is the y distance between the two ends of the elements, and  $l(t) = \sqrt{(dX)^2 + (dY)^2}$ .

Taking the stiffness matrix as an example, the finale transformed element matrix can be calculated by:

$$k_{transformed} = [T]' \cdot [k] \cdot [T] \quad (7.21)$$

### 7.3.2. 3-D local matrix transformation

However, since the model to be constructed is in three dimensions, the local matrices change. Furthermore an extra transformation of the element and thereby matrices, is needed to determine the position of an element in a 3-D coordinate system.

The three-dimensional local element matrices are:

$$[m] = \begin{bmatrix} mt & 0 & 0 & 0 & 0 & 0 \\ 0 & mn & 0 & 0 & 0 & 0 \\ 0 & 0 & mb & 0 & 0 & 0 \\ 0 & 0 & 0 & mt & 0 & 0 \\ 0 & 0 & 0 & 0 & mn & 0 \\ 0 & 0 & 0 & 0 & 0 & mb \end{bmatrix} \quad (7.22)$$

Where:

$$mb = \frac{1}{2} \cdot elementmass \quad (7.23)$$

Here,  $mb$  is the bi-normal mass which are off course the same as the normal and the tangential mass.

$$[ma] = \begin{bmatrix} at & 0 & 0 & 0 & 0 & 0 \\ 0 & an & 0 & 0 & 0 & 0 \\ 0 & 0 & ab & 0 & 0 & 0 \\ 0 & 0 & 0 & at & 0 & 0 \\ 0 & 0 & 0 & 0 & an & 0 \\ 0 & 0 & 0 & 0 & 0 & ab \end{bmatrix} \quad (7.24)$$

Where:

$$ab = \frac{1}{2} \cdot \rho \cdot c_{an} \cdot \frac{\pi}{4} \cdot D^2 \cdot l(t) \quad (7.25)$$

Here,  $ab$  is the bi-normal added mass.

$$[c] = \begin{bmatrix} ct & 0 & 0 & 0 & 0 & 0 \\ 0 & cn & 0 & 0 & 0 & 0 \\ 0 & 0 & cb & 0 & 0 & 0 \\ 0 & 0 & 0 & ct & 0 & 0 \\ 0 & 0 & 0 & 0 & cn & 0 \\ 0 & 0 & 0 & 0 & 0 & cb \end{bmatrix} \quad (7.26)$$

Where:

$$cb = \frac{1}{2} \cdot \rho \cdot c_{cn} \cdot D \cdot l(t) \quad (7.27)$$

Here,  $cb$  is the b-normal *drag – relativevelocity*.

$$[k] = \begin{bmatrix} kt & 0 & 0 & -kt & 0 & 0 \\ 0 & 0 & 0 & 0 & 0 & 0 \\ 0 & 0 & 0 & 0 & 0 & 0 \\ -kt & 0 & 0 & kt & 0 & 0 \\ 0 & 0 & 0 & 0 & 0 & 0 \\ 0 & 0 & 0 & 0 & 0 & 0 \end{bmatrix} \quad (7.28)$$

Where  $kt$  remains the same.

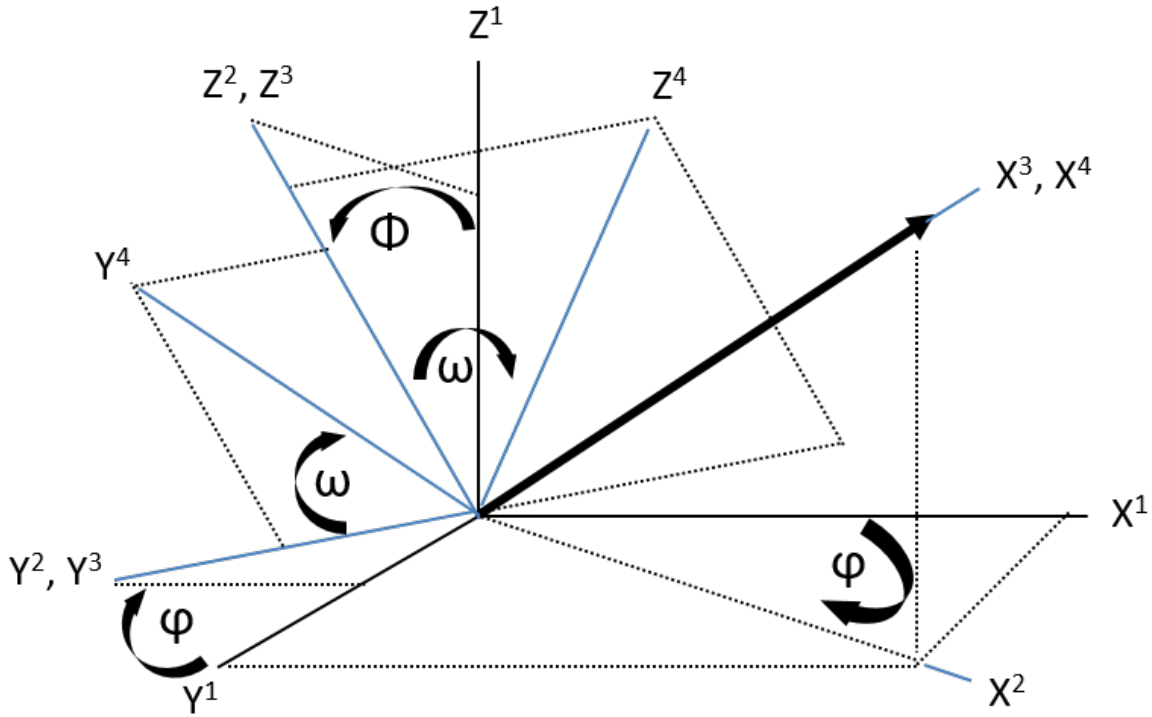


Figure 7.12: Representation of a 3-D transformation of a global to local coordinate system

The three-dimensional element matrices have to be transformed as to support a 3-D environment. An additional direction called the bi-normal direction is introduced. The transformation of a global coordinate system into a local coordinate system has two steps in this thesis. However, an additional step can be introduced for 'torsion', which is not of interest in this theses, since it is neglected.

The steps involved in this transformation are:

1. Start with global reference frame
2. Turn reference around Z-axis  $\varphi$
3. Turn reference around Y-axis  $\Phi$
4. Turn reference around X-axis for roll/torsion  $\omega$

The directional matrices used for this transformation enable the previously stated steps. The first transformation as according to the steps, is around the z-axis. Which is enable by matrix 7.29

$$[T_\varphi] = \begin{bmatrix} \cos(\varphi) & \sin(\varphi) & 0 & 0 & 0 & 0 \\ -\sin(\varphi) & \cos(\varphi) & 0 & 0 & 0 & 0 \\ 0 & 0 & 1 & 0 & 0 & 0 \\ 0 & 0 & 0 & \cos(\varphi) & \sin(\varphi) & 0 \\ 0 & 0 & 0 & -\sin(\varphi) & \cos(\varphi) & 0 \\ 0 & 0 & 0 & 0 & 0 & 1 \end{bmatrix} \quad (7.29)$$

The second transformation is around the y-axis and is enabled by matrix 7.30

$$[T_\Phi] = \begin{bmatrix} \cos(\Phi) & 0 & \sin(\Phi) & 0 & 0 & 0 \\ 0 & 1 & 0 & 0 & 0 & 0 \\ -\sin(\Phi) & 0 & \cos(\Phi) & 0 & 0 & 0 \\ 0 & 0 & 0 & \cos(\Phi) & 0 & \sin(\Phi) \\ 0 & 0 & 0 & 0 & 1 & 0 \\ 0 & 0 & 0 & -\sin(\Phi) & 0 & \cos(\Phi) \end{bmatrix} \quad (7.30)$$

Combining these two Matrices into one generates one complete transformation matrix. Again using vector notation, with  $Cx = dX/l(t)$ ,  $CY = dY/l(t)$ ,  $CZ = dZ/l(t)$ , and  $Cxy = \sqrt{((dX)^2 + (dY)^2)}/l(t)$

$$[T] = \begin{bmatrix} Cx & Cy & Cz & 0 & 0 & 0 \\ -Cy/Cxy & Cx/Cxy & 0 & 0 & 0 & 0 \\ -(Cx * Cz)/Cxy & -(Cy * Cz)/Cxy & Cxy & 0 & 0 & 0 \\ 0 & 0 & 0 & Cx & Cy & Cz \\ 0 & 0 & 0 & -Cy/Cxy & Cx/Cxy & 0 \\ 0 & 0 & 0 & -(Cx * Cz)/Cxy & -(Cy * Cz)/Cxy & Cxy \end{bmatrix} \quad (7.31)$$

The obtained matrix can subsequently be used to transform the the local drag, added mass and stiffness matrix of each element. Into matrices that transform global input to local and back to global.

$$c_{transformed} = [T]' \cdot [c] \cdot [T] \quad (7.32)$$

$$ma_{transformed} = [T]' \cdot [ma] \cdot [T] \quad (7.33)$$

$$k_{transformed} = [T]' \cdot [k] \cdot [T] \quad (7.34)$$

After the transformation has been performed for each element. The complete system matrix can be assembled. Which is the subject of the next paragraph. The mass matrix does not need transformation, since it is independent of time and space. However the mass matrices of all elements need to be assembled into one system mass matrix.



### 7.3.3. 3D matrix assembly

The basic principle of the assembly procedure, is the connection of the local matrices of the elements that are directly connected in the system. Visually this procedure is explained in figure 7.13. Where one can see the element matrices as gray and blue overlapping rectangles, with the black circles representing the nodes. The two blue rectangles which are 'split' indicate the method of connecting the elements when they are not directly in sequence. The system presented in this figure has eight elements and seven nodes.

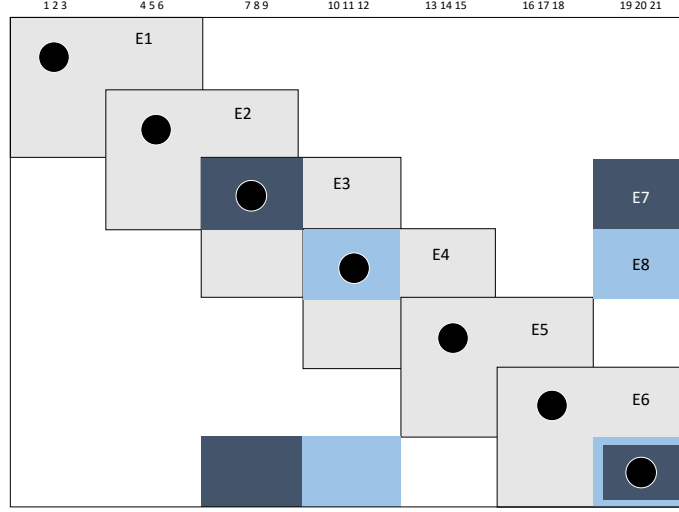


Figure 7.13: Visual representation of individual element matrices combined into one system matrix

By following this procedure for the mass, added mass, drag and stiffness matrix, and subsequently defining the buoyancy and gravity forces, the system can be modeled correctly. The last step is the introduction of depth dependent current velocity. Where the depth of an element, determines the endured current velocity. After this procedure the system can be solved according to the complete set of discrete differential equations. Connected through the system matrix construction.

For this model the system is solved explicitly through the following procedure:

$$\ddot{x} = A \setminus B \cdot (x - Ls) + A \setminus P \cdot (((x - Ls) - V)) \cdot (abs((x - Ls) - V)) + A \setminus D \quad (7.35)$$

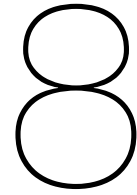
$$[B] = -([M] + [Ma]) \setminus [K] \quad (7.36)$$

$$[P] = -([M] + [Ma]) \setminus [C] \quad (7.37)$$

$$[D] = ([M] + [Ma]) \setminus [f] \quad (7.38)$$

Where  $A, B, P$  are matrices of the size  $2 \cdot DOF \times 2 \cdot DOF$ , and  $P, Ls, V$  are vectors of the size  $2 \cdot DOF \times 1$ , and  $A$  is the Identity matrix. Where  $f$  is the force vector,  $Ls$  the initial length vector for the top and bottom bar,  $V$  the current velocity vector,  $x$  is the input vector for distance and velocity, and  $\ddot{x}$  the acceleration output. In MATLAB the system could be solved with the use of an explicit ordinary differential equation solver, of which several exist. Thereby, the problem could be considered 'stiff'. Meaning that the solution being sought is varying slowly, but there are nearby solutions that vary rapidly, so the numerical method must take small steps to obtain satisfactory results. Which in turn means a stiff solver needed to be used. The most efficient solver was in this case found to be 'ode15s'.





## Model evaluation

The evaluation of the model has been done on through two tests. The first test is a simulation of the 'window-shade drogue' (drogue) in a straight current, to determine if the intended behavior of the drogue indeed occurs (turning normal to the current). Which is, based on the proposed assumption of the hydrodynamic center, expected to occur in an unstable manner. The second test is a simulation of the 'Window-shade drogue' with the exact same environmental forcing parameters and dimensions as in one of the tests performed by William A. Vachon. The goal of this simulation is to analyze if the three-dimensional model shows similar weathervaning behavior as the anchor experimentally tested at full scale. If so, this would mean the model can be considered partially validated.

Input parameters for all simulations:

- Anchor size of:  $2.25 \times 9.83$  which results in  $C_d \cdot A = 57.47 \text{ [m}^2\text{]}$
- Anchor depth of 24 meters, which is the same depth as used by William A. Vachon during full scale ocean tests.
- Ballast weight 1.5 times the max expected drag force

Environmental parameters for the first simulation:

- Summed wind and current force on the buoy:  $F_x = 0 \text{ [N]}$ ,  $F_y = 17.08 \text{ [N]}$
- Surface current representing both forces:  $V_x = 0$ ,  $V_y = 0.2326$
- Current at anchor depth:  $V_x = 0 \text{ [m/s]}$ ,  $V_y = 0 \text{ [m/s]}$

Environmental parameters for the second simulation:

- Summed wind and current force on the buoy:  $F_x = -5.52 \text{ [N]}$ ,  $F_y = 16.05 \text{ [N]}$
- Surface current representing both forces:  $V_x = -0.1322$ ,  $V_y = 0.2255$
- Current at anchor depth:  $V_x = 0.116 \text{ [m/s]}$ ,  $V_y = 0.088 \text{ [m/s]}$

During both test the most important evaluation criteria was the angle of the anchor with the surface current, and with current at anchor depth if it existed. Figure 8.1a shows the method of angle calculation, where the smallest angle between the current vector and the anchor screen is determined from the left side. However, if the anchor is to turn 180 degrees the angle will subsequently be calculated from the right side. Figure 8.1b shows a schematic of the anchor orientation and force representation in a straight tow. Which is used to explain anchor behavior depicted in the presented graphs.

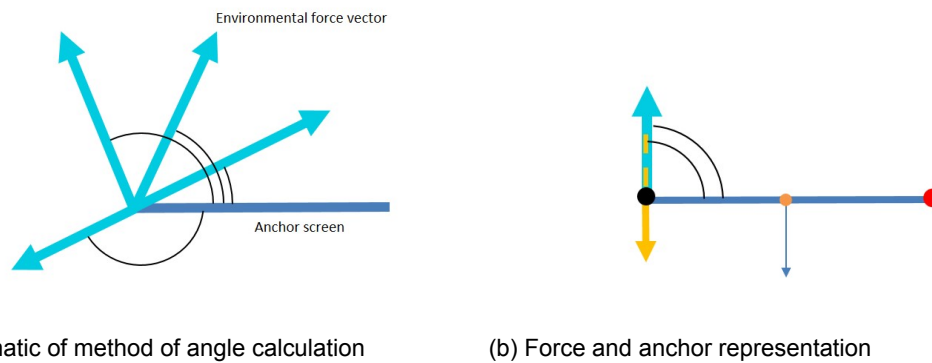


Figure 8.1: Visual explanation of the representation and the calculation of the angle of attack

## 8.1. Test 1

The first simulation was run for 3600 seconds with a straight surface current as stated in the list above (see Figure 7.2a). The initial conditions were not at the steady state but at 22 meters below the waterline. Meaning that at the start of the simulation the anchor sinks and experiences a shock load. Subsequently the current acting on the surface buoy starts pulling the anchor through the water. Unexpectedly the anchor does not turn normal to the current and is unstable during the whole simulation. As depicted in Figure 8.9a the angle varies between 0 and 180 degrees, for both the angel of attack with the uniform current and the relative current. Furthermore the spacial anchor path oscillates with an amplitude of around ten meters, and it can be seen that the right and left side of the anchor follow the same path for a high percentage of the time. Which indicates that the anchor moves parallel to its relative velocity vector.

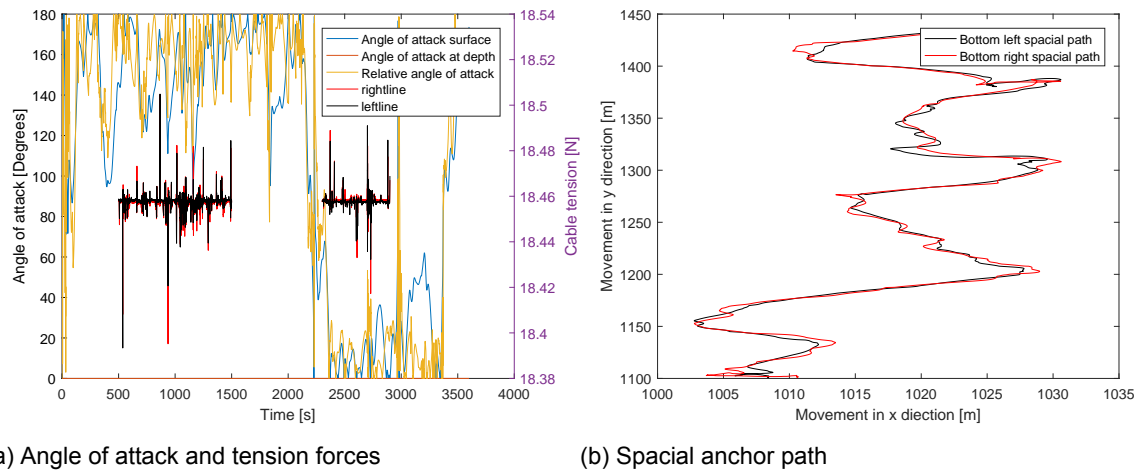


Figure 8.2: Results of the first test of the window drogue in surface current only

The behavior of the 'Window-shade drogue can be explained based on the tension in the two lines connected to the anchor (see Figure 7.1). After assessing the tension in the lines connected to the anchor which is shown in Figure 8.9a, but enlarged in Figure 8.3. One can see why the moment generated by the change of hydrodynamic center location does not turn the anchor normal to the current. The tension timetrace shows that during the first 2000 seconds the force in the leading line (in this case the left line) is higher than in the trailing line. Causing the system to weathervane around the leading line instead of around the center-line. This tension is caused by the normal and viscous drag force acting on the anchor screen, pulling the lower side of the screen slightly backwards, thereby rotating about the leading top node, and increasing the load on the leading line. However, the force difference is minimal and a small error or shock can tip the anchor around, thereby switching the leading and trailing edge (Which happens at 2200 seconds into the simulation). Figure 8.3a and 8.3b show the time traces of the tension when the respectively the left line is the leading side and when the right line is the leading side, and clearly show the minimal tension difference causing this irregular behavior.

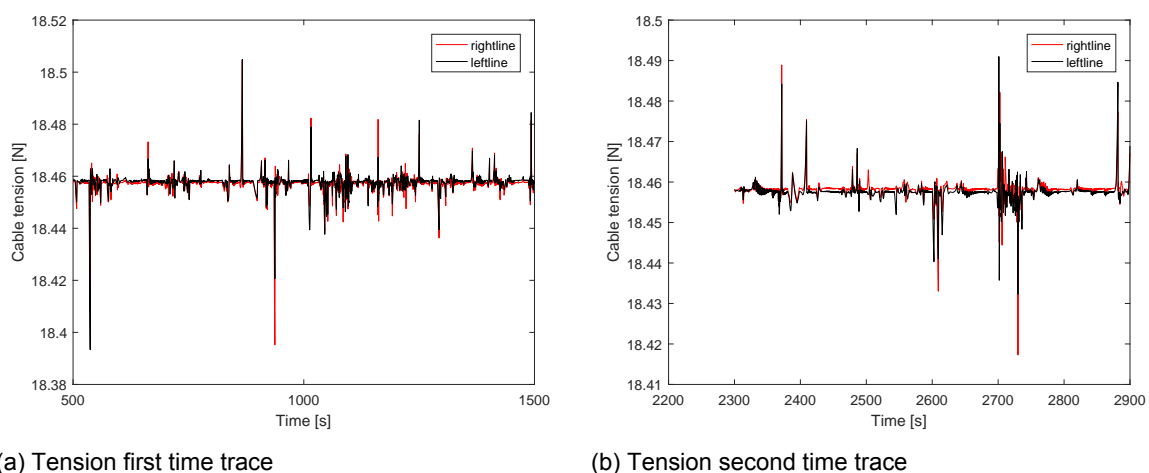


Figure 8.3: Time traces of the tension in long anchor lines

Since this behavior is unwanted for the 'correct' functioning of the 'Window-shade drogue', the tension effect on the turning point was further investigated. The lines attached to the drogue were tested for different lengths (seen in Figure 8.4a ), of which one variation with pretension. The result of which can be seen in the boxplot in Figure 8.4b.

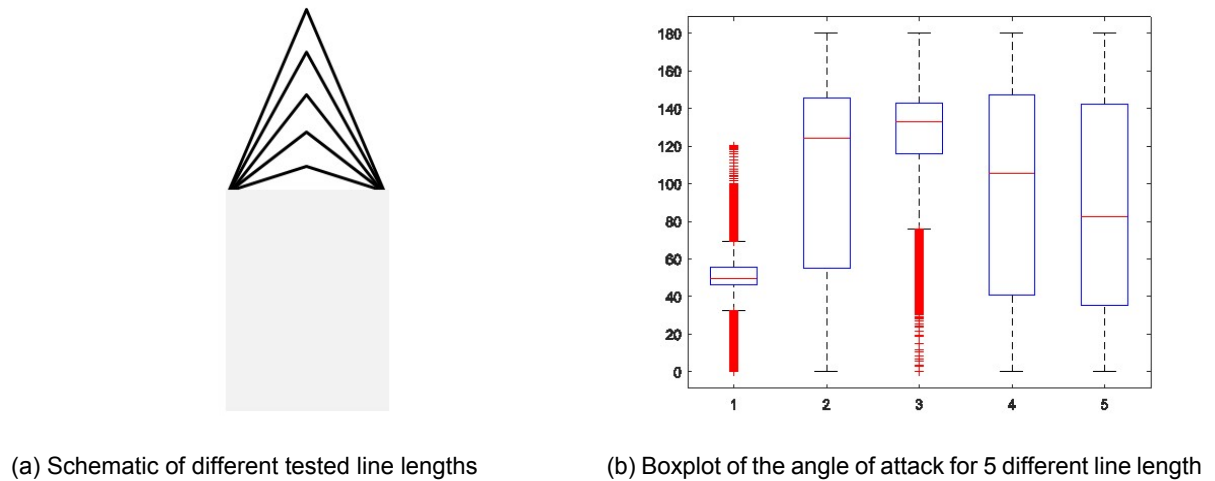


Figure 8.4: Effect of line length

It appeared from these results that the weathervaning behavior of a drogue with pretensioned lines was considerably better than without pretensioned lines. Figure ?? shows the time traces of the drogue with the shortest lines (pretensioned). The time traces of the tension can be seen in Figure 8.6.

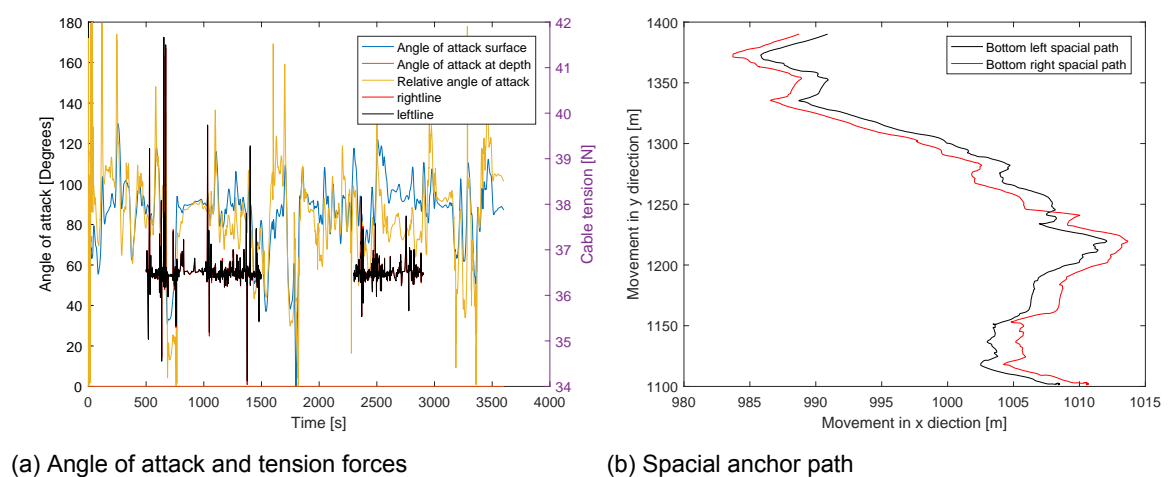


Figure 8.5: Results of the first test of the window drogue in surface current only

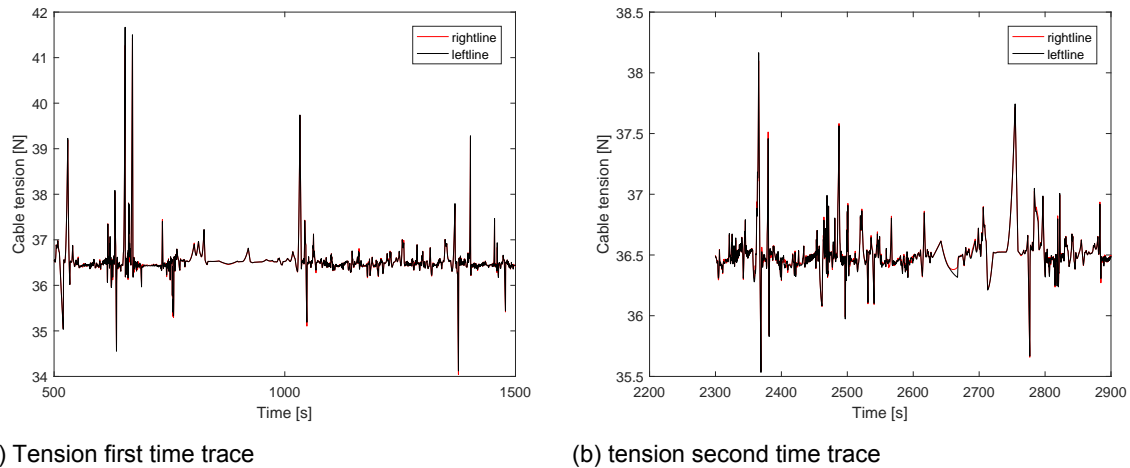


Figure 8.6: Time traces of the tension of pretensioned anchor lines

The behavior of the drogue with pretensioned lines is completely different from the behavior of drogue with long lines, and can be explained based on hydrodynamic behavior following from the change of hydrodynamic center location depending on the angle of attack. When the drogue is at a 90 degree angle of attack there is no moment acting on screen, since the hydrodynamic center is at the center line. However, small deviations away from the 90 degree angle, due to the initial conditions or due to numerical errors, cause the screen to generate a horizontal lift force. Due to this lift force the anchor starts moving to one side, thereby creating a relative current velocity in the opposite direction of the movement. The relative velocity vector and screen have at that moment a small angle of attack, which means the hydrodynamic center will be at the leading edge with respect to the relative velocity. Causing a restoring moment that forces the angle back to a 90 degrees angle of attack. However due to the inertia of the anchor and the low damping in bi-normal and tangential direction the anchor overshoots this 90 degrees orientation, causing a periodic motion around the 90 degrees angle of attack.

Figure 8.7 shows the difference between the behavior of a 'Window-shade drogue' with and without pretensioned lines, in respectively Figure 8.7a and Figure 8.7b. From these schematics it appears that if a 'Window-shade drogue' configuration would be used as a sea-anchor, it should be configured with pretensioned lines. Meaning that when the anchor is pulled through the water (as in this test) the hydro dynamic behavior is most uninfluenced with pretensioned lines. However, it has be noted that in these simulations there is no torsion stiffness included. Which is though to have a big effect on the hydrodynamic behavior as well. This aspect will therefor be analyzed in a one-degree of freedom model at the end of this chapter.

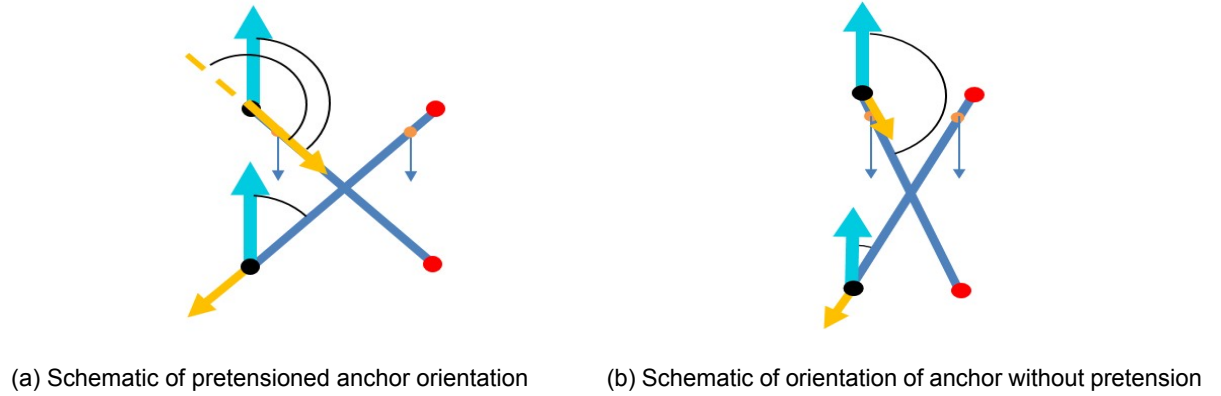


Figure 8.7: Schematic of anchor orientation with and without pretension

## 8.2. Test 2

During full scale Ocean tests performed by William A. Vachon [43], it became apparent that the hypotheses of the anchor turning normal towards the relative current direction, seemed untrue. As seen in Figure 8.10b the anchor orients itself in a 'slip' position. The anchor did not turn normal to the dominant surface current or normal to the current at anchor depth, but is oriented parallel to the relative velocity vector. The second test discussed in this section of the thesis, is intended to compare the behavior of the modeled drogue to the experimental test results depicted in Figure 8.10b. The initial conditions were the same as for test 1 and the environmental forcing was as stated in the list at the beginning of the chapter. The angle of attack of the anchor with the surface current and the current at anchor depth was calculated as in Figure 8.1a. The results of the test can be seen in Figure 8.8 and Figure 8.9, for respectively the anchor with lines under pretension and the anchor with long lines.

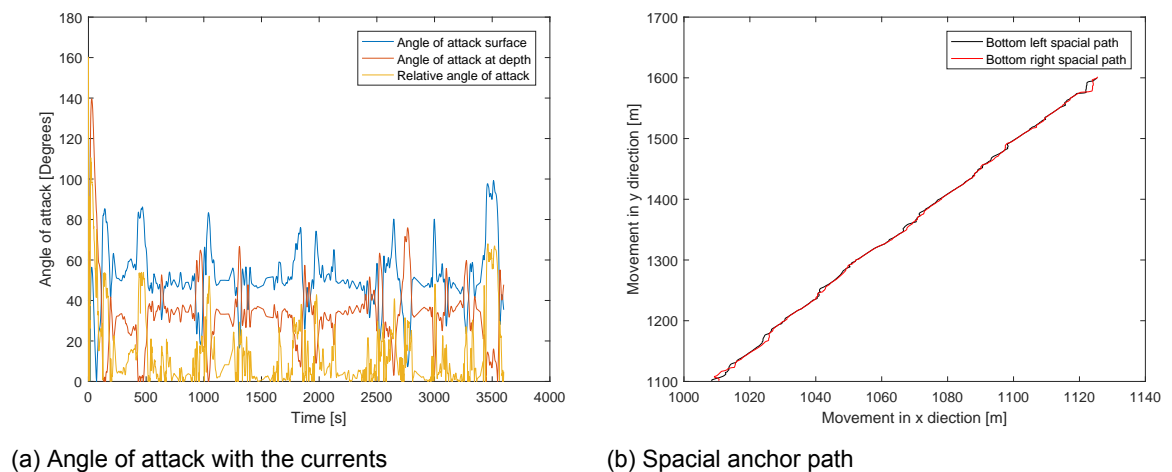


Figure 8.8: Time traces of the anchor with pretensioned lines



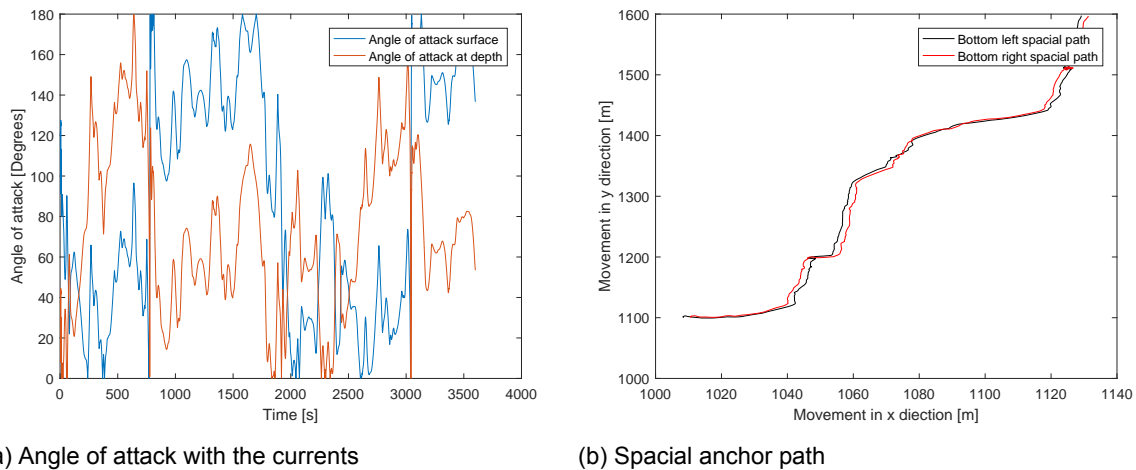


Figure 8.9: Time traces of the anchor without pretensioned lines

The results of the drogue with pretension in the lines shows a remarkably similar behavior as the 'Window-shade drogue' tested by William A. Vachon during large scale ocean tests [43]. The drogue does not turn normal to the subsurface current but turn parallel to the relative current direction (See overlapping of left and right path in Figure 8.9b). The angle with the surface current varies has a median around 45-50 degrees and the angle of attack to the subsurface current has a median around 25-30 degrees (see Figure ??). Which is similar to the angles depicted in Figure 8.10b. The drogue with long lines shows a behavior that is a lot less similar to the recorded behavior. As in test 1 the drogues has a leading edge due to tension difference in the line connected to the anchor. This difference causes the anchor to lean towards the surface current, thereby increasing the angle of attack to the subsurface current. Which can be seen in the Figure 8.9b, where the spacial path of both sides of the anchor do not always overlap. It thereby has to be noted again, that the difference in tension force between both lines is so small that when torsional line stiffness would be introduced in the model, both pretensioned and unpretensioned drogues could show different hydrodynamic behavior. However, the torsional stiffness in a line of 24 meters length could be considered to be zero. Furthermore, considering the similarities between the anchor with pretensioned lines and the measured orientation by William A. Vachon, one could argue that the current model shows realistic behavior. The model is therefor considered to be partially validated.

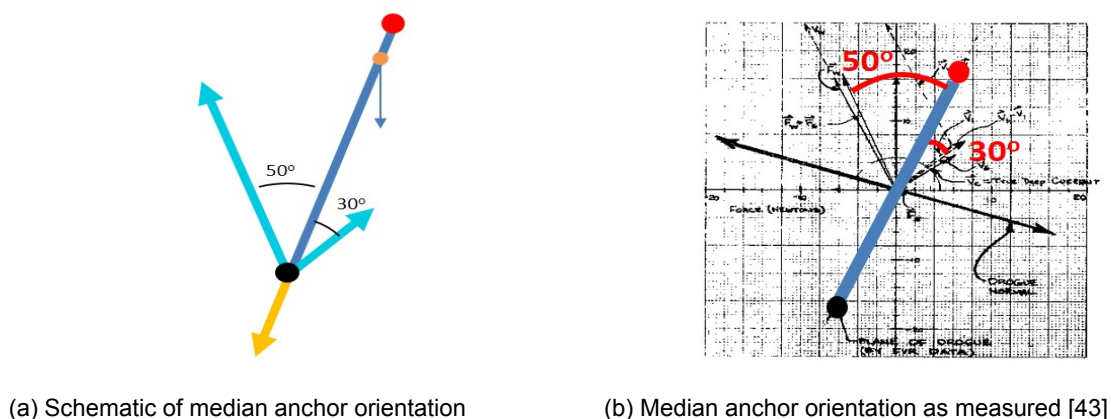


Figure 8.10: Schematics of median anchor orientation simulated and measured



## Sea-anchor evaluation

### 9.1. One degree of freedom stability analysis

Besides the three-dimensional analysis of the 'Window-shade drogue', an additional stability analysis is performed for a one degree of freedom anchor system. Meaning an anchor that only has torsional freedom around a central vertical axis. Figure 9.1 shows this configuration, where  $U$  is the uniform flow velocity,  $\theta$  is the angle of attack,  $\gamma = 90^\circ - \theta$  (in other sections this is  $\theta$ ), and  $\alpha$  is relative angle of attack. Furthermore, the dashpot simulates the structural damping and the torsion spring, torsional stiffness.

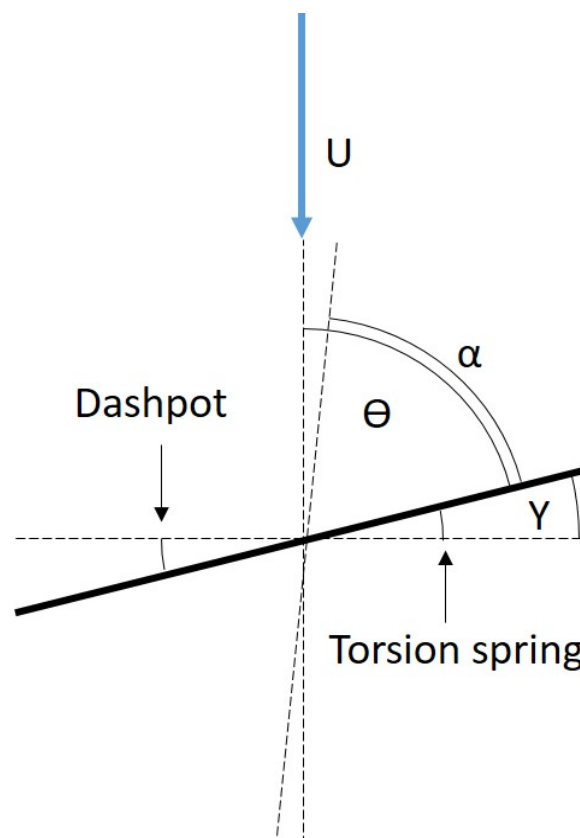


Figure 9.1: One degree of freedom anchor schematic

According to Robber D. Blevins such a system is susceptible to a form of instability called

torsional galloping (all non circular cross sections are ) since self induced oscillating fluid forces can enhance the systems movements [4]. Meaning that the systems energy increases due to a uniform current flow, but subsequently levels out when the effective damping term becomes zero. Therefor it was considered to be of importance to understand the parameters that influence the stability of such a system, and thereby influence the stability of the 'Window-shades drogue'. The obtained information about the stability could subsequently be used as a basis to design a new anchor. Or as a basis for future studies with respect to a 'Window-shade drogue'. Thereby there are specifically two parameters of interest when one would want to adopt the 'Window-shade drogue' behavior, while maintaining the existing dimensions and material of the anchor itself. These two parameters being torsional stiffness and structural damping, since both can be changed by a simple reconfiguration. For example by the introduction of a high torsion cable, and a chain impact damper [4].

According to several articles on torsional galloping of a vertically hinged plate in a uniform flow, the other aspects that influence stability are, the aspect ratio of the plate (or anchor screen), and the velocity of the uniform current [3], [36], [10]. Thereby a specific structural damping and torsional stiffness is assumed in most papers, and the effect of an increase in current velocity is examined. Research on the effect of structural damping and torsional stiffness is therefor an interesting addition to the current body of knowledge. Furthermore, most current analyses discuss instability of a plate at a small angle of attack, whereas this section discusses the instability at high angles of attack. The equation of motion to describe the behavior can be seen in equations 9.1 to 9.3. Where  $\ddot{\theta}$  is the angular acceleration,  $\dot{\theta}$  the angular velocity, and  $\theta$  the angle. Furthermore  $\zeta_{\theta}$  is the structural damping,  $\omega_{\theta}$  the torsional eigenfrequency,  $k$  the torsional stiffness,  $I$  the inertia, and  $I_{66}$  the added moment of inertia.  $\rho$  is the water density,  $A$  the surface area of the plate,  $U$  the uniform flow velocity, and  $C_m$  the steady moment coefficient.

$$(I + I_{66}) \cdot \ddot{\theta} + b \cdot \dot{\theta} + k \cdot \theta = 0 \quad (9.1)$$

Where:

$$b = 2 \cdot (I + I_{66}) \cdot \zeta_{\theta} \cdot \omega_{\theta} \quad (9.2)$$

Resulting in equation of motion of the torsional response:

$$(I + I_{66}) \cdot \ddot{\theta} + 2 \cdot (I + I_{66}) \cdot \zeta_{\theta} \cdot \omega_{\theta} \cdot \dot{\theta} + k \cdot \theta = \frac{1}{2} \cdot \rho \cdot U^2 \cdot D^2 \cdot C_m \quad (9.3)$$

Thereby the moment coefficient has to be determined experimentally, and is therefor assumed to have a dependency on the angle of attack as discussed in section 7.2.6. Furthermore, Robber D. Blevins explains that most galloping analyses utilize quasi-steady fluid dynamics [4]. In which the fluid force acting on the structure is assumed to be only dependent on the instantaneous relative velocity. Thereby opening up the possibility to measure the aerodynamic or hydrodynamic coefficients with static tests. However, this assumption is only valid if the frequency of vibration of the structure is far away from the frequency at which vortex shedding occurs. Meaning that the following statement should hold [4].

$$\frac{U}{(f_n \cdot D)} > 20 \text{ or } \frac{U}{(f_n \cdot D)} < 1 \quad (9.4)$$

Where  $U$  is the current velocity,  $D$  is the width of the anchor screen, and  $f_n$  is the natural frequency in Hz. If this statement is true, quasisteady theory can be used and the equation of motion (9.3) can subsequently be linearized for small relative angles of attack [35], but can also be linearized for large angles of attack. Meaning that the instantaneous angle and relative angle are almost the same. To enable the linearization one has to simplify the angle of attack, which varies over the whole width of the anchor screen, to be evaluated at one single point at

a distance  $R_c$  from the center of rotation. The linearization of angle of attack for large angles can subsequently be calculated as:

$$\alpha = \theta - \arctan\left[\frac{R_c \cdot \dot{\theta} \cdot \sin \gamma}{U - R_c \cdot \dot{\theta} \cdot \cos \gamma}\right] \quad (9.5)$$

$$\simeq \theta, \text{ for } \alpha \simeq 90^\circ \quad (9.6)$$

Furthermore, the relative velocity can be linearized as:

$$U_{rel}^2 = (R_c \cdot \dot{\theta} \cdot \sin \gamma)^2 + (U - R_c \cdot \dot{\theta} \cdot \cos \gamma)^2 \quad (9.7)$$

$$\simeq (U - R_c \cdot \dot{\theta})^2, \text{ for } \alpha \simeq 90^\circ \quad (9.8)$$

$$\simeq U^2 - 2 \cdot R_c \cdot U \cdot \dot{\theta}, \text{ for low velocities} \quad (9.9)$$

By subsequently considering that  $C_m = CM \cdot \frac{U_{rel}^2}{U^2}$ , and expanding CM about  $\alpha = 90$ , equation 9.3 can be written as:

$$(I + I_{66}) \cdot \ddot{\theta} + 2(I + I_{66})\zeta_\theta \omega_n \cdot \dot{\theta} + k \cdot \theta = \frac{1}{2} \rho U_{rel}^2 A (C_m|_{\alpha=90} + \frac{dC_m}{d\alpha}|_{\alpha=90} + \dots) \quad (9.10)$$

The final step in the linearization process, is to substituted the  $U_{rel}$ , and to conclude from Figure 7.10 that  $C_m|_{\alpha=90} = 0$ . Thereby  $R_c$  can be considered to be at the leading edge for small angles of attack, but will her be assumed to be right between the axis and the leading edge [4]. After which, with some rearranging, the equation of motion is:

$$(I + I_{66}) \cdot \ddot{\theta} + (2(I + I_{66})\zeta_\theta \omega_\theta + \rho U R_c A \frac{dC_m}{d\alpha}) \cdot \dot{\theta} + (k - \frac{1}{2} \rho U^2 A \frac{dC_m}{d\alpha}) \cdot \theta = 0 \quad (9.11)$$

From this linearized equation of motion it can be seen that the anchor has two possible types of instability. The first, which is dependent on the effective damping term, is dynamic instability. The second, which is dependent on the effective stiffness term is static instability. Which occur when respectively the effective damping is negative, and when the effective stiffness term is negative. As mentioned earlier both terms are thereby dependent on the current velocity, and on the dimensions of the anchor screen. Furthermore, torsional galloping exists when the effective damping term becomes zero. Which can only happen when  $\frac{dC_m}{d\alpha}$  is negative ( $\alpha$  in degrees). Figure 7.10 shows that the slope of the moment coefficient is indeed negative ( $-0.1848$ ) and almost constant up to  $\theta = + - 50^\circ$ . Which means that considering slow oscillations the required stiffness and damping to maintain stability can be calculated. The boundary of the stability can be found when the effective damping and effective stiffness are zero, and thus:

$$k = \frac{1}{2} \rho U^2 A \frac{dC_m}{d\alpha}|_{\alpha=90} \quad (9.12)$$

$$\zeta_\theta = \frac{-\frac{1}{2} \rho U R A \frac{dC_m}{d\alpha}|_{\alpha=90}}{2(I + I_{66})\omega_\theta} \quad (9.13)$$

Where:

$$\omega_\theta = \sqrt{\frac{k - \frac{1}{2} \rho U^2 A \frac{dC_m}{d\alpha}|_{\alpha=90}}{I + I_{66}}} \quad (9.14)$$

From formula 9.11 it can be seen that static instability can only occur when  $\frac{dC_m}{d\alpha} \geq 0$ , because the torsional stiffness would otherwise have to be negative. Which in means that

in the oscillation range of interest ( $\theta = + - 55^\circ$ ) no static instability will occur, since the slope of the moment coefficient line is negative in this interval. On the other hand it can be seen in equation 9.12 that when  $\frac{dC_m}{d\alpha} \leq 0$  galloping can occur, and which is dependent on the velocity of the uniform flow. Subsequently for the calculation of the required structural damping to prevent instability or galloping, the following parameters were used:

Table 9.1: Parameters for one degree of freedom stability analysis

Parameter	value	unit
Surface current	0.6	m/s
Speed reduction	10	%
$U_{max}$	0.54	m/s
Width D	2.25	m
Height H	9	m
Plate area	$D \cdot H = 20.25$	m
$C_d$	2.5	.
$C_{ma}$	2.5	.
Re	$\frac{U_{max} \cdot D}{viscosity} = 2.7 \cdot 10^5$	.
R	$D \cdot \frac{1}{4} = 0.5625$	m
mass M	$\frac{3}{2} \cdot \frac{1}{2} \rho A C_d U_{max} \cdot \frac{1}{9.8} = 381$	kg
Inertia I	$\frac{mass \cdot D^2}{12} = 161$	$kg \cdot m^2$
Added inertia $I_{66}$	$\frac{1}{6} \cdot \pi \cdot \rho \cdot (D/2)^4 \cdot H \cdot C_{ma} = 2.15 \cdot 10^3$	$kg \cdot m^2$

From the calculations that followed, could be concluded that when no additional torsional stiffness would be introduced, and thereby the effective stiffness is completely dependent on the hydrodynamic stiffness, the natural frequency would be  $\omega_\theta = 0.1669$  degrees/s,  $\omega_\theta = 9.5652$  rad/s. Therefor  $f_n = 1.5223$  Hz, and the reduced velocity  $U_{re} = 0.1577$ . Which means that the frequency of vortex shedding and the frequency of torsional vibration of the structure do not coincide, since the value is below one. Substantiating that in this case linear theory is applicable. Thereby the damping ratio would need to be at a minimum of  $\zeta_\theta = 0.0869$  to prevent the system from galloping, and thereby to ensure a stable system. If torsional stiffness is subsequently introduced to further limit the movements of the anchor screen, the natural frequency will change, and thereby the required structural damping will change. The required damping and stiffness to prevent instability is thereby dependent on the velocity of the uniform flow. A lower flow velocity would result in a lower natural frequency, which results into a requirement for a higher damping ratio. While the velocity term in equation 9.12 results in a lower damping ratio requirement.

Furthermore, coming back to possibility of vortex shedding. An increase in flow velocity and an increase in torsional stiffness can result in a higher natural frequency, which in turn effects the reduced velocity (equation 9.4), and therefor the chance on vortex shedding. Another method of analyzing of vortex shedding might occur is based on research performed by Fernandes et al, which shows that the Strouhal number will be around 0.2 for a vertically hinged plate in uniform flow [9]. Therefor the vortex shedding frequency can be approximated to be:

$$f_s = \frac{St \cdot U}{D} \quad (9.15)$$

Which results in a shedding frequency of 0.048 Hz, and which is very different from the natural frequency of the system without the introduction of additional torsional stiffness (1.5223 Hz). Based on these results it can be concluded that for the situation in which the anchor is towed straight through the water at maximum surface current and at a speed reduction of 10%, the anchor will remain stable at a structural damping ratio of 0.09. However, when the speed decreases: the effective torsional frequency decreases, the required damping ratio for stability changes and the reduced velocity changes. Thereby possibly making linear theory

invalid. Furthermore, as shown the system is statically stable in a straight tow without any additional torsional stiffness.

## 9.2. Sea-anchor design

The performed analyses on the 'Window-shade drogue' shed light on a few issues considering the applicability of the drogue for the use as a Ocean Cleanup sea-anchor. The first being that the 'Window-shade drogue' seems to be quite unstable, and the second being that for the drogue to generate lift in a specific intended direction, the system had to be redesigned.

Solving both issues required an iterative process in testing design options and performing some additional test on the 'Window-shade drogue'. These additional test where to see if the 'Window-shade drogue' could be adopted for generating lift. William A. Vachon indicated that introducing an unbalance of weight at the bottom of the drogue, could cause a the drogue generate lift in unwanted directions, which in the case of an Ocean Cleanup sea-anchor could be beneficial. However, when analyzing this behavior it could be seen that the unbalance caused the drogue to eventually turn parallel to the current.

The subsequent steps were focused on adapting the anchor to generate lift in a specific required direction, and to decrease the standard deviation of the angle of attack. Since the latter indicates instability, and the first is needed to open the barrier perpendicular to the flow. The first design step was to introduce a weight on the mooring-line at 24 meters water depth, and to reduce the submerged sea-anchor weight to zero. While at the same time the tension on the anchor screen was kept at 1.5 times the maximum expected drag force [43]. This could be done by increasing the buoyancy force on the top rigid rod of the anchor. The configuration can be seen on the left side in Figure 9.2a, where the mass on the mooring-line is indicated with a black sphere. In this configuration the anchor would always stay at required depth, independent of the relative current velocity.

The sea-anchor was subsequently tested under a one directional surface current, and tested for a rectangular shape and a thin long triangular shape (see Figure )9.2b. The rectangular sea-anchor has an evenly distributed weight at the top and bottom, causing the system to be able to twist in it's plane around the center of the screen. With a triangular anchor this is not the case. When the top bar turns away from the horizontal plane in the vertical plane, a moment is introduced by the weight at the tip of the anchor. Which is caused by the fact the the turning of the top bar reduces the tension in one side of the anchor and increases it at the other side, restoring the anchor to the intended position. Therefor the thin triangular configuration of the anchor was used all the results presented in this chapter. Thereby acknowledging the fact that a thing triangular anchor has a complicated dependency of the hydrodynamic center location on the angle of attack. As discussed in the section on model assumptions in chapter 7, step wise linear dependency was used in the model. Whereby the hydrodynamic center moves towards the leading edge and not towards the trailing edge. The latter having a negative effect on anchor stability when positioned under an angle.

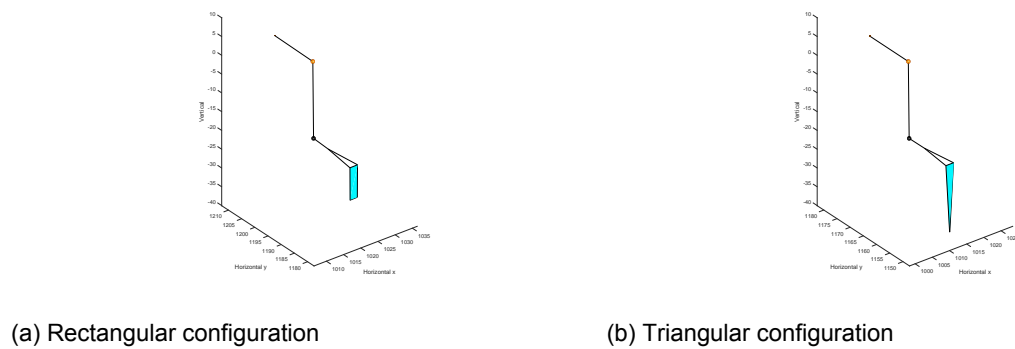


Figure 9.2: Adopted anchor configurations

To be able to evaluate these anchors, two new angle measurement methods had to be introduced. The first method involved the measurement of the angle of attack and the relative angle of attack. To be able to constantly assess the anchors orientation over a time trace, the angle was calculated counter clockwise from the respective force vector to the anchor. This method can be seen in Figure 9.3a. Subsequently an additional angle was introduced to determine the direction of the relative current. Being the compass angle to define the direction of the relative velocity vector, while the anchor was being towed in a straight line (see Figure 9.3b).

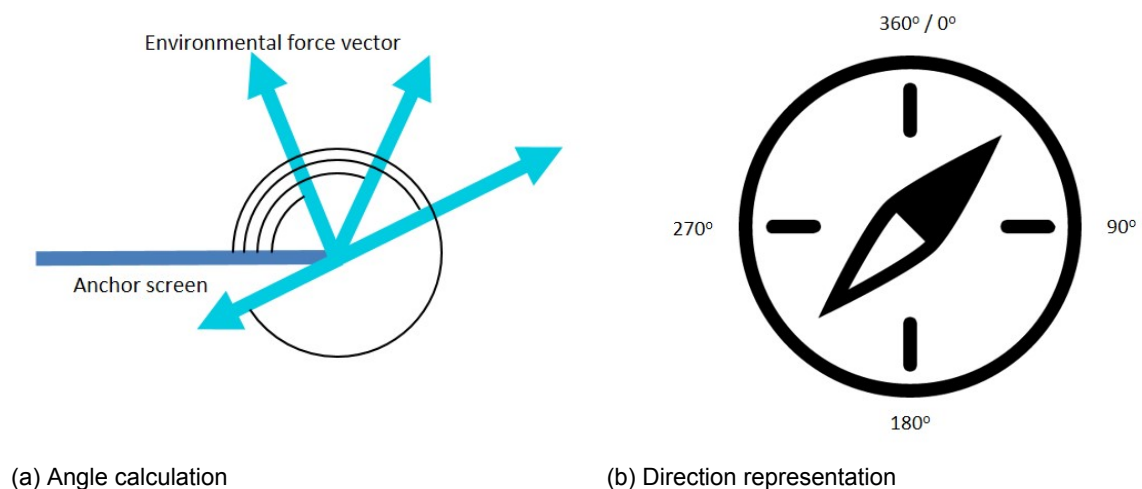


Figure 9.3: Angle calculation and relative velocity direction representation

Figure 9.4a shows the result of a straight tow of the triangular anchor. Whereby Figure 9.4b gives an explanation of the legend. Based on new information from the Ocean Cleanup, indicating a maximum surface current of  $1.2m/s$ , the anchor was towed under a surface current velocity of  $1.2m/s$  while the uniform flow at anchor depth had a velocity of zero. Figure 9.4a shows that the angle of attack of the anchor with the uniform flow, remains around  $270^\circ$ , meaning an angle of attack of  $90^\circ$  according to aeronautical definition. On the other hand Figure 9.4a also shows that the relative angle of attack varies around the  $270^\circ$ . Indicating that the anchor moves from left to right under very small actual angles of attack, and thereby creating an unstable apparent current.



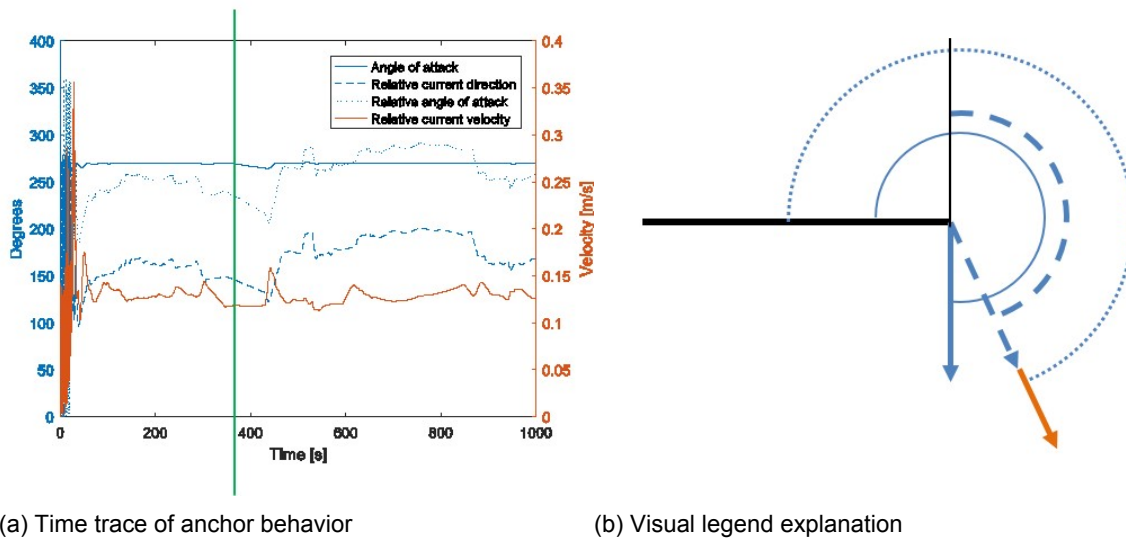
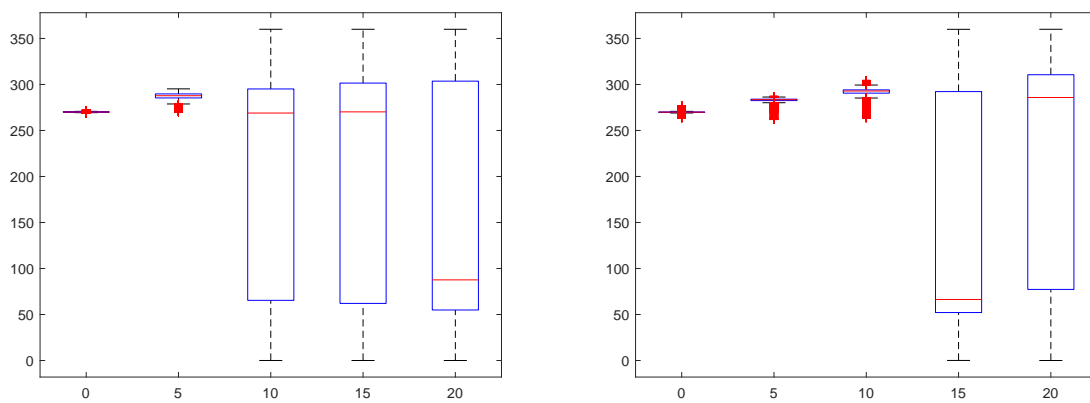


Figure 9.4: results of straight tow of the triangular adopted anchor

The anchor was subsequently forced under different angle of attack by reducing the cable length of one of the cables connected to the anchor. This was done for both the situation in which the hydrodynamic center is dependent on the relative angle of attack and for a situation where that would not be the case. With the intend of showing the stabilizing or destabilizing effect of hydrodynamic center dependency on the angle of attack. Which has to be investigated more thoroughly in future studies. The results of theses test are shown in the box-plots in Figure 9.5 Where the horizontal axis indicates the forced angle, and the vertical axis the angle of attack. It can be seen that the anchor with the hydrodynamic center always in the middle of the anchor, has a stable position towards the uniform flow up to a forced angle of ten degrees, but starts to become unstable above this angle. Furthermore, the anchor with hydrodynamic center dependency on the angle of attack, becomes unstable at a force angle of  $15^\circ$ .



(a) Anchor with hydrodynamic center always in the center (b) Anchor with hydrodynamic center angle dependent

Figure 9.5: Boxplots of angle of attack versus forced anchor angle

Examining the forced angle of  $20^\circ$  for the anchor with hydrodynamic center dependency on the angle of attack, one has to look at Figure 9.6, where Figure 9.6b shows the schematic

representation of the lines at a time of around 360 seconds. From these Figures it becomes clear that the anchor becomes unstable under a force angle of  $20^\circ$  due to the relative angle of attack and the related direction of the relative current. When the anchor is positioned under an angle a lift force is generated and the anchor starts moving in the direction of the lift force. At the same time the lift forces increases as the angle of attack increases, until at some point the relative angle of attack changes from below  $360^\circ$  to over  $0^\circ$ , resulting in a relative current that tips over the anchor. Subsequently the same effect is induced towards the other side as the anchor line is now shorter at the opposite side.

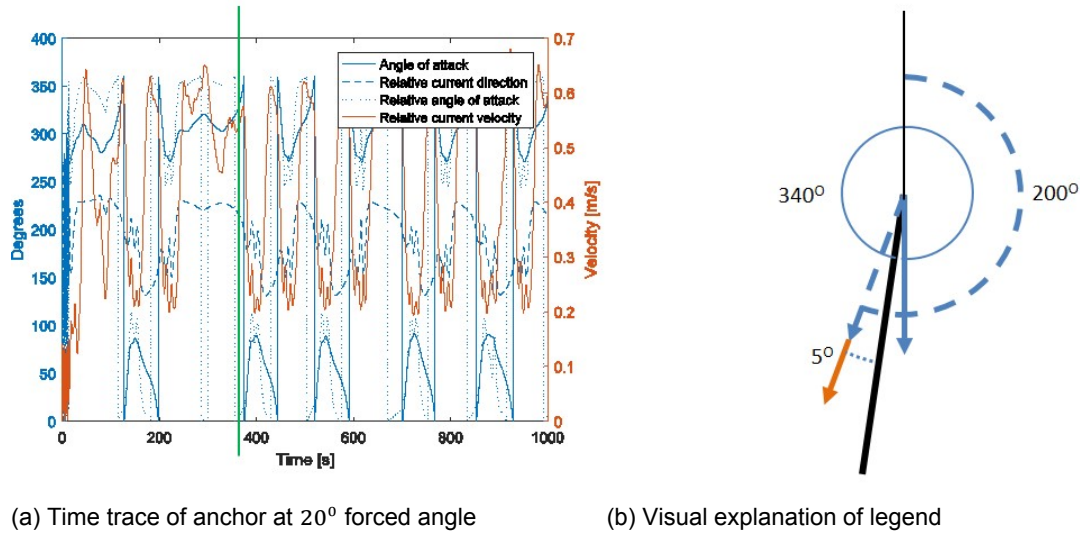


Figure 9.6: Result of anchor with hydrodynamic center dependency under a forced angle

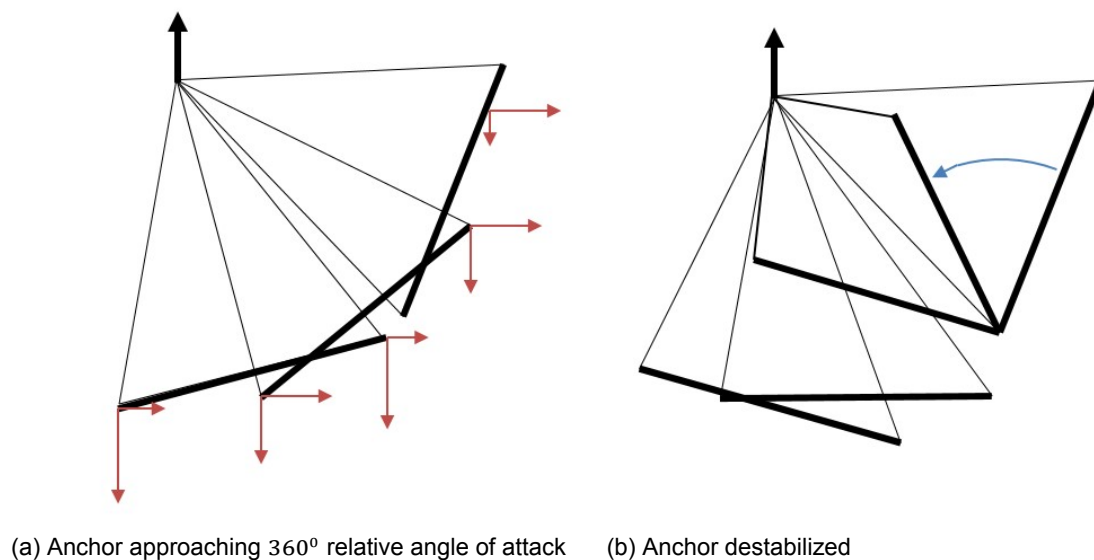


Figure 9.7: Visual explanation of anchor behavior

This overshoot of the  $360^\circ$  relative angle of attack can be seen to be related to accelerations of the anchor. As in Figure 9.6a the relative angle of attack quickly rises when the relative velocity vector is steep. In order to investigate this dependency the mass, the

normal added-mass, and bi-normal added-mass, were varied. A better understanding of this dependency was thereby thought to be necessary to be able to design methods of preventing instability. Figure 9.8 shows boxplots of mass variations, with the angle of attack on the vertical axis. Figure 9.8a shows the effect of a variation in mass [1.5, 15, 150 times the maximum expected dragload] on the angle of attack. Figure 9.8b shows the effect of a variation in mass on the angle of attack when the added-mass in normal direction is ten times lower than originally assumed. Figure 9.8c shows the effect of different levels of added-mass [kg] in bi-normal direction on the angle of attack, at a mass of 15 times the maximum drag load.

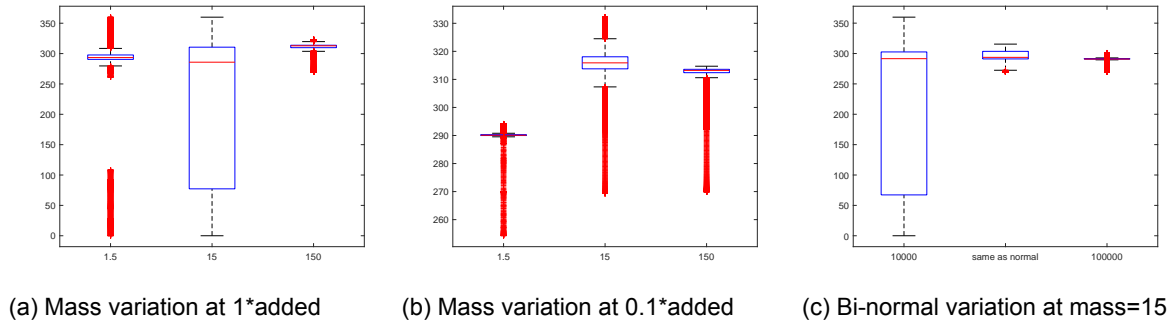


Figure 9.8: Boxplots with the angle of attack versus mass variations

Figure 9.8 indicates that an increase in mass can either stabilize or destabilize the anchor. Which is due to the fact that at a certain increase of mass the anchor still accelerates quickly but does not decelerate quick enough to prevent the relative angle to increase over  $360^\circ$ . While an even larger increase prevents the anchor from accelerating all together. Furthermore, the reduction of bi normal added mass reduces the amount of lift generated due to acceleration forces. Thereby the anchor system stabilizes. On the other hand, decreasing the bi-normal added-mass reduces the forces needed to accelerate the anchor into the direction of the generated lift, whereas increasing the bi-normal added-mass increases the forces needed for acceleration. Figure 9.9 shows the effect of an increase in bi-normal added-mass since this was considered to be most effective and most realistic to enable in any future anchor design.

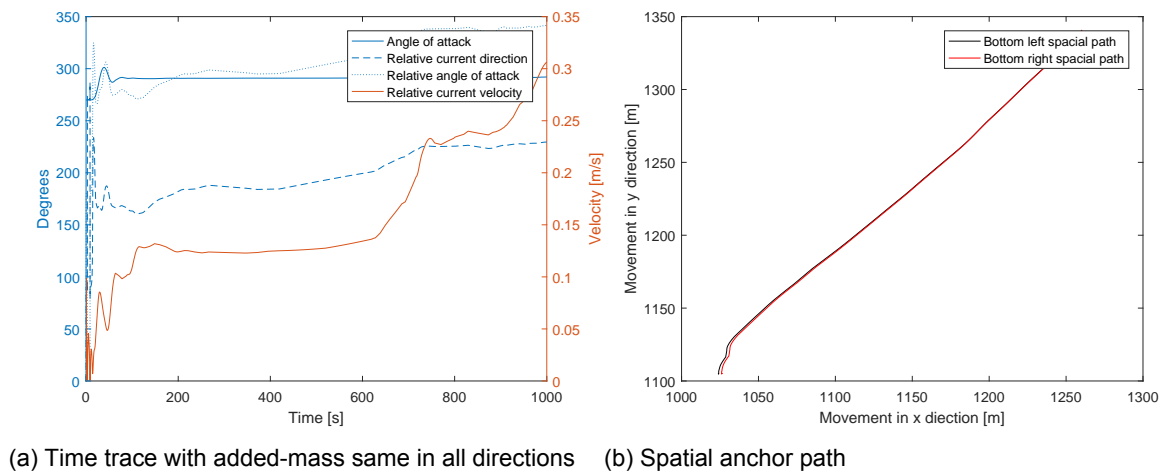


Figure 9.9: Result of an anchor with high bi-normal added-mass

From Figure 9.9a it can be seen that the anchor is stable during the complete simulation

but that the relative angle of attack slowly rises towards  $360^\circ$ . Thereby Figure 9.9b shows that the anchor starts of normal to the uniform flow but quickly streams parallel to the relative velocity. This in turn indicates that the system is inherently unstable since the anchor will always approach a parallel orientation with the relative current. From which point, any acceleration could destabilize the anchor. The only solutions in the the presented anchor design to prevent this destabilization was to replace the cables connector to the anchor by rigid bars. Any potentially destabilizing acceleration would then be counteracted by the towing force induced by the uniform flow. Figure 9.10a shows the time trace of the anchor with rigid bars to force the anchor under an angle of  $20^\circ$ , resulting in an angle of attack with the uniform flow of  $30^\circ$ . Thereby figure 9.10b shows a path without any instabilities, with the anchor oriented parallel to the relative current.

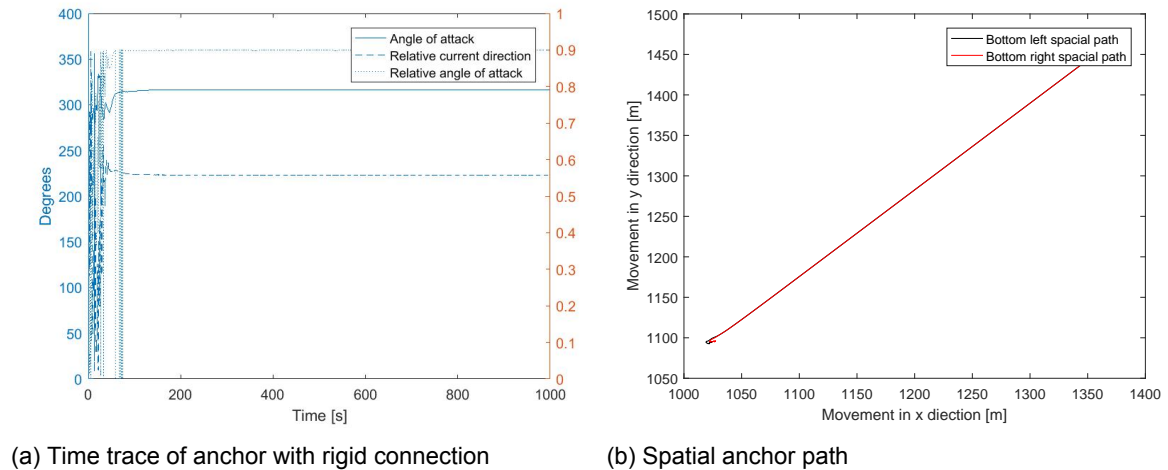


Figure 9.10: Result of an anchor with rigid bars to force the angle

It has to be noted that for these simulations the hydrodynamic center was modeled to be at the leading edge. Depending on the eventual size and shape of the anchor, this location could also be at the trailing side or at the center. As shown in Figure 9.5 this could potentially destabilize the anchor. However it is presumed that the use of a rigid construction to force the angle of attack, can overcome these instabilities. Furthermore, a limitation to the selection of the triangular anchor configuration is that research indicates that an insolence triangle might move through the water in a helical pattern [26], [2]. Which in turn might also hold for the thin triangle with small aspect ratio. Experimental research would have to be performed to analyze if this behavior indeed will occur. To conclude, it was determined that since a suitable anchor was now designed, the process should continue to the construction of a three-dimension concept model. When this would be achieved, the anchors could be reanalyzed as part of the system, since other behavior such as fishtailing was expected to occur.

## **Part IV**

# **Concept feasibility**



# 10

## Three-dimensional concept model

After a preliminary sea-anchor was designed, the complete mobile cleaning concept needed to be modeled. Chapter 10 discusses the process that was needed to convert the three-dimensional anchor model into a three-dimensional concept model. The chapter starts with the definition of test cases needed to evaluate the concept. subsequently, the evaluation criteria that are needed to quantitatively judge the concept feasibility are set-up. In section 10.2, the actual foundation of the model is discussed. Whereby new and additional assumptions are presented, the system set-up is discussed, and the verification of the model by means of convergence tests is shown. Following from the first three-dimensional model and first simulation results, the system was subsequently adopted during an iterative process (which is discussed in chapter 11), with the intend to solve issues around the efficiency and functionality of the system. This process eventually led to the three configurations seen in Figure 10.1 Of which in turn multiple variations where tested under the design cases, which will be discussed in chapter 11.

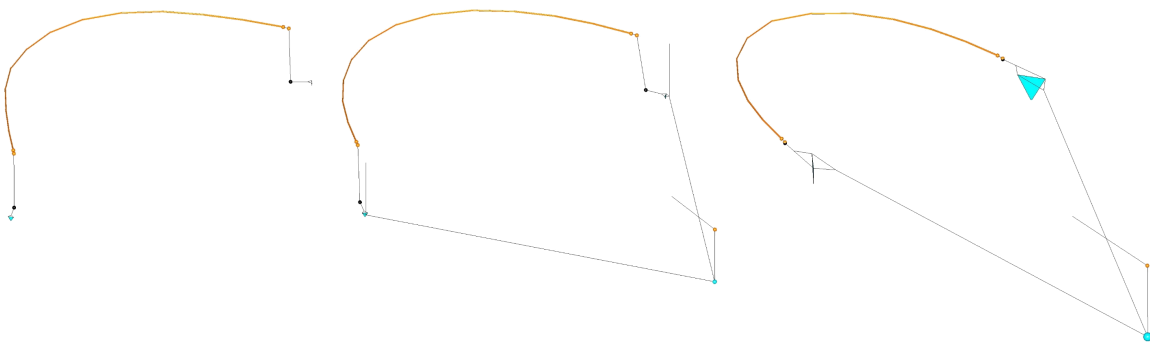


Figure 10.1: Three basic system designs derived from the high level concept selected in chapter 3

## 10.1. Test-cases and evaluation procedure

To test and evaluate the high level concept selected in chapter 4, it was of importance to define the most critical factor in the concepts feasibility. Meaning that it had to be determined which factors with regard to concept performance would be of highest influence. These factors could be the effect of current conditions, wind conditions, and wave conditions, on Mesoscale motions or on system scale motions. But could also be factors such the effect of wave conditions on line/barrier loads, plastic retention, or sea-anchor behavior.

To evaluate which factors would be of most importance the Value Drivers were reassessed, and the it was considered which factor were likely able to be mitigated and which would be completely dependent on the in chapter 4 selected concept. The Value Drivers seen in Figure 1.4, show that the efficiency of the system is regarded as most important after inspirational and environmental impact, which have been assessed previously. Whereby the efficiency is dependent on the amount of Plastic, per kilometer boom, that is caught per week. In chapter 2 it was shown that the plastic in the Great Pacific Garbage Patch is for the largest part completely submerged in the first two meters of the water column [34]. Furthermore, in chapter 4 it is explained that research performed by the Ocean Cleanup showed that a speed reduction of 10%, together with a current following behavior similar to plastic, would result in the highest efficiency. Besides this, the concept selected in chapter 4 is for the largest part completely submerged, and its 'shape retention' is enabled by hydrodynamic force. Lastly, experimental research by the Ocean Cleanup indicated that drag forces on the boom due to waves can be neglected with respect to current.

Together, all these arguments lead to the conclusion that most dominant factor in system feasibility was the current driven system behavior. To determine the exact current conditions present at the intended deployment location, data form the HYbrid Coordinate Ocean Model (HYCOM) was analyzed. The data included in the HYCOM model is continuously updated based on measurements, new simulations and predictions [6]. The data provides insight into surface currents but also provides information on the current depth profile seen in Figure 4.2a. The information from the HYCOM model and literature on ocean current flow, indicated that the current velocity vectors are highly variable in space and time, or more specifically, in the horizontal and vertical plane. Meaning that at one set of coordinates, provide by HYCOM, the current over depth varies in velocity and direction (see Figure 4.2a). Furthermore, the surface current varies in direction, with a 10th percentile 36 degrees/hr, a median of 16 degrees/hr, and a 90th percentile of 12 degrees/hr. Figure 11.14 shows the probability calculation of rate of direction change for six locations in the Great Pacific Garbage Patch over ten years, for the median case. Which was subsequently determined to be 16 degrees/hr.

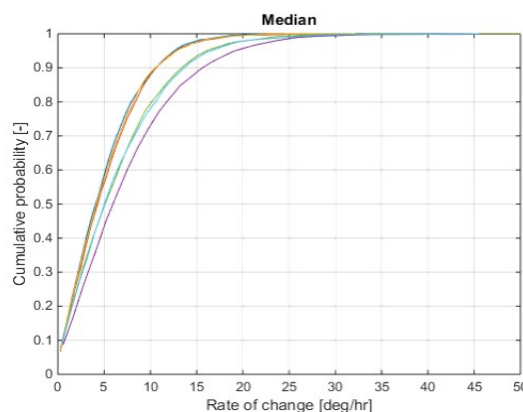


Figure 10.2: Probability of median rate of change of the surface current direction

This rate of current direction change was thought to be of high influence on the systems



feasibility. As discussed in earlier in this section, the system should be able to follow the plastic as precisely as possible, and since the plastic follows the current [34], the system should follow the current as precisely as possible. To be able to determine these effects of the current on the system, a clear definition of system efficiency and functionality had to be defined. It was thereby chosen that the concept would be tested under median current conditions and if proven to be feasible, other conditions would subsequently be tested. The test conditions were:

1. Straight median current, with the current over the entire water column in the same direction
2. 16 degrees/hr change of current direction for 81000 seconds to simulate one complete turn
3. Current returns back into a straight line to identify if the system is able to recover if failed

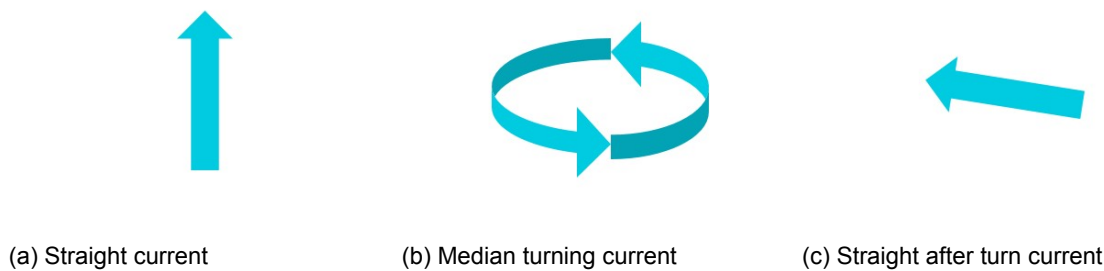


Figure 10.3: The three different test executed for the concept feasibility analysis

### 10.1.1. Functionality

The system is defined to be functioning when the state of the system indicates that it is operating within its defined limits. These limits are subsequently defined as maximum relative spatial element movements, from which system is thought to be able to reattain its convergence state, after it endured a changing current direction.

The first limit is the crossing of an element such as the anchor (or the barrier itself), of the line between the two outer nodes of the barrier. Whereas the second type of limit is the crossing of the extended line of the line between the two outer nodes of the barrier (depicted in Figure 10.4). Meaning that the anchors or barrier pass around the outer barrier nodes. When the limits are exceeded it is defined to be a system failure. Either the barrier has been scrambled into an unwanted shape, or the anchor has past a line after which it might generate lift in the wrong direction. During the simulations the systems state is constantly evaluated and if a limit is exceeded it is noted as a failure in functionality. Where a crossing of the red line in Figure 10.4 is an inner span failure, and a crossing of the orange line is an outer span failure. Due to the complexity of the system it was decided that the system should be able to operate without such failures, since the real life behavior after such a failure could not be predicted.

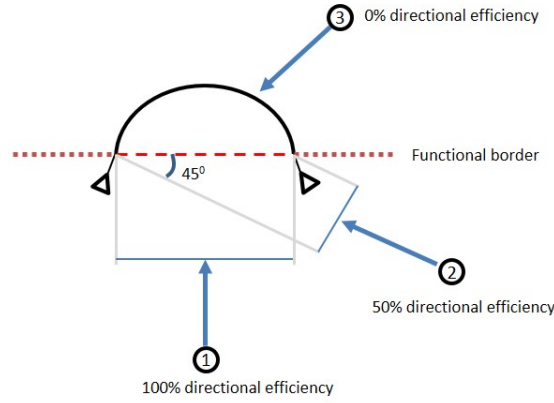


Figure 10.4: Visualization of functional limits and projected span width

### 10.1.2. Efficiency

The efficiency of the system can be considered from three different perspectives. The first would be the directional efficiency, which defines the ability of the system to follow the current and maintain a 90 degrees angle between the span of the 'catching opening', and the direction of the current. From this perspective a current coming from direction 3 in Figure 10.4, would result in an directional efficiency of 0%.

The formula for directional efficiency introduces a term called 'effective span' and 'real span', where effective span is calculated as the width of the span project at a 90 degrees angle to the current, and the real span is calculated as the real time distance between the two outer nodes of the barrier.

$$\text{Directionalefficiency} = \frac{\text{effectivespan}}{\text{actualspan}} \cdot 100 \quad (10.1)$$

The second type of efficiency is defined as 'opening efficiency', and indicates the ability of the system to maintain the span width at the same level as during the straight convergence test (discussed in 10.2.3). When the span width decreases the 'opening efficiency' decreases. The optimal span width, which would result in a 100% 'opening efficiency' is called 'convergence span'. It is important to note that the 'opening efficiency' for some systems can exceed 100%, since when no line is attached between the two outer barrier nodes, the opening can increase above the 'convergence span'. In fact this increase would actually result in a larger ocean surface coverage and therefor result in a larger efficiency.

$$\text{Openingefficiency} = \frac{\text{actualspan}}{\text{convergencespan}} \cdot 100 \quad (10.2)$$

The final type of efficiency is called total efficiency, and is defined as the effective span over the convergence span. It indicates the total efficiency of the system since it takes into account which ocean surface area has been covered in respect to what could have been covered if the system would have perfectly followed the current with a 90 degrees angle to the direction of the current.

$$\text{Totalefficiency} = \frac{\text{effectivespan}}{\text{convergencespan}} \cdot 100 \quad (10.3)$$

### 10.1.3. Anchor evaluation

Besides the evaluation of functionality and efficiency of the system, the sea-anchor behavior is discussed based on their angle of attack over time and on the resulting spacial path. As discussed in chapter 6, it was expected that the anchors could start fishtailing [46]. The direction of the lines connecting the anchor to the system will be in a different direction the the relative current. possibly causing an unstable equilibrium. It is this unstable equilibrium that could cause fishtailing, and it could be further enhanced by the fact that the angle between the tension force and drag force on the anchor will be small [46].

## 10.2. Assumptions

For the construction of the three-dimensional system model the same lumped mass approach was used as for the sea-anchor model. The model was simply extended by introducing more elements with the correct physical properties and required connections. Besides that, the same drag and added mass coefficients where used. With the screen of the barrier being considered as a vertical positioned flat plate. The screen of the barrier was assumed to have circumscribing cylinder with a diameter of the screen height as added-mass volume.

The stiffness for the lines in the system was again chosen to be as low as reasonably possible, which came down to the selection of the materials in table 10.1. However, according to Van den Boom [44], the mooring-line tension would effect the the dynamic behavior of the light weight surface system. This means that when the system will be simulated in wave conditions, the material of the lines and barrier should be varied to analyze difference in behavior. As to the size of the system and the required anchor dimensions, the base case defined in chapter 4 was used. The values attributed to this base case can also be seen in table 10.1.

As for the number of elements/nodes used in the model, the barrier and anchors were presumed to be the primary driver behind hydrodynamic behavior. Whereas the other elements would mostly influence behavior through tension forces. This, in combination with the need for computational efficiency, led to the assumption that only the number of nodes for the barrier would be determined through convergence tests. The anchors were assumed to be tensioned in such a ways that they would behave as a flat plate, and the number of nodes was therefor limited to 4 per anchor (as in the sea-anchor model). The other lines in the concept are all modeled as single elements with variable stiffness. Thereby simulating tethers that can go 'slack'.

Furthermore there are several other limitations to the model:

- The buoyancy of the floating elements is modeled as a thin cylinder
- Free surface effects are not incorporated
- The effects of actual flow of the fluid around the elements is unknown
- The hydrodynamic center of the barrier elements is not dependent on the angle of attack
- There is no torsional stiffness in the system
- There is no bending stiffness in the system

The buoyancy of the surface floating elements was introduced at the appropriate masses, where the element behavior was simplified to be a thin vertical cylinder. This oversimplification was done to reduce the amount of vibrations, which considerably reduced computation time, and can be justified since during the test cases no waves were introduced, or of interest. In the case that waves need to be simulated, the buoyancy of the floating elements will have to represented by a cylinder or an ellipse, depending on the design of the barrier. Furthermore, free surface effects have to be incorporated in these conditions. The model presented

herein is completely submerged and only experiences forcing due to current loading.

For a more detailed analyze on system behavior it is important to investigate experimentally how the fluid actually flows around the barrier, and how the hydrodynamic center of the barrier relates to the angle of attack of the barrier to the flow. Both effects could seriously influence the behavior of the system but can only be determined experimentally or with the use of computational fluid dynamics. In the here presented model, the flow of the water is assumed to have no effect on the forces on the barrier, whereas in reality the water flowing under the barrier will generate a complex pressure distribution, which could either increase or decrease the closing force of the barrier, depending on the depth of the screen. The angle of attack of the barrier, to the incoming flow, could have a similar effect. Xavier Ortiz, David Rival and David Wood, state that with a small aspect ratio, which is the case for the barrier in the horizontal plane, the hydrodynamic center moves to the leading edge [31]. Depending on the orientation of the barrier towards the incoming flow, this could result in a higher closing force or in a lower closing force. All in all, the situation is extremely more complex than simulated in the basic model presented in this thesis. However, it was presumed that if the model discussed here would indicate that the system is feasible, efforts could be made to perform more detailed analysis.

As with respect to the torsional and bending stiffness, the limitations have foremost to do with the ability to model other concepts, and secondly they have influence on the systems behavior. The influence on system behavior has mostly the torsional stiffness which is not incorporated. The bending stiffness can be neglected due to the selected concept, which makes uses of a flexible barrier and flexible lines. The lack of torsional stiffness on the other hand could have significant effect on the sea-anchor behavior. The movements of the anchor are currently less constraint than with the simulation of torsional stiffness. However, this can be justified, since if the concept proves feasible under these less constraint assumptions, it will likely also be feasible when torsional stiffness is incorporated.

### 10.3. System set-up

The system was build by using the previously sea-anchor model as a bases. Since the high level concept selected in chapter 4 consists of two anchors and one flexible barrier in between, the complete system could simply be modeled by connection more flexible elements to the anchor, giving them the correct material and dimensional properties, and subsequently connecting them at the correct nodes. The properties can be seen in table 10.1.

Table 10.1: System parameters

System element	Size	Material	E Modulus
Barrier	1.37 km	Polyester	$3.05 \cdot 10^6$
Cables	1-1000 m	Polyester	$3.05 \cdot 10^6$
Anchor rudder	172 m <sup>2</sup>	Nylon	$3.30 \cdot 10^5$
Surface rudder	3962 m <sup>2</sup>	Nylon	$3.30 \cdot 10^5$

In terms of modeling the local matrices had to be connected in a manner that represents the system. This set-up can be seen in the form of the assembled system matrix for system 1 (Figure 10.1, left), depicted in Figure 10.5.

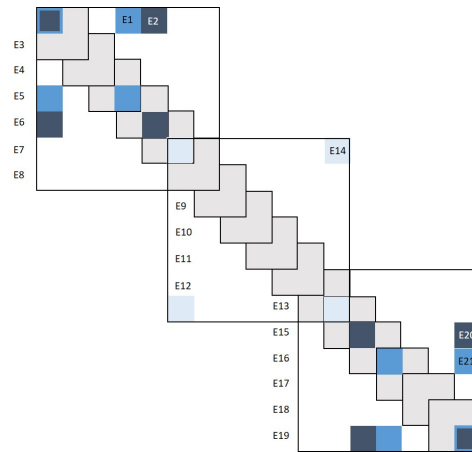


Figure 10.5: Matrix assembly of the first model

## 10.4. Convergence test

After finalizing the three-dimensional system model, several convergences test were executed, during which the drag force and 'closing force' were measured, and was determined which minimal amount of nodes was required to converge both in force on the system as in shape of the system. The convergence tests were performed for different barrier lengths with the same span width, and the 'closing force' was measured by analyzing the force in a spring between the two outer nodes. The different barrier lengths were presumed to be influencing the system behavior in different ways, and therefor the necessary convergence tests needed to be performed. The resulting amount of nodes varied between the 8 and 12 depending on the length of the barrier. However, the number of nodes required for a inline load case, determined through this method, was different from the number of nodes needed when the system undergoes a current that changes direction. In this case the shape of system can become complex, and 8 to 12 nodes for a barrier length of 1.37 kilometers therefore showed unrealistic behavior. To ensure the number of nodes would be sufficient, every basic configuration of the three main concept variations, was tested for convergence in a rotating current direction. Starting with the number of nodes determined in the straight convergence tests, the rotating current would be simulated multiple times, with a increased number of nodes for every simulation. When the concept in two subsequent simulations had the same shape and position, convergence was said to be met. For the first system this came down to the three test depicted in Figure 10.6 From which was determined that 24 nodes was sufficient.

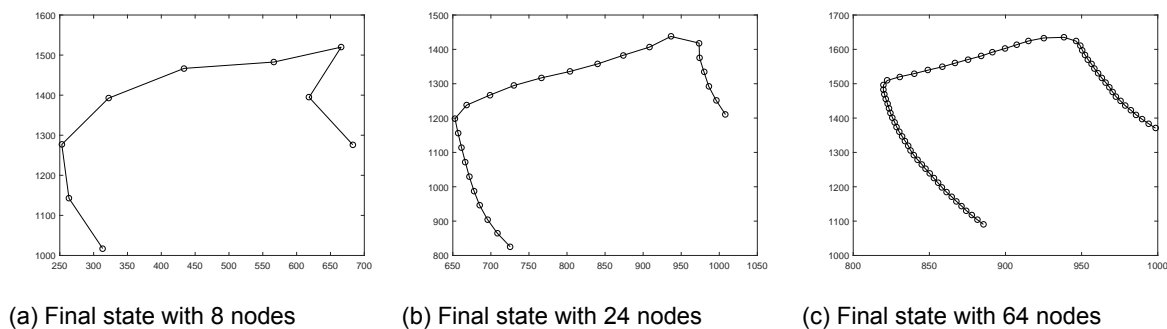


Figure 10.6: Convergence test for system 1



## Concept evaluation

In order to accomplish the final objective, the selected concept was submitted to the test program defined in chapter 10. The concept was subsequently altered to solve apparent issues. This resulted in an iterative innovative process, through which 11 concept variations were designed and tested. These 11 variations exist out of 3 main variations that are significantly different with respect to each other: the Hydroforce-boom, the Hydroforce-boom with anchor connector, and the Hydroforce-boom with surface rudders. This section will elaborate on the reasoning behind the design steps and will evaluate system performance and behavior based on time traces of the directional en opening efficiency.

### 11.1. Hydro-force boom

The first simulated concept system seen in Figure 11.1b is the three-dimensional model of the concept selected in chapter 4 (see Figure 11.1a).

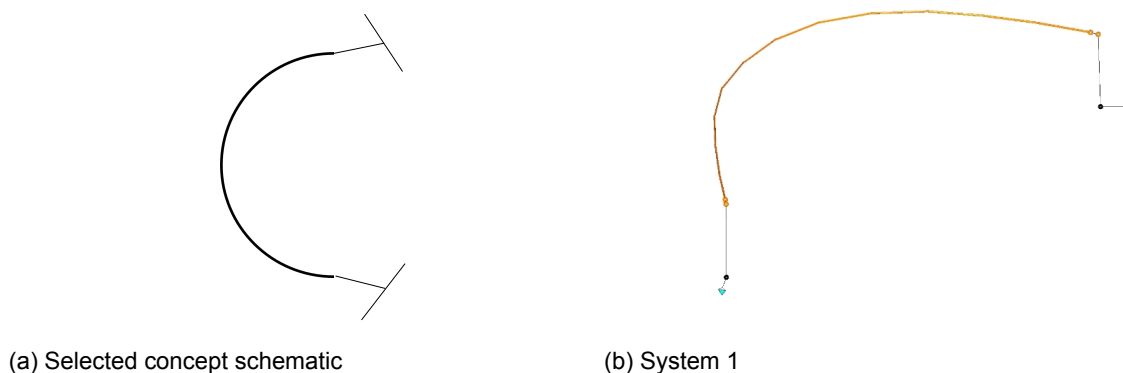


Figure 11.1: Selected concept schematic and three-dimensional model

The system was tested according to the defined test program, in a straight current, changing current direction, and in a straight current following the turn. The system showed a high opening and directional efficiency in a straight current, but was unable to properly follow the changing current direction. During the straight current test both anchors were analyzed and special attention was given to potential fishtailing behavior. This behavior was expected to occur because the behavior of the barrier was presumed to lead to an unstable equilibrium of the anchor. Which, according to Wichers, could lead to fishtailing, and thereby create high mooring loads and unwanted behavior [46]. Figure 11.2 shows the time trace of the behavior of the left anchor during the straight current test of system 1. In which the same convention

for the legend is used as in chapter 9. Thereby an explanation regarding the depicted angles is necessary. Where in chapter 9 the anchor was forced under an angle to generate a lift force to the right, the anchor presented here generates a lift force to the left. Therefore the angle relative angle was expected to be between  $180^\circ$  and  $270^\circ$ , of which the latter means an actual angle of attack of  $90^\circ$ .

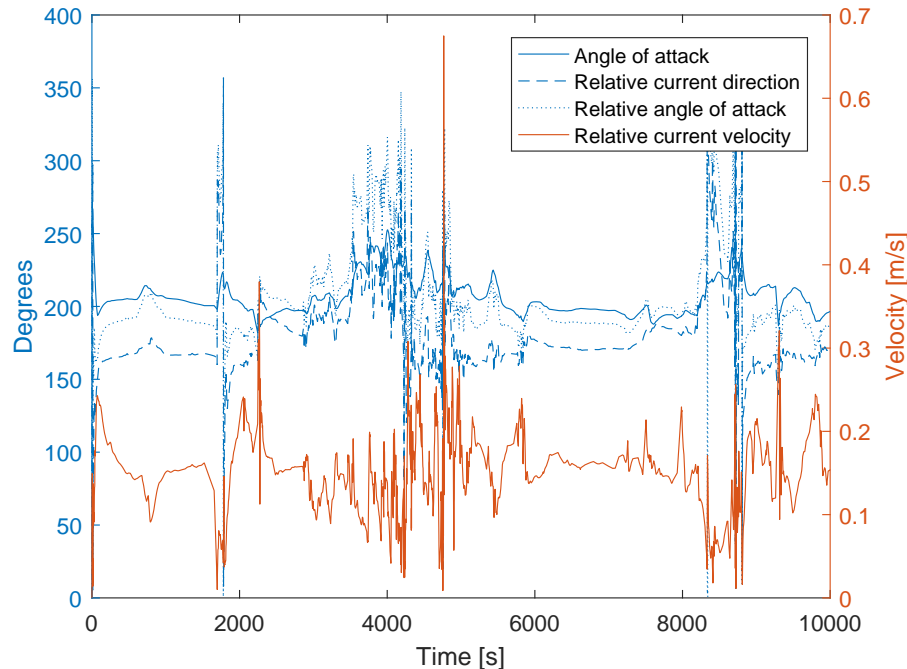


Figure 11.2: Time trace of the left anchor with rigid angle forcing

From the graph it can be seen that the relative angle of attack has a mean around  $180^\circ$  degrees, which means the relative angle of attack with the leading edge has a mean around  $0^\circ$ . This is what one would expect based on the data presented in chapter 9, but it is also clear that the anchor has unstable moments, after which it returns to the mean position. This behavior is caused by the fact that the barrier is pushed forward by the current but at the same time exerts a closing force. This closing force, which is caused by the barrier being contracted, creates an unstable equilibrium for the anchor, by creating a relative velocity which has a small angle with the current velocity at anchor depth. Which is according to Wichers a situation in which fishtailing occurs [46].

Nonetheless, the system performs as intended in a straight current. The barrier remains open and the span opening of the system remains at an angle of  $90^\circ$  degrees with the incoming current. However, when the current started to turn counter clockwise, the drag force exerted by the current increased at the trailing side of the barrier while decreasing at the leading side (the side that is forward into the current with respect to the other side). Since the trailing side and leading side are only connected by the barrier, the drag force spread the system into almost a straight line, after which first the anchor at the leading side turned around the mooring line it was directly attached to, and secondly the anchor at the trailing side did the same. The system had hereby completely failed to follow the flow, and the current was subsequently directed towards the wrong side of the barrier. Since the anchors had turned around their respective mooring-lines, they exerted a lift force that led to a slowly decreasing span width. Although the barrier took on a more curved shape and started turning, the force on the leading side quickly decreases again, and the barrier fails to make a turn. Subsequently the barrier crosses itself (system is considered scrambled), and the barrier could not recover, since one of the anchors generated lift in the direction of the other anchor. The decrease of drag



force on the leading side of the barrier was identified to be the main driver in the inability of the system to adequately follow the current. Therefore a method had to be designed to ensure that the leading side of the barrier would experience more force when the turn initiates. Besides this a method had to be designed to prevent the anchor from turning around the connected mooring-line. These two methods came respectively in the form of a 'cross-line' seen in Figure 11.3a, and in drag spheres connected to the anchors seen in Figure 11.3b. The 'cross-line', is a cable between the two outer nodes of the barrier, and acts as blockade for the trailing anchor. This blockade was intended to ensure that the barrier would not be pushed into a straight line, and that a curvature would form in the trailing side of the barrier. Thereby creating a 'sail' for the current to act upon when turning. The drag spheres on the other hand was intended to increase the curvature of the barrier in a straight current, after which this curvature could also act as a 'sail' when the current started turning.

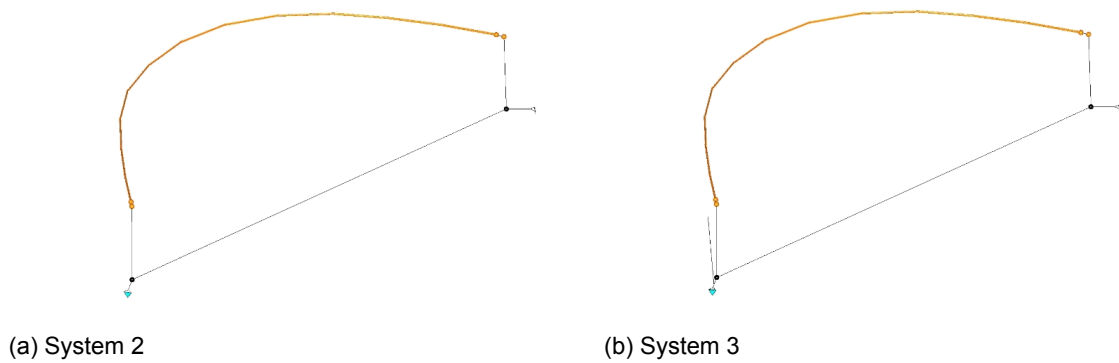


Figure 11.3: The first two variations of the selected concept

Both methods showed a improvement in overall efficiency, however both systems still failed (first failure moment indicated by red \* in Figure 11.10), and had a window of zero directional efficiency. The drag sphere worsened the effect of barrier being pushed into a straight line and the cross-line only slightly improved the opening efficiency, while intended to improve directional efficiency.

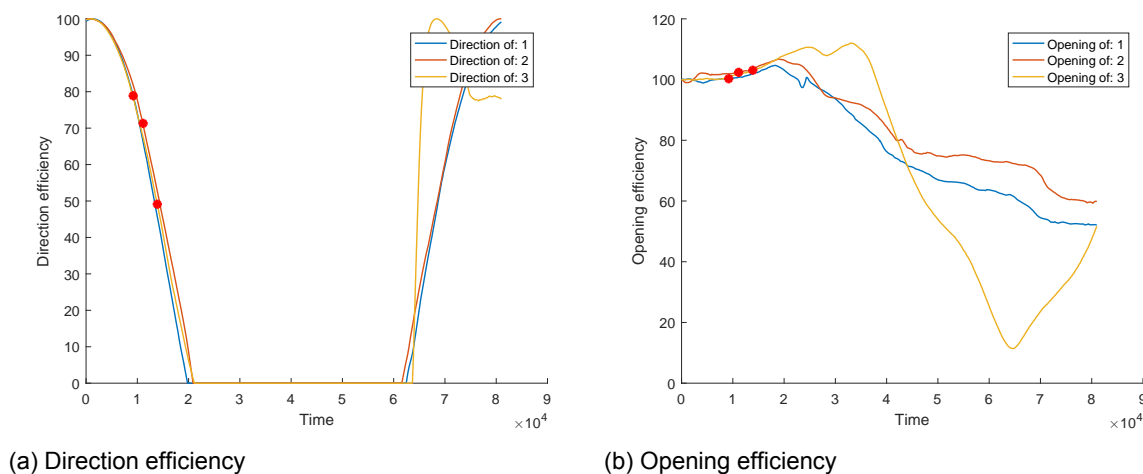
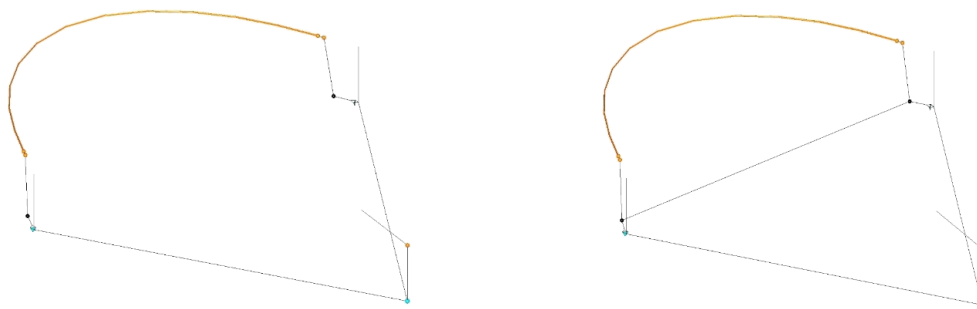


Figure 11.4: Time trace of the Direction and Opening efficiency of the first three variations, with indication of first moment of failure

The output from these simulations showed that a concept was needed that had 1 turning point. The anchors had too much freedom in the first variations, leading to a failure of the system early in the process of the changing current direction. Furthermore, the turning of the system was prevented by the drag on the leading anchor, the reduction of drag on the leading side, and by the fact that the trailing edge is pushed away by the current. Thereby failing to act as a turning point.

## 11.2. Hydroforce-boom with anchor connector

The introduction of the anchor connector was the first step in the search for a single turning point. It connected the anchors, thereby limiting their freedom, and introduced a single drag sphere in the center-line of the system (see Figure 11.5a). The drag sphere is supported by a mooring-line and surface buoy, which is connected to a surface line pointing in the direction of the current. Besides that, the same system, but with cross-line was introduced, since it had shown to improve the opening efficiency (see Figure 11.5b).

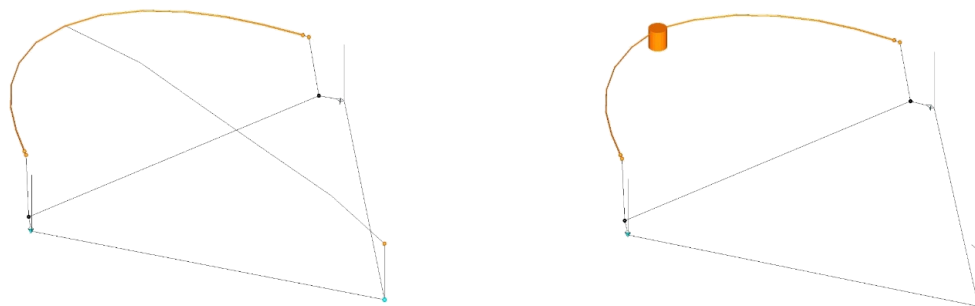


(a) System 4

(b) System 5

Figure 11.5: The first two variations of the system with anchor connector

However, although the moment at which failure occurred was delayed both systems did not show any significant improvement with respect to the designs of systems 1, 2 and 3 (see Figure 11.10). The subsequent design changes were the introduction of a 'drag-line' and a pilot anchor, seen in Figure 11.6a and 11.6b. The introduction of the drag line was thought to improve the turning of the system, since this high drag line (or screen) was expected to be forced parallel into the current flow. Whereas the pilot anchor, being a large drag area, was thought to be able to pull the system leading anchor around the trailing anchor.



(a) System 6

(b) System 7

Figure 11.6: The concept variations with anchor connector with drag-line and pilot anchor

However, the introduction of the drag-line reduced system efficiency and scrambled the system when the current turned. The pilot anchor on the other hand showed improvements in directional efficiency and a even further delayed the moment of failure (see Figure 11.7). Nonetheless, although the pilot anchor showed improvements in efficiency, the system was still not able to follow the changing current direction.

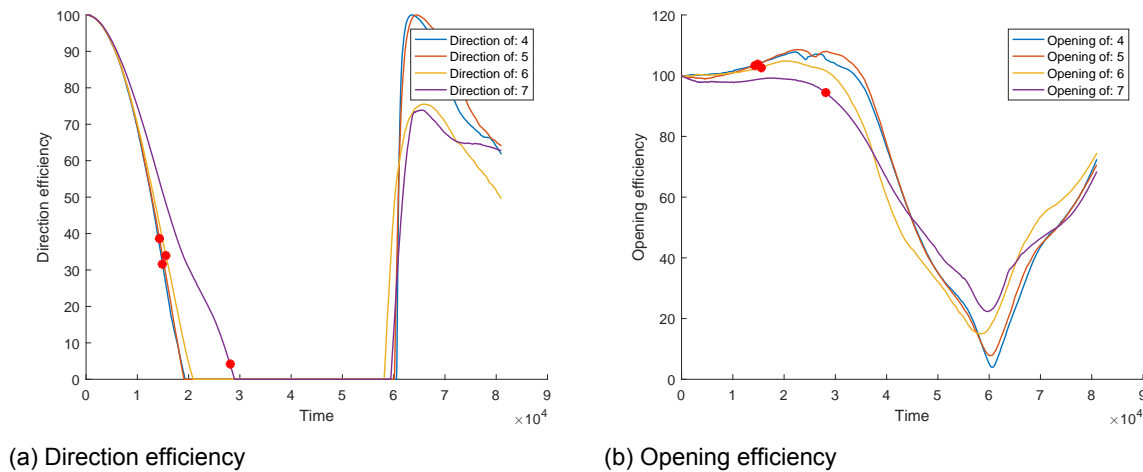


Figure 11.7: Time trace of the Direction and Opening efficiency of the anchor connector variations, with indication of first moment of failure in red

All in all the anchor connector didn't improve the systems efficiency and the connector introduced extra lines which would increase the change of entanglement. However, the pilot anchor as a separate component was thought to be effective, and could function as a retention area at the same time. The main problem with the systems, that were designed up to this point, was the sea-anchor at the leading side of the system. Which, in combination with the reduced drag force on the leading side, prevented the system from turning around the anchor on the trailing side. Therefore a new system had to be designed without submerged anchor rudders.

## 11.3. Hydroforce-boom with surface rudders

To be able to omit the use of subsurface rudder anchors, surface rudders were introduced (see Figure 11.8a). However, the main reason why they were not part of the selected concept, was the required size. The rudders used in this configuration have a base width of 95 meters and a depth of 85 meters, forming an insolvency triangle. The size of the anchor is extreme since the maximum angle before failing is limited and the rudders themselves therefore introduce significantly more surface drag. Furthermore they are connected to a single drag sphere, which increases the closing force even more, but is needed to enable a single turning point. The reason why the angle is limited is due to the fact that the anchors in this configuration were not forced under an angle with rigid bars. The required size of rigid elements was presumed to be unrealistic, although the anchor itself of course also had a single rigid element. Additional analyses into the systems behavior with rigid angle forcing have to be performed.

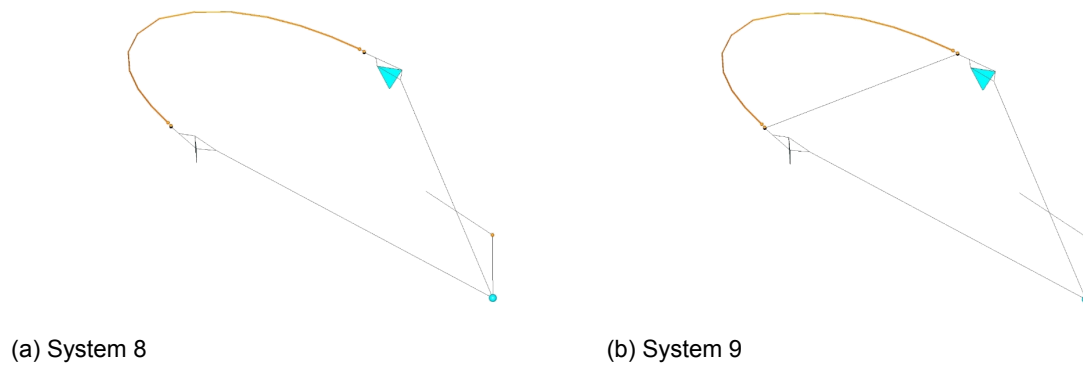


Figure 11.8: The first two variations of the selected concept

The surface rudder system was subsequently tested with a cross-line, smaller front drag-line (which only had a large area from the span line to the point of the barrier), and a pilot anchor (respectively Figure 11.8b, 11.9a, and 11.9b).

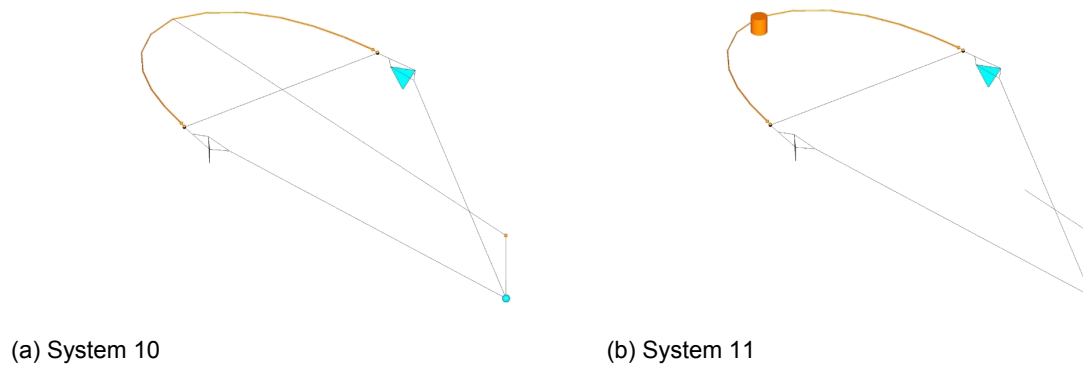


Figure 11.9: The first two variations of the selected concept

As expected, the systems 8-11 showed a different weathervaning behavior than the systems 1-7. All variations initially turn with the changing current direction, but 30000 seconds into the turn the current takes over the trailing side of the barrier and directional efficiency drops to zero. At this moment in time the barrier is pushed inward from the wrong side of the system and the system fails (as indicated by the red \* sign). The closing force of the barrier decreases since the load is of the sea-anchor, and the barrier is forced to open (see increase in opening efficiency Figure 11.10b). Furthermore, the opening efficiency of the system with pilot anchor is considerably lower due to the increased drag load of the surface system. However, the directional efficiency of the system with pilot anchor is slightly higher than that of the other configurations. Large anchor could be used for this configuration to support the additional drag load induced by the pilot anchor.

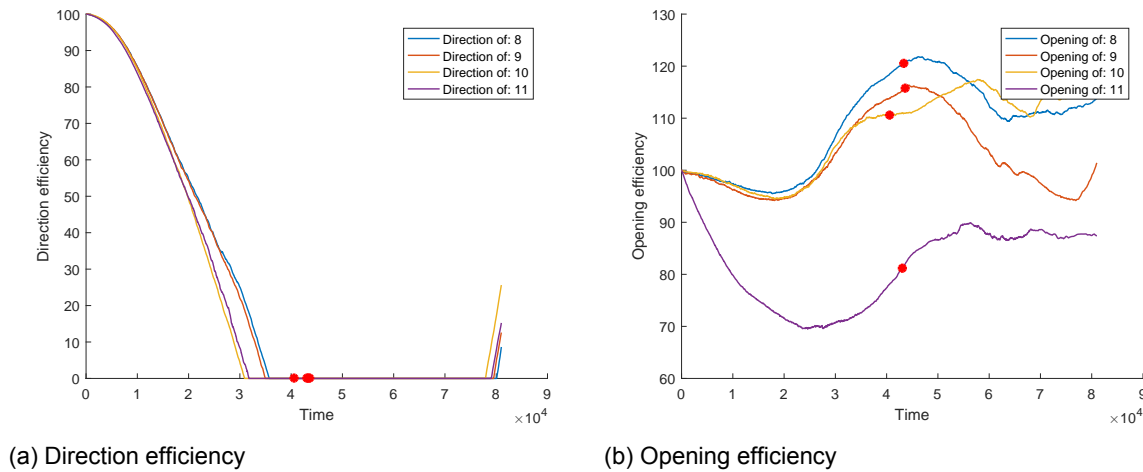


Figure 11.10: Time trace of the Direction and Opening efficiency of the surface rudder variations, with indication of first moment of failure in red

## 11.4. Concept variation evaluation

The design steps that were undertaken up in this research showed improvement in system performance, but all variations still endured 'system failure'. With the failure indicating that the system or its components have respectively taken on a shape or position from which the system can possibly not reattain its intended configuration. Some systems got scrambled up to a point from which they could not reattain the convergence state when the current took on a one directional flow. Whereas other systems could reattain there convergence state, but of which was unclear if they would be able to do so in any condition. Which was primarily the case for systems with submerged anchors, for which was assessed that their was a high risk of entanglement. For the surface-rudder system this risk was reduced to a minimum, however their still appeared to be a risk of the system to be pushed 'outside-in'. Which means that when the current turns fast around the system, the point of the barrier could be pushed through the inner span-line between the two rudders. This in turn could lead to unrecoverable system failure.

Figure 11.11 shows that system 7 has performed best overall, which was primarily due to the improve directional efficiency, caused by the introduction of the pilot anchor. Furthermore, the surface rudder systems have a higher opening efficiency than all the other systems, with the exception of the system with pilot anchor. However, the improved opening efficiency has no effect on the concepts feasibility since the current comes from the wrong direction of the barrier for more than 50% of the turn.

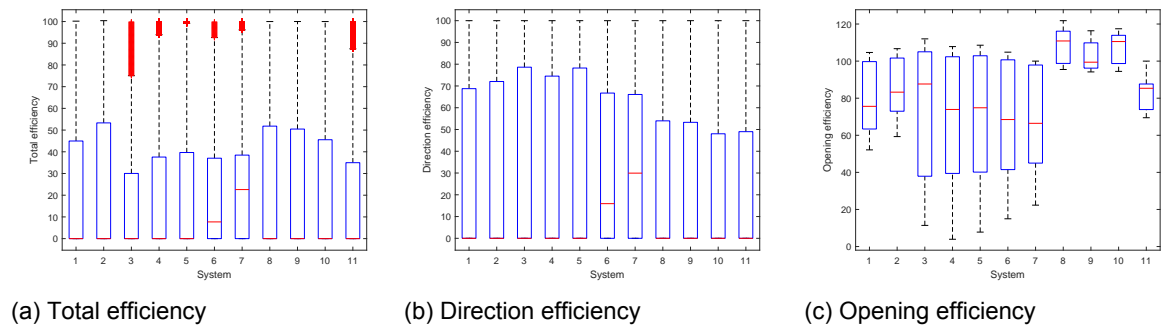


Figure 11.11: Boxplots of the total, directional, and opening efficiency of all system variations

Besides these systems, the exact same system variations were tested with a longer barrier, since this was expected to be of effect on the way the barrier is pushed 'straight' during a changing current direction. The results of the longer barrier, which was 2km long, can be seen in Figure 11.12.

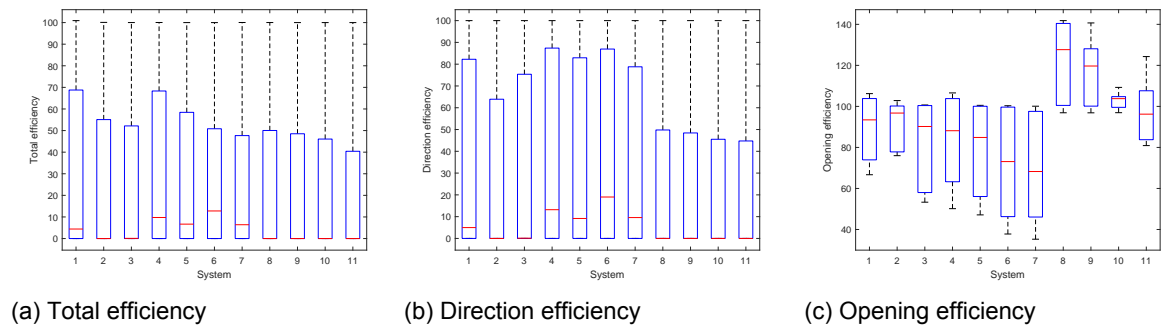


Figure 11.12: Boxplots of the total, directional, and opening efficiency of all system variations for the longer barrier

The results of the longer barrier systems indicate that the barrier length did indeed have an influence on the system performance. The longer barrier systems seem to turn better with the current due to the existence of a large curvature at of the barrier at the leading side, pulling the system around it's central point. However, as with the other systems, the current takes over on the trailing side and directional efficiency drops to zero. Furthermore, since all systems have failed the turning current test, the recover test was not of any value. If systems would show to be able to recover, they might still have become entangled since the elements only interact at their connected nodes.

In hindsight some of these findings might seem trivial, however at the time of system design iterations, the poor current following ability of the system was unknown. Furthermore, it has to be noted that the Ocean Cleanup, who were at the same time conducting research into the second high level concept in chapter 4 (designed in this thesis), came to the same results regarding current following ability of a similar but semi rigid system (using Orcaflex). As a result of these findings it was determined that a new type of system needed to be designed.

## 11.5. Proposal of a new concept

The new system would have to be able to either follow the current more precisely, or be able to catch plastic from all directions. Furthermore, the system would have to be able to always reattain the intended shape. Any situation regarding changing current direction should ultimately not lead to system damage or failure. Besides the fast changing current direction at relatively low current velocity, the system should be able to operate in day-to-day conditions. The day-to-day conditions only came into consideration during the final period of the research presented herein, and appeared to have a strong negative influence on system feasibility. In some situations the current was seen to decrease to a velocity of almost zero, after which the direction changed 180 degrees and the current velocity increased. Practically no system would be able to follow the current in such a situation. This led to new innovative design phase, taking into account all new knowledge.

The new additional value drivers for this process were defined to be:

1. The system should be able to catch plastic from all directions, meaning it either should use 1-way-gate barrier or it should be able to 'flip' (barrier curvature goes to zero, after which the barrier takes on a curvature on the other side of the span line). Meaning that the directional efficiency should be redefined.
2. The system should always be able to return to the intended state. Meaning that no failure is allowed to occur.
3. The system should at all times maintain an opening efficiency of at least 50%. Meaning the system should not be able to get completely scrambled.

These value driver subsequently had to be combined with the previous knowledge on concept behavior and the knowledge on the high level concept defined in chapter 3. It was thereby assumed that the new concept still needed to be completely flexible for the following reasons:

1. it was assumed that a flexible barrier would be considerably more easy the scale in size (length)
2. a flexible barrier is better applicable when the barrier needs to be able to 'flip', when the current direction changes
3. a flexible barrier was presumed to have better wave following characteristics
4. a flexible barrier would be better capable of enduring the significant cyclic loading due to waves
5. a flexible barrier is easier to install
6. a flexible barrier can be produced against lower costs
7. the Ocean Cleanup was researching rigid alternatives

Secondly the rudders needed for a flexible system were analyzed. The research in chapter five indicated that a long thin triangular sea-anchor with bars to force the anchor under a required angle, would be the most effective. Furthermore, the surface anchors were more applicable in preventing entanglement due to the surface boundary. Besides this the rudder-anchor could be kept considerably smaller since the relative current velocity is considerably higher at anchor depth. With both systems however the problem remained, that the anchors could generate lift force in the wrong direction if the system was to be pushed 'inside out', or if the anchors would turn around the directly connected mooring-line.

Taking into account all these risks and considerations, two types of anchor/system configurations were designed. The first being a flexible or semi-rigid barrier with stiff 100 meter deep anchor bars attached to the ends (see Figure 11.13a). In this configuration the anchors are

forced under an angle with rigid bars, and are not able to turn around the connection point in the horizontal plane. Besides that the anchor bar has a high torsional stiffness connection to the barrier and the complete anchor system is thereby also not able to rotate around the barrier end. If the current would change direction with 180 degrees, the anchor can flip around the bending point in the vertical plane. This results in the anchors always being able to generate a lift force to open the barrier perpendicular to the current.

The second configuration is an anchor designed with a rigid, triangular bottom and top rod configuration, with the two angles of 30 degrees and one of 120 degrees (see Figure 11.13b). Subsequently the anchor was made to run from the surface all the way down to anchor depth (see Figure ??). In this configuration the anchor rudder system would function as a surface rudder pushing outward, and the anchor would at the same time function as an anchor-rudder pushing outward. This being enabled by the difference in relative current direction. The new anchor was presumed to be able to deliver a high lift force with low additional drag force, due to its large surface area and optimal angle of attack. However the anchor could still rotate, which would diminish the systems ability to return to convergence state under all design cases. As a result the anchor and boom were specially redesigned and connected to the anchor to prevent this behavior (see Figure 11.13b). In this configuration the surface barrier and anchor barrier would always generate a drag force in the opposite direction, thereby creating a tensioned ellipse. If the anchor would turn around the connection point, the force of the barrier and anchor barrier would subsequently ensure that the anchor would regain the required position.

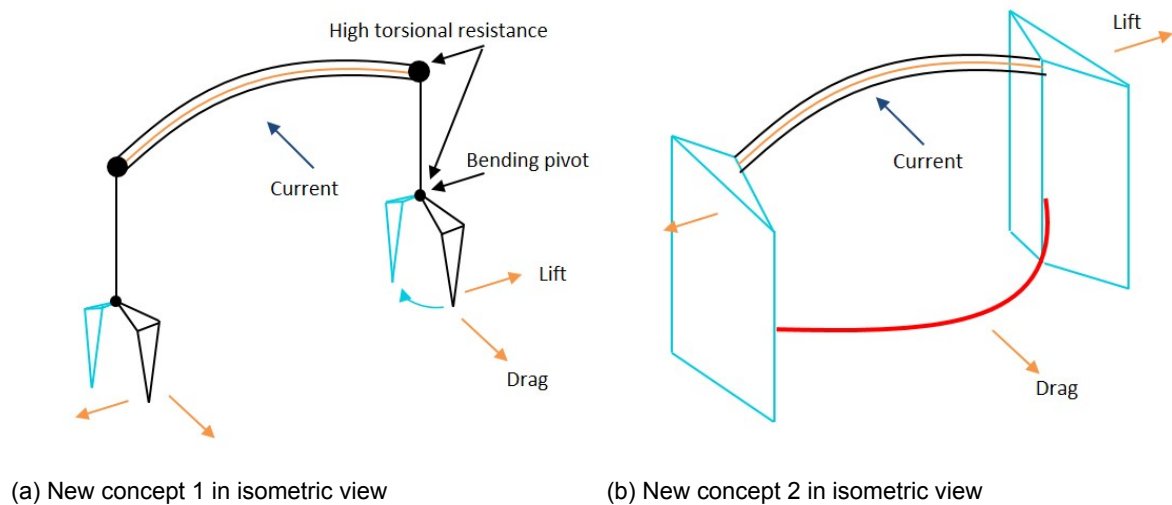


Figure 11.13: New concept schematics

Subsequently these new systems would have to be simulated under all defined design cases, during which no failures are allowed to occur. However, since the new systems are able to 'flip', a crossing of the inner span line could not be considered a failure, and after a crossing of the outer span line, the systems are presumed to be able to return to the intended state. Therefore no failures could be defined or were expected to occur. As to efficiency, the definition of 'opening efficiency' can be kept the same, whereas the definition for 'directional efficiency' has been changed as can be seen in Figure 11.14).



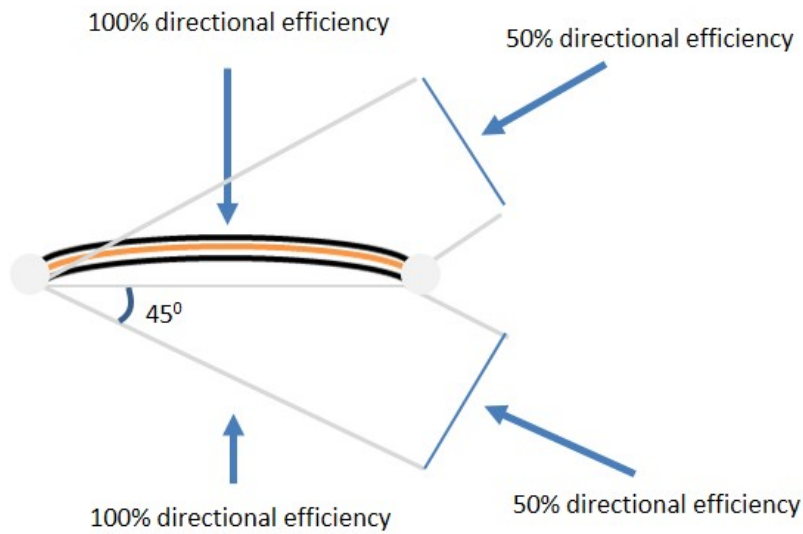
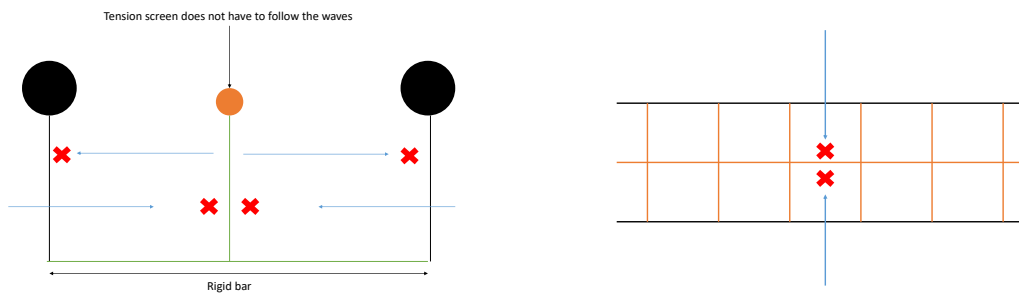


Figure 11.14: Visualization of new efficiency determination

The total efficiency of the system could subsequently be calculated by:

$$Totalefficiency = \frac{effectivespan}{convergencespan} \cdot 100 \quad (11.1)$$

The barrier configuration for the proposed concept, should be able to catch plastic from all directions to enable a 100% directional efficiency when the current is at a 90 degrees angle to the barrier, from any of the two sides. A barrier system that can provide this functionality can be seen in Figure 11.15. The barrier uses a 1-way-gate principle defined in chapter 4, to catch plastic from both directions. The screen in the middle of the barrier holds the tension from the current and wave drag, and is not required to follow the waves. Rigid bars are extended perpendicular from the barrier, to which completely decoupled flexible barriers are attached that are able to follow the waves. An extraction ship could use a suction mechanism or a large shovel system to empty the barrier while sailing past it.



(a) Proposed barrier cross-section

(b) proposed barrier top view

Figure 11.15: Proposed barrier for the new concept



**Part V**

**Research evaluation**



# 12

## Discussion

A reflection on the presented thesis can only be done by a separate discussion of every part. The research went through four different phases that all contributed to the objective of making a conceptual design but have independent results that can be used for future research. It are these results that will be discussed in this chapter. Thereby the part on concept generation is used to reflect on the overall process.

### 12.1. Part: Concept generation process

The process through which the conceptual design was developed, improved and evaluated, has been presented in line with scientific guidelines, and can therefore be easily used for further research. Starting of with the definition of the alternative systems Value Drivers (see Figure 1.4), followed by a method of convergent research, a broad solution space was defined, which included cleaning strategies as well as strategy specific concepts. All of which were based on a thorough analysis of the strategy sub-functions and required solution principles. Whereby the sub-functions and solution principles were depicted in a morphological overview, after which the resulting working structures were rated through a multi-criteria analysis (see Figure 4.6). Following from this rating process a passive cleaning strategy was selected to be the most suitable, and two strategy specific concepts were subsequently proposed to be analyzed on a more detailed level. The first being a concept that uses a pressurized floating membrane to retain shape and plastic (see Figure 4.5, number 4), was proposed to be analyzed experimentally. The second being a concept that makes use of hydrodynamic force to retain shape (see Figure 4.5, number 1), was proposed to be analyzed with the use of a numerical tool.

Although the research approach had been clearly defined there were several decision gates that had to be met without the proper information. Starting with the selection of the passive strategy for further analysis. Although the passive strategy did indeed score highest in the multi-criteria analysis, other strategies could have been good options in hindsight. The required cleaning speed of 10% relative reduction is considerably lower than presumed at the time (50% reduction), which would mean that drones at low speed could also be very effective. Besides that, the high directional variability of the current, which sparked the need for an alternative system in the first place, is considerably higher than expected during the concept generation phase. At a median direction change of 16 degrees/hr (see Figure 11.14) an actively controlled system could be a lot more efficient. Furthermore, the passive strategy scored extremely high on the inspirational criterion. Which is the most important Value Driver, but also the most difficult to substantiated. Potentially the best working strategy and system can receive the highest amount of funding, but in the absence of scientific evidence the inspirational criterion was judged on the current success of a passive approach.

As to the strategy specific concepts it was decided to analyze the feasibility of the Hydroforce-boom. This decision was mainly based on the bases of simplicity and efficient use of material. However, in hindsight the actual operating conditions should have been analyzed more thoroughly before making a decision on system plausibility. Not only could this have lead to the selection of one of the other concepts, but different concepts might also had been designed. Furthermore, the risks of entanglement in a highly dynamic environment should have been taken more seriously. Any system with more than one line subsurface has significant risk of entanglement and should therefor be avoided.

## **12.2. Part: Experimental test program**

Shortly after the selection of the passive concept the opportunity arose to participate in a HYDRALB+ experimental test program. At the time, the concept formulation process had just started and a experimental program had to be set-up within four weeks. As a result the Liquid Island concept was chosen to be investigated on a qualitative level, whereas a version of the 'Parachute' was proposed to be tested for the determination of hydrodynamic coefficients.

In hindsight the Liquid Island was not particularly plausible on a environmental bases and the determined coefficients would not been very helpful in the simulation of a completely flexible concept. Besides this the received feedback indicated that the submitted proposal did not clearly show the state of the project, and is was difficult to asses future implications (Appendix A). Both of which were valid arguments since the research only started 2 months before submission.

## **12.3. Part: Sea-anchor feasibility**

### **12.3.1. The approach**

The first phase that followed the selection of the Hydroforce-boom for feasibility analysis, was the feasibility analysis of the most critical component present in all formulated concepts: the sea-anchor. For the selected concept a sea-anchor was needed that could both slow down the system to the required speed and that could generate a lift force to open the barrier perpendicular to the incoming flow. A three-dimensional model was constructed for the design and analysis of the sea-anchor. Whereby a literature overview provided full scale test results of a similar system, based on which the three-dimensional model could be partially validated. The research found in the literature focused on the 'Window-shade drogue', which is a sea-anchor used for meteorological research and which consist out of a tensioned screen that could easily be adopted to generate lift. During full scale ocean tests this anchor was intended to turn it's screen normal to the relative current direction, but proved to turn parallel to the flow. The three-dimensional model that needed to be constructed for the design and evaluation of a ocean Cleanup sea-anchor was subsequently developed to model this unwanted 'Window-shade drogue' behavior, as to validate the model. Finally the 'Window-shade drogue' was adopted and suitable sea-anchor was designed and tested.

The taken approach resulted in a suitable anchor but if the approach would have been more structured, other alternative anchor systems might have been developed. The structured approach for the high level concept design taken in the concept generation part could for example have been expanded to the design of a sea-anchor. On the other hand the focus of the thesis was on development of a conceptual design of the complete concept and a more detailed analysis on sea-anchor design could have resulted in the inability to simulate the complete concept. Nonetheless, the use of an existing sea-anchor system as a basis (the 'Window-shade drogue') resulted in the design of a very similar type of anchor system. Whereas the use of a morphological overview, with sub-functions and solution principles could have resulted in a different and perhaps more (or less) effective sea-anchor.

Furthermore, the use of experimental data form 1975 to partially validate the model was

effective, but it remains unsure if the obtained experimental data is completely reliable. As described in the research report by William A. Vachon the measuring equipment used at the time was inaccurate. Leading to the fact that the obtained median anchor position used for model validation could also be inaccurate. Besides this, the partial validation of the model is based on one data point and can therefore only be used as a basic reality assessment.

### 12.3.2. The results

The results of the sea-anchor feasibility part should be discussed on three levels. The model validation, the stability analysis of a one-degree of freedom sea-anchor model, and the design of the final sea-anchor.

Presented in Figure 8.10, one can see the final partial model validation. Where Figure 8.10a indicates the median of the time trace presented in 8.8a. Thereby it can be seen that the anchor is quite unstable around the mean but does indeed show the same behavior as recorded from the experiment. This modeled unstable behavior has partially to do with the lack of torsional stiffness in the model, and due to the fact that the only damping is based on a velocity squared term (no structural damping and high Reynolds number). Although both are coarse simplifications, it is interesting to see that modeled anchor behavior still resembles the recorded behavior. Thereby it has to be noted that the anchor is only connected to a thin 24 meter long cable, and the actual torsional stiffness would therefore not be too far off. Furthermore, the assumed hydrodynamic center dependency on the angle of attack (see section 7.2.6), also seems to be appropriate since the model shows similar behavior.

To assess the effect of torsional stiffness and damping on the stability of the anchor, a one degree of freedom model was constructed. Thereby quasisteady theory was assumed, and the equation of motion was linearized around a 90 degrees angle of attack (see equation 9.11). Although this is substantiated, there are cases in which a linearized approach would not be appropriate due to for example a fast rotation of the screen and thereby a large relative angle of attack, or due to a reduced velocity in the interval of 1 to 20. Whereby the frequency of structural vibrations comes close to the vortex shedding frequency. In these cases the anchor's behavior cannot be described by instantaneous angles. Furthermore, the rotation of the plate or anchor screen could lead to an increase in vortex shedding. Torsional flutter has thereby been proven to occur when the frequency of vortex shedding is close to the oscillating frequency of the plate, and lock-in takes place. Which subsequently can increase the vibrations and result in auto-rotation. During which the anchor enters an unbounded rotation and stabilizes at a constant angular velocity [15]. It can therefore be argued that to determine the actual stiffness and damping needed to maintain stability, a more extensive model is needed.

The design and evaluation of the final sea-anchor has many simplifications that would need to be substantiated when the anchor goes into a detailed design phase. The first being the hydrodynamic center dependency on the angle of attack for the slender triangular anchor, which was assumed to be the same as for a rectangular anchor such as the 'Window-shade drogue', while this dependency is a lot more complicated. The second being the simplification of the anchor representation as four nodes, which removes the possibility to model in plane anchor screen tension. And the third major simplification being the mooring-line the adopted design, which is simply a cable with a weight at the bottom to maintain the anchor at the required depth.

Figure 9.4 shows the results of the final anchor with a tether connection under a straight tow, and Figure 9.6 shows the results under a straight tow, but with the anchor forced under an angle of 20 degrees. Thereby it can be seen that the anchor becomes unstable at a forced angle of 15 degrees (Figure 9.5), but that an anchor with the hydrodynamic center always in the middle of the anchor screen, becomes unstable at 10 degrees. The time traces in Figure 9.6 indicate that the reason of instability is due to the fact that the anchor approaches a  $0^\circ$

angle of attack with the relative current and thereby become unstable. However the results of Figure 9.5 thus give an impression of the sensitivity of the assumption of the hydrodynamic center dependency on the angle of attack. Meaning that the anchor could in real life either be more stable or less stable, depending on the shape and aspect ratio.

Figures 9.8 give an overview of a simple parametric study on the dependency of the anchors stability on the mass and added-mass of the system. It gives an explanation and substantiation of the time trace in Figure 9.6, where the decrease of the apparent angle that go hand in hand with accelerations of the system. Based on these figures it is explained that instability of the anchor is mass dependent, but in order to fully substantiate this claim, a extensive parametric study would have to be performed. Thereby, besides mass, several parameters should be varied, including the hydrodynamic center. This parametric study would give the possibility to optimize the anchor in the detailed design phase. Furthermore, the anchor with a rigid connection to position the anchor under an angle shows a stable behavior (see Figure 9.10). However, besides the parametric study, simulations under different angles, different current speeds, and different connection configurations would have to be performed to obtain a complete understanding of the anchor stability.

## 12.4. Part: Concept feasibility

The finale three-dimensional model of the complete concept was tested in median current conditions in one direction, a 360 degrees changing direction and a straight current following the end of the turn. These conditions were presumed to strongly effect system feasibility, but other conditions might have had even more negative impact on the systems feasibility. Thereby since no definition of feasibility existed, three types of efficiency were defined, and the definition of failure was determined. These efficiency and failure definitions were specifically set-up and had no basis in literature. Other definitions could have been used but the end result would have been the same if the concept design was kept the same.

Furthermore the basic design variations were tested for convergence through a series of tests in changing current conditions. Every test had a duration of 81,000 seconds and if two subsequent end positions (and end shapes) of the systems were the same, the system was said to be converged. While this approach is valid for these specific cases, the system might still not have enough nodes to cover a realistic behavior in any case. To be able to guarantee this additional convergence analysis should be performed.

The subsequent design of system variations was a unstructured and innovative process through which apparent issues were tried to be solved step by step. However, in hindsight it can be seen that although the design iterations resulted in small improvements, every flexible system would inevitably fail in a rotating median current condition. A better approach would therefor had been to perform an in depth analysis of the behavior of the first concept simulation. After which subsequently a totally new concept could have been designed.

The in chapter 4 selected concept was simulated under all three conditions of which only the changing current direction proved to be of relevance. All systems had a 100% opening and directional efficiency in a straight current, but failed soon after the current started turning. Due to these failures the third test results were unnecessary to discuss since all systems could have get entangled in in a resembling real life situation.

The final results presented in chapter 11 (Figure 11.11) show that all concept variations fail under a rotating current. After which is claimed that a concept with a flexible barrier will inevitably fail. However, although multiple concept variations have been tested, various other configurations could have been designed, of which the feasibility is unsure. Furthermore, the tests of the Hydroforce-boom with surface rudders, have not been performed with rigid anchor forcing (a rigid connection to force the angle of attack), which could have potentially increased the chance on concept feasibility.



## Conclusion & Recommendations

The research presented in this thesis has provide a thorough analysis of a possible conceptual design for an alternative Ocean Cleanup system. Thereby the thesis has accomplished the objective assigned by the Ocean Cleanup: Develop a conceptual design of a mobile Great Pacific Garbage Patch plastic catching system. The conclusions and recommendations that can be made are presented in their relation to the parts of their topic.

### 13.1. Part: Concept feasibility

#### 13.1.1. The conclusions

The main conclusion following from the concept feasibility analysis is that: a concept that uses hydrodynamic forcing to retain shape by inducing tension with anchor rudders, is unfeasible when the system is designed to catch plastic from one side. It became apparent that a direct reduction of drag forces on the leading side of the barrier (the side that is first encounters the flow), in combination with the large drag area of the submerged anchor rudders, prevented the system from turning when the current direction changed. Besides this it became clear that a system with two separate anchors would inevitably fail since the designed anchors could turn around their attachment point, thereby generating lift in the wrong direction and closing the barrier. Following from these conclusions two new main system variations were designed and tested. Of which one variation had connected anchor rudders and the other variation had surface rudders and an drag sphere as sea-anchor. Both showed different types of improvements but it was evident that no system would be able to follow the changing current direction. Furthermore, the anchors showed stable behavior (Figure 11.2) but are sometimes forced out the equilibrium position due to barrier-anchor interaction, which causes the apparent current angle to decrease to zero and tip the anchor. However, since a rigid angle forcing is used the anchor returns to the equilibrium position. If a flexible anchor connection was used the system would have failed.

Therefor two new systems are proposed at the end of the last chapter on concept feasibility. This new system can catch plastic from all directions and is presumed not be able to fail, since there are no lines that can get entangled and the anchors cannot generate lift in the wrong direction.

#### 13.1.2. The recommendations

1. Use the presented model to simulate the two newly proposed concepts
2. Introduce torsional stiffness to enable the modeling of concept 1 (see Figure ??)
3. Analyze behavior in the same conditions as presented
4. Introduce bending stiffness in the barrier of both concepts if they are not feasible

5. If the concept(s) prove feasible in current conditions, analyze the behavior in day to day conditions
6. If the concept(s) prove feasible in all current conditions, model the barrier as a horizontal ellipse
7. Simulate the wind and wave forces and asses total concept feasibility
8. If concept(s) prove feasible make scale model and test it through HYDRALAB+ program with the here presented program as a basis
9. If concepts do not prove feasible, return to the solution space in chapter 4 and start analyzing the gate-wheel and Liquid Island concept

## 13.2. Part: Sea-anchor feasibility

### 13.2.1. The conclusions

The main conclusion from the sea-anchor feasibility analysis is that: a sea-anchor that can generate a stable lift force can be designed by forcing an anchor screen under an angle with a rigid connection, and thereby preferably giving the anchor a high added-mass in the bi-normal direction. If the rigid connection is not implemented the anchor seems to be unstable due to a small relative angle of attack, created by lift forces. With these destabilizing lift forces being dependent on the mass and added-mass of anchor. At a low anchor mass the system quickly accelerated when the angle of attack changes, whereas at a higher bi-normal added-mass, these accelerations are reduced and the anchor stability increases. Besides this the first anchor design had to be adopted to prevent it from twisting around its vertical plane. This can be done by changing the anchor shape in a slender triangle, of which the mass at the tip would create a restoring moment when the top bar twisted.

These design optimization's hold true for the sea-anchor as a separate system but are even more important for the sea-anchor implemented in the complete system. As the sea-anchor with rigid connection shows no instabilities as a separate system, but does show some instabilities as part of the complete system. This is due to the fact that the forces in the system try to close the barrier opening, through which the anchor is not only pulled forward but also side-wards. Thereby creating an unstable equilibrium.

Furthermore, the three-dimensional sea-anchor model is partially validated since a modeled 'Window-shade drogue' shows similar behavior as recorded during a full scale ocean test performed by William A. Vachon [43]. Thereby an interesting dependency of the drogues behavior on the connected cable tension was identified. Meaning that the 'Window-shade drogue' behavior with pretension in the lines is completely dependent on the hydrodynamic coefficients of the anchor screen, while without pretension the anchor is forced parallel to the dominant surface current. This effect was caused by the relocation of the drogues turning point from the center-line of the system to the leading edge. The pretensioned drogue on the other hand proved to turn normal to the surface current due to the fact that the hydrodynamic center of the drogue moves to the leading edge at small angles of attack, which results in a restoring moment.

Besides this, a one degree of freedom analysis of the 'Window-shade drogue' proved that a minimal damping ratio of 0.09 is required to prevent dynamic instability (effective damping  $\leq 0$ ) at a straight tow in a current of 0.54 m/s (90% of the max surface current of 0.6 m/s). Thereby it is shown that the hydrodynamic stiffness of the one degree of freedom anchor, is enough to prevent static instability (effective stiffness  $\leq 0$ ). However, for both analyses holds that they are performed with the use of quasisteady theory. Therefor the result is only applicable for a straight tow.

### 13.2.2. The recommendations

1. With respect to the newly proposed systems one new anchor needs to be modeled (system 2 Figure ??)
2. For the anchor of system 1 holds that torsional and bending stiffness should be introduced in the model
3. For both anchors holds that a parametric study on the influence of the hydrodynamic center dependency on the angle of attack, is necessary to determine the stability of the anchor
4. Experimental research and additional literature should subsequently be performed to identify the most suitable anchor aspect ratio and shape
5. A conceptual design analysis is advised to design the anchor of system 1 with a high added-mass in bi-normal direction
6. A non-linear analyses on the one degree of freedom system stability could provide insight in anchor stability in all conditions
7. A two dimensional analyses of the finally proposed anchor with a fixed rotation point, could be performed to better understand the cause of instability/stability

### 13.3. Additional recommendations

1. If all systems fail, the design process in the part 'Concept generation' can be used as a new basis
2. The HYDRLAB+ proposal, discussed in chapter 5 can be used to submit a new test program for the final concept



# Bibliography

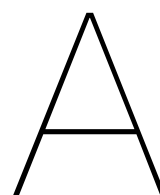
- [1] A Andersen, U Pesavento, and Z Jane Wang. Unsteady aerodynamics of fluttering and tumbling plates. *Journal of Fluid Mechanics*, 541:65–90, 2005. ISSN 1469-7645.
- [2] Anders Andersen, Umberto Pesavento, and Z Jane Wang. Analysis of transitions between fluttering, tumbling and steady descent of falling cards. *Journal of Fluid Mechanics*, 541: 91–104, 2005. ISSN 1469-7645.
- [3] Mohammadmehdi Armandei and Antonio Carlos Fernandes. Stability analysis of a yawing flat plate into the water current. In *ASME 2012 31st International Conference on Ocean, Offshore and Arctic Engineering*, pages 623–629. American Society of Mechanical Engineers, 2012.
- [4] PW Bearman. Flow-induced vibration. by robert d. blevins. van nostrand reinhold, 1977. 363 pp.£ 13.75. *Journal of Fluid Mechanics*, 89(01):206–207, 1978.
- [5] Robert D Blevins. Flow-induced vibration. 1990.
- [6] Eric P Chassignet, Harley E Hurlburt, Ole Martin Smedstad, George R Halliwell, Patrick J Hogan, Alan J Wallcraft, and Rainer Bleck. Ocean prediction with the hybrid coordinate ocean model (hycom). In *Ocean weather forecasting*, pages 413–426. Springer, 2006.
- [7] Matthew Cole, Pennie Lindeque, Claudia Halsband, and Tamara S Galloway. Microplastics as contaminants in the marine environment: a review. *Marine pollution bulletin*, 62 (12):2588–2597, 2011.
- [8] RG Dong. *Effective mass and damping of submerged structures*. Department of Energy, 1978.
- [9] AC Fernandes and S Mirzaeisefat. Flow induced fluttering of a hinged vertical flat plate. *Ocean Engineering*, 95:134–142, 2015.
- [10] Antonio Carlos Fernandes and Mohammadmehdi Armandei. van der pol-duffing modeling for torsional galloping. In *ASME 2014 33rd International Conference on Ocean, Offshore and Arctic Engineering*, pages V09BT09A009–V09BT09A009. American Society of Mechanical Engineers, 2014.
- [11] Antonio Carlos Fernandes, Sina Mirzaei Sefat, Fabio Moreira Coelho, and Mario Ribeiro. Towards the understanding of manifold fluttering during pendulous installation: Flow induced rotation of flat plates in uniform flow. In *ASME 2010 29th International Conference on Ocean, Offshore and Arctic Engineering*, pages 603–609. American Society of Mechanical Engineers, 2010.
- [12] Annalisa Griffa, AD Kirwan Jr, Arthur J Mariano, Tamay Özgökmen, and H Thomas Rossby. *Lagrangian analysis and prediction of coastal and ocean dynamics*. Cambridge University Press, 2007. ISBN 113946308X.
- [13] J Hall and E Kerut. Development of a meteorological and oceanographic drifting buoy system. In *OCEAN 75 Conference*, pages 56–69. IEEE.
- [14] David Michael Hargreaves, Bruce Kakimpa, and John S Owen. The computational fluid dynamics modelling of the autorotation of square, flat plates. *Journal of Fluids and Structures*, 46:111–133, 2014. ISSN 0889-9746.

- [15] David Michael Hargreaves, Bruce Kakimpa, and John S Owen. The computational fluid dynamics modelling of the autorotation of square, flat plates. *Journal of Fluids and Structures*, 46:111–133, 2014.
- [16] B Hofland. 2d physical model tests for the ocean cleanup. report, 2015.
- [17] Robin M Robin M Hogarth. *Judgement and choice: The psychology of decision*. Number Sirsi) i9780471914792. 1987.
- [18] R Holler. Hydrodynamic drag of drogues and sea anchors for drift control of freefloating buoys. In *OCEANS’85-Ocean Engineering and the Environment*, pages 1330–1335. IEEE.
- [19] Scott G Isaksen. Creative problem solving. *GIFTED CHILD QUARTERLY*, 49(04):343, 2005.
- [20] Garbis H Keulegan and Lloyd H Carpenter. *Forces on cylinders and plates in an oscillating fluid*. US Department of Commerce, National Bureau of Standards, 1956.
- [21] T Kukulka, G Proskurowski, S Morét-Ferguson, DW Meyer, and KL Law. The effect of wind mixing on the vertical distribution of buoyant plastic debris. *Geophysical Research Letters*, 39(7), 2012. ISSN 1944-8007.
- [22] LC-M Lebreton, SD Greer, and JC Borrero. Numerical modelling of floating debris in the world’s oceans. *Marine Pollution Bulletin*, 64(3):653–661, 2012. ISSN 0025-326X.
- [23] Henry A McKenna, John WS Hearle, and Nick O’Hear. *Handbook of fibre rope technology*. Elsevier, 2004.
- [24] Sina Mirzaeisefat and Antonio Carlos Fernandes. Stability analysis of the fluttering and autorotation of flow-induced rotation of a hinged flat plate. *Journal of Hydrodynamics, Ser. B*, 25(5):755–762, 2013.
- [25] Edward C Monahan and Elizabeth A Monahan. Trends in drogue design. *Limnology and Oceanography*, 18(6):981–985, 1973. ISSN 1939-5590.
- [26] SR Munshi, VJ Modi, and T Yokomizo. Fluid dynamics of flat plates and rectangular prisms in the presence of moving surface boundary-layer control. *Journal of Wind Engineering and Industrial Aerodynamics*, 79(1):37–60, 1999. ISSN 0167-6105.
- [27] John Nicholas Newman. *Marine hydrodynamics*. MIT press, 1977. ISBN 0262140268.
- [28] Pearn P Niiler and Jeffrey D Paduan. Wind-driven motions in the northeast pacific as measured by lagrangian drifters. *Journal of Physical Oceanography*, 25(11):2819–2830, 1995. ISSN 1520-0485.
- [29] PP Niiler, AS Sybrandy, Kenong Bi, PM Poulain, and D Bitterman. Measurements of the water-following capability of holey-sock and tristar drifters. *Oceanographic Literature Review*, 5(43):429, 1996. ISSN 0967-0653.
- [30] James O’Donnell, Arthur A Allen, and Donald L Murphy. An assessment of the errors in lagrangian velocity estimates obtained by fgge drifters in the labrador current. *Journal of Atmospheric and Oceanic Technology*, 14(2):292–307, 1997. ISSN 1520-0426.
- [31] Xavier Ortiz, David Rival, and David Wood. Forces and moments on flat plates of small aspect ratio with application to pv wind loads and small wind turbine blades. *Energies*, 8(4):2438–2453, 2015.
- [32] Gerhard Pahl and Wolfgang Beitz. *Engineering design: a systematic approach*. Springer Science & Business Media, 2013.
- [33] Umberto Pesavento. *Unsteady aerodynamics of falling plates*. Thesis, 2006.

- [34] Julia Wiener Reisser, Boyan Slat, Kimberly Denise Noble, Katherine Du Plessis, Meredith Epp, Maira Carneiro Proietti, Jan de Sonnevile, Thomas Becker, and Charitha Pattiaratchi. The vertical distribution of buoyant plastics at sea: an observational study in the north atlantic gyre. 2015. ISSN 1726-4189.
- [35] I Robertson, L Li, SJ Sherwin, and PW Bearman. A numerical study of rotational and transverse galloping rectangular bodies. *Journal of Fluids and Structures*, 17(5):681–699, 2003.
- [36] Ali Bakhshandeh Rostami and Antonio Carlos Fernandes. Simulation of fluttering and autorotation motion of vertically hinged flat plate. In *ASME 2015 34th International Conference on Ocean, Offshore and Arctic Engineering*, pages V001T01A001–V001T01A001. American Society of Mechanical Engineers, 2015.
- [37] T Sarpkaya. Forces on cylinders and spheres in a sinusoidally oscillating fluid. *Journal of Applied Mechanics*, 42(1):32–37, 1975. ISSN 0021-8936.
- [38] Jami J Shah, Santosh V Kulkarni, and Noe Vargas-Hernandez. Evaluation of idea generation methods for conceptual design: effectiveness metrics and design of experiments. *Journal of mechanical design*, 122(4):377–384, 2000.
- [39] Carlos Guedes Soares and Y Garbatov. *Ships and Offshore Structures XIX*. Crc Press, 2015.
- [40] Ken Takagi and Miho Nagayasu. Ray theory for predicting hydroelastic behavior of a very large floating structure in waves. *Ocean engineering*, 34(3):362–370, 2007.
- [41] W Vachon. Current measurement by lagrangian drifting buoys-problems and potential. In *OCEANS’77 Conference Record*, pages 639–645. IEEE.
- [42] William A Vachon. Scale model testing of drogues for free drifting buoys. 1973.
- [43] William A Vachon. Instrumented full scale tests of a drifting buoy and drogue. Report, DTIC Document, 1975.
- [44] HJJ Van den Boom. Dynamic behaviour of mooring lines. In *BOSS Conference, Delft*.
- [45] Chien Ming Wang, Eiichi Watanabe, and Tomoaki Utsunomiya. *Very large floating structures*. CRC Press, 2007.
- [46] JEW Wichers et al. On the slow motions of tankers moored to single point mooring systems. In *Offshore Technology Conference*. Offshore Technology Conference, 1976.
- [47] Fritz Zwicky et al. Discovery, invention, research through the morphological approach. 1969.







HYDRALAB+



# A.1. Application form



HYDRALAB+: transnational access to the major and unique experimental hydraulic and hydrodynamic facilities



## 1. Title of the proposal

*Feasibility study of a mobile plastic catching system*

## 2. Requested facility/facilities

*DHI Offshore Wave Basin*

## 3. User Group Leader's full name and title

*Prof. R.H.M. Huijsmans*

## 4. Affiliation of User Group Leader

Name and full postal address of the institute/company, including department:

*Delft University of Technology. Faculty of Mechanical, Maritime and Materials Engineering. Department Maritime & Transport Technology, Section Ship Hydromechanics & Structures*

*Male/Female: Male*

*Tel.: +31 15-27 83598*

*E-mail: R.H.M.Huijsmans@tudelft.nl*

*Fax.: +31 15-27 81836*

*Web-site: www.tudelft.nl*

## 5. Details of all other persons participating in the project

#	Title	Family name	First name	Gender (M/F)	Birth year	Nationality	Institution	E-mail	New User (Y/n)
2	PhD	Sainte-Rose	Bruno	M	1985	French	Ocean Cleanup	<a href="mailto:bruno.sainte-rose@theoceancleanup.com">bruno.sainte-rose@theoceancleanup.com</a>	y
3	PhD student	Laguna	Antonio	M	1984	Mexican	TU Delft	<a href="mailto:a.jarquinlaguna@tudelft.nl">a.jarquinlaguna@tudelft.nl</a>	y
4	PhD student	Van der Kolk	Nico	M	1985	Dutch	TU Delft	<a href="mailto:n.j.vanderkolk@tudelft.nl">n.j.vanderkolk@tudelft.nl</a>	n
5*	PhD student	van der Mheen	Mirjam	F		Dutch	UWA	<a href="mailto:mirjam.vandermheen@theoceancleanup.com">mirjam.vandermheen@theoceancleanup.com</a>	n
6	MSc	Schöneich-Argent	Rosanna	F	1991	German	Ocean Cleanup	<a href="mailto:rosanna.schoeneich-argent@theoceancleanup.com">rosanna.schoeneich-argent@theoceancleanup.com</a>	y
7	MSc student	Delfos	Bram	M	1991	Dutch	TU Delft	<a href="mailto:bram.delfos@student.tudelft.nl">bram.delfos@student.tudelft.nl</a>	y
8	MSc student	De Feijter	Theotimus	M	1991	Dutch	TU Delft	<a href="mailto:t.s.j.defeijter@student.tudelft.nl">t.s.j.defeijter@student.tudelft.nl</a>	y
9	MSc student	Flick	Johanna	F	1989	Dutch	TU Delft	<a href="mailto:j.m.p.flick@student.tudelft.nl">j.m.p.flick@student.tudelft.nl</a>	y

\*will most likely not be able to visit the facility

## 6. Names and access period of those that made use of the access programme to this facility in previous EC framework programmes:

*None*

- 7. Estimated number of access days requested;** *(this includes the time needed for building the test setup, testing and calibration when necessary, experiments, and removal of the test setup)*
- 

23 (thereof 15 in the offshore basin)

- 8. Estimated total number of the visiting person-days:**  
*(Sum of the days of presence at the installation of all the members of the visiting team)*
- 

60

- 9. Most appropriate period for the experiments?**  
*Are there any constraints for the period when you may or may not perform the experiments?*
- 

*Preferred period is in the summer of 2016.*

- 10. Tentative list of instrumentation requested** *(contact us for information; if you also use your own instruments, please give the characteristics)*
- 

*Mooring system with roller support mounted in the basin  
Video cameras  
Underwater video cameras  
Potentiometer  
Force transducer  
Motion capturing system  
Wave gauges  
Current speed sensor*

*For more details see the description of the Research Proposal in appendix 12.*

- 11. Description of proposed work (four A4)**
- 

*See appendix 11.*

- 12. Technical details and specifications of the planned experiments (maximum of one A4 page)**
- 

*See appendix 12.*

- 13. References**
- 

*[1] Cole, M., et al. (2016). "Microplastics Alter the Properties and Sinking Rates of Zooplankton" Environmental Science and Technology*

*[2] Lecture notes, Experimental Methods in Marine Hydrodynamics, 2014*

*[3] Wang, C. M., et al. (2007). Very large floating structures, CRC Press.*

*[4] Takagi, K. and M. Nagayasu (2007). "Ray theory for predicting hydroelastic behavior of a very large floating structure in waves." Ocean Engineering **34**(3–4): 362-370.*



## A.2. Feedback



Title:	<b>Feasibility study of a mobile plastic catching system</b>	
User group leader:	Prof. R.H.M. Huijsmans	
<i>SECTIONS 1 – 3: to be completed by providers (before distributing this form to USP members)</i>		
<b>1.</b>	<b>User group is eligible and project is feasible and fits within the logistics of the host institute</b>	<b>y</b>
Remarks:		
<b>2.</b>	<b>Conformity with objectives of the EC</b>	<b>A</b>
	<i>training of researchers in the use of these installations</i>	<b>a</b>
	<i>stimulating collaboration in the team and with host institute expected</i>	<b>a</b>
	<i>priority to Users having not normally access to similar installations</i>	<b>y</b>
	<i>percentage of female users in user group</i>	<b>%</b>
	<i>percentage of First time Users in user group</i>	<b>%</b>
	<i>number of nationalities in user group</i>	
Remarks:		
<b>3.</b>	<b>The amount of access required for the project</b>	<b>A</b>
Remarks, suggestions to adapt the number of required access days, etc.		
<i>SECTIONS 4 - 6: to be completed by USP members</i>		
<b>4.</b>	<b>Relevance of the possible outcome of the project</b>	<b>B2</b>
	<i>relevant within a long term development or to the theme of climate change adaptation</i>	<b>b3</b>
	<i>direct utilisation of the possible outcome (result is directly useful in practice)</i>	<b>b2</b>
Remarks:		
<p>This is a very tentative proposal that deals with ocean pollution rather than climate change. The information might eventually be useful but at some time in the future. The concept and the development are innovative and exciting for clean-up of marine litter.</p> <p>There is no direct indication that there is a climate change component in this proposal. There is an environmental component that weakly argues that microplastics could have an influence on the carbon cycle, however, the aim of the proposed system is to catch larger plastics.</p> <p>Results won't have direct utilization, but long term development of the system might rely on the data.</p>		
<b>5.</b>	<b>Scientific level of the proposal</b>	<b>B2</b>
	<i>content of the proposal</i>	<b>b3</b>
	<i>need to use this specific installation</i>	<b>b1</b>
	<i>effectiveness of the research approach / technical feasibility</i>	<b>b1</b>
	<i>experience in other (small scale) facilities or in field experiments</i>	<b>b1</b>
	<i>competence of the team (Users Group)</i>	<b>b2</b>
Remarks to improve the proposal, suggestions to combine proposals, etc.:		
<p>A very interesting proposal with highly innovative content. The potential outcome is of societal and environmental importance. Ties into existing literature are presented.</p> <p>The structure of the proposal is however not easily read in a continues manner, some vital information was kept in an appendix, which made it complex and confusing. A better structure would make a clearer</p>		

<p>justification of what is being planned.</p> <p>Existing experience on previous physical model tests is valuable, however, there is no clear indication that the proposed system has undergone other model tests at smaller scale. Data storage plan is good, as it allows for sharing with others.</p> <p>Publication strategy is a bit vague; however, inclusion of educational and dissemination aspects is appreciated.</p> <p>The team interaction is not well described, who is contributing what. The CV for the team leader is missing and the involvement of the team leader is not clear. The European collaboration dimension should be strengthened, so the proposal doesn't appear as a DUT project alone.</p> <p>More details of the so-called “mega-scale numerical model” should be provided. It is not clear at what stage the project is in, and therefore it is hard to judge if the project is suitable within Hydralab+.</p>	
<b>6.</b>	<p><b>CONCLUSION</b></p> <p><b>B2</b></p>

Meaning of the ratings: A/a = good; B/b = acceptable, but should be improved; C/c = poor, reason for rejection.

A1: excellent  
A2: very good  
A3: good  
B1: good, but should be improved on some minor items  
B2: acceptable, but should be improved on certain items  
B3: acceptable, but needs improvement on important item  
C1: poor, there is a reason for rejection  
C2: poor, there are a number of reasons for rejection  
C3: very poor, should be rejected